Ecological Archives M076-016-A1, A2, A3

Craig A. Aumann, Lisa A. Eby, and William F. Fagan. 2006. How transient patches affect population dynamics: the case of hypoxia and blue crabs. *Ecological Monographs* 76:415–438.

How transient patches affect population dynamics: the case of hypoxia and blue crabs

Appendices

Authors: Craig A. Aumann[1], Lisa A. Eby[2] and William F. Fagan[1]

Affiliation:
1 Department of Biology, University of Maryland, College Park MD
2 Wildlife Biology Program, University of Montana, Missoula MT

Address correspondence to:
Craig Aumann
Department of Biological Sciences
University of Alberta
Edmonton, AB Canada T6G 2E9
Email: caumann@ualberta.ca
Phone: (780)-492-1289

February 12, 2006

Contents

List of Figures

List of Tables

A Model Development

A.1 Overview of Model Operation

The overall model consists of four main components: 1) environmental variables including salinity, temperature, depth and dissolved oxygen; 2) clams; 3) background prey; and 4) individual crabs. The environmental variables, clams and background prey are all modeled at the scale of individual fine-level triangles, crabs are modeled as individuals and move from triangle to triangle. While the first three model components are updated every 24 hours, individual crabs are updated on average once per hour and even more frequently if crabs interact. Since environmental variables alter habitat variables (clams and background prey), and since all of these are relevant to crab response in the estuary - environmental, habitat, and crab density all vary spatially and temporally.

To represent the spatial variation in the environmental and habitat variables, the overall model domain is discretized into small triangles (Appendices A.2 & A.3). The clam and background prey models operate within the environmental conditions of each of these triangles (Appendix A.4) while individual crabs respond autonomously to the above conditions (Appendix A.5). This appendix focuses on providing and justifying the particular implementation assumptions made. The model is implemented using the object-oriented language C++. All parameter values (and associated references used to justify them) are summarized in Table C.1.

A.2 Discretization of Estuary to Represent Environment, Habitat and Facilitate Crab Movement

Given a closed boundary specification of the Neuse, the estuary is discretized into a series of triangles by applying an external mesh generation program (**NETGEN** written by Joachim Schoeberl available at `http://www.hpfem.jku.at/netgen/`). The initial set of coarse triangles is read into the model and refined (Bänsch, 1991) to create a series of nested conforming triangles at different levels (Fig A.1). For our purposes, the advantages of this approach are that it allows representation of more complex domains than is possible with rectangular basis elements, the nested conforming triangulation facilitates the crab movement algorithm (Appendix A.5.4) by enabling fast determination of which fine-level triangle a crab is on, and finally it allows a discrete representation of the continuous environmental variables. If required, this nested triangulation could also enable multigrid methods to be used to numerically solve more detailed partial differential equation models (e.g., Braess, 1997) of the environmental variables.

The coarsest discretization in the nested triangulation is constructed to contain the fewest possible triangles while still adequately representing the estuary. The nested triangulation used consists of four refinement levels representing 89, 218, 498 and 1079 triangles with each triangle having an average unscaled area (Appendix A.6) of $\approx 2.5\times10^6$, 1.0×10^6, 4.5×10^5, 2.1×10^5 m^2, respectively. The degree of refinement is chosen based on the degree of spatial resolution desired for environment variables, clam, and crab densities.

A.3 Generating the Environment Variables

The depth of the Neuse estuary was obtained from a bathymetric map (NOAA, Map 11552) at a resolution of 500 m × 500 m. These depths are interpolated to the nodes on the finest level triangulation as shown in Fig A.1. Depth, $D(x, y)$ (m), is the only environment variable that does not vary temporally. The variables temperature, bottom salinity and DO all vary spatially and temporally. The actual mechanisms causing variations in temperature, salinity and DO are not explicitly modeled. Instead, the modeling goal is to create environment variables which are realistic inputs for the model and, particularly in the case of DO, which can be altered. Temperature, salinity and DO have both deterministic, spatial and temporally varying random components. Representing these variables spatially is done using a discrete representation over the estuary (Appendix A.2). The random component (Appendix A.3.1) is created by pre-generating Gaussian random fields, $X(x, y, t)$, (Ripley, 1987) with mean 0, variance 1 and a particular spatial and temporal correlation structure which are then transformed to create the temperature (Appendix A.3.2) and salinity (Appendix A.3.3) variables and the disturbance regime altering bottom water dissolved oxygen (DO) (Appendix A.3.4).

A.3.1 Random Field Generation

The entire 2D model estuary is enclosed in a rectangle that is discretized into a total of N_x and N_y points in the x and y directions, while the number of points used over the time interval (March 16th to November 14th) is N_t. This leads to a series of rectangles in space and time. Gaussian random fields are generated over this rectangular grid using a FFT algorithm (Dietrich & Newsam, 1993) with filter:

$$\eta(x, y, t) = \xi(x, \sigma_x) \otimes \xi(y, \sigma_y) \otimes \xi(t, \sigma_t) \tag{A.1}$$

where

$$\xi(x, \sigma) = \frac{\exp\left(-\frac{x^2}{2\sigma^2}\right)}{\pi^{1/4}\sigma^{1/2}}. \tag{A.2}$$

The correlation between locations are governed by the parameters σ_x, σ_y, and σ_t. Points separated by distances of more $\approx 3\sigma$ are not very correlated. The number of discretization points (N_x, N_y and N_t) are chosen so that $\sigma_i/\triangle_i > 2$ for $i = x, y, t$ where $\triangle_i$ is the constant distance between discretization points (Dietrich & Newsam, 1993). The random fields are generated independently each year for the 245 days between March 16 and November 14th. No randomness is present in these environment variables for the remaining time period (November 15th to March 15) that the model runs over. Because the temperature in the estuary is low during this period, a crab's respiration and growth rates will also be low and the lack of spatial heterogeneity in environmental variables will not homogenize the crab population. Finally, the values of the generated random field are interpolated from the rectangular grid onto the finest triangulation of the estuary and exported to a file. As the crab model runs, the appropriate values are read in every 24 hours. Pre-generating these variables lessens the computational burden.

A.3.2 Temperature

Bottom water temperatures in the Neuse range between 4 and 32° C (Borsuk et al., 2001b; Selberg et al., 2001). The temperature field consists of deterministic and random components and is given by:

$$T(t, d_s)_{\text{final}} = T_{\text{mean}}(t) + T_{\text{depth}}(t) + 1/2 \left(1 + \sqrt{1 - d_s}\right) X \tag{A.3}$$

The first part of the temperature field is deterministic and was obtained by fitting time-series data of bottom water temperature from a single location in the Neuse (LT11 near the bend in Fig A.2). These data were fit to a sinusoidal function where time, t, is in hours:

$$T_{\text{mean}}(t) = 18.3 + 10 \sin\left(\frac{2\pi}{365 * 24}(t - 3020)\right). \tag{A.4}$$

The second term in Eqn (A.3) alters T_{mean} depending on the depth $D(x, y)$ at a given location (x, y) and the season:

$$T_{\text{depth}}(t) = -2\left(1 - \exp\left(-\frac{D^2}{8}\right)\right) * \sin\left(\frac{2\pi}{365 * 24}(t - 3020)\right), \tag{A.5}$$

causing deeper areas to be slightly (up to 2°C) warmer in winter and colder in summer (the reverse for shallower areas) to reflect estuarine patterns (Fig A.3).

The Gaussian random field, X, in Eqn (A.3) is generated with $\sigma_{x,T}$, $\sigma_{y,T}$, and $\sigma_{t,T}$ set to 1000 (m), 800 (m) and 48 (hrs) respectively based on the data presented in Luettich Jr. et al. (1999) and Selberg et al. (2001). The degree of variation in the final field is assumed to decrease toward the eastern boundary of the estuary. Let $d_s = d(x, y)/d_{\text{max}}$ be the proportional horizontal distance from the western most boundary of the estuary and d_{max} (m) the maximum horizontal length of the estuary. See the online appendices for movies and Appendix B.2 for further summary of this and the other environment variables.

A.3.3 Bottom Water Salinity

Summertime salinity values generally range between 0.8 to ≈ 18 practical salinity units (psu) and the estuary is less saline in the spring and becomes more saline as the summer progresses (Luettich Jr. et al., 1999; Borsuk et al., 2001b). Bottom salinity, S_{bot} (psu), depends on depth, average temperature and the distance toward the eastern-most boundary of the estuary. Let $\zeta = \sin\left(\frac{2\pi}{365*24}(t - 3020)\right)$ (from Eqn A.4) and let X denote the Gaussian random field (Appendix A.3.1) generated with $\sigma_{x,S}$, $\sigma_{y,S}$, and $\sigma_{t,S}$ set to 1000 (m), 800 (m) and 48 (hrs). The maximum salinity in the deepest parts of the estuary is given by:

$$S(t)_{\text{deep}} = \begin{cases} 8\sqrt{d_s} + 2\sqrt{d_s}(\sin(X) + 1) + 5(1 + \sqrt{d_s})\,\zeta & : \zeta > 0 \\ 8\sqrt{d_s} + 2\sqrt{d_s}(\sin(X) + 1) & : \zeta \leq 0. \end{cases} \tag{A.6}$$

The first two terms term causes salinity to increase toward the mouth of the estuary, while if $\zeta > 0$ (which occurs between May 6 to Nov 4) a seasonal component is also added. Depth is accounted for by scaling $S(t)_{\text{deep}}$:

$$S(t)_{\text{bot}} = S(t)_{\text{deep}} \left(1 - \frac{\exp\left(-D^2/2.25\right)}{2}\right). \tag{A.7}$$

Thus, shallower parts of the estuary are always less saline than deeper parts.

A.3.4 Bottom Water Dissolved Oxygen

The Neuse is characterized as an intermittently-mixed estuary with wind being the primary mechanism controlling vertical mixing (Luettich Jr. et al., 1999; Borsuk et al., 2001b) temporarily dissipating bottom water hypoxia. Hypoxia is typically defined as dissolved oxygen concentrations (DO) ranging from 0.2 to 2 mg/L with anoxic conditions occurring below 0.2 mg/L. Over an entire year, DO in the Neuse ranges from 0.1 to 10.6 mg/L with hypoxic conditions developing intermittently during summer, lasting from a few days to weeks and varying intra and inter seasonally (Selberg et al., 2001). Empirically, the duration of continuous hypoxia at a given location is about 9 days in the deep parts of the estuary which experience multiple hypoxic episodes throughout the summer. The primary mechanisms causing hypoxia at any location in the estuary is oxygen usage by the biomass and sediments (which is temperature dependent) while the primary mechanisms dissipating hypoxia are oxygen diffusion from the surface waters (which is also a temperature dependent process) and random wind events that mix the oxygen rich surface waters with the oxygen depleted bottom waters.

The model for DO (mg/L) results from greatly simplifying a more complex model (Mauersberger, 1983) obtained using the principle of mass conservation:

$$\frac{\partial DO}{\partial t} + \triangledown(DO\,\mathbf{v}) + \mathrm{div}(\mathcal{J}(DO)) = DO_{\text{source}} - DO_{\text{sink}} \tag{A.8}$$

which captures the important mechanisms of advection, dispersion, sources and sinks. Advection is the processes whereby DO is carried along by a current, $\mathbf{v}$, and is represented by the second term on the LHS. The dispersion term, $\mathcal{J}(DO)$ (m/hr), represents the effective diffusion consisting of molecular diffusion, turbulent "eddy diffusivity" and other types of random mixing processes. DO_{source} (mg.L^{-1}.hr^{-1}) represents sources of oxygen into the system (re-aeration from the surface and random wind-mixing events) and DO_{sink} (mg.L^{-1}.hr^{-1}) sinks due to biological and chemical oxygen demand.

Because the Neuse has a very long residence time (Luettich Jr. et al., 1999; Kim, 1990), the advection term, $\mathbf{v}$, is considered insignificant. Under calm conditions that favor the formation of hypoxia, $\mathcal{J}$ is dominated by molecular diffusion which is small (Hyer et al., 1971) and thus will be considered insignificant. The overall sink term is split into two components: oxygen demand from sediments and demand from clam and background biomass. Similarly, the source term is split into a component dealing with re-aeration from the surface and a second component, Z, dealing with random mixing events (i.e., wind) and is used to control the shape, duration and extent of hypoxia in the model estuary. This yields:

$$\frac{\Delta DO}{\Delta t} = DO_{\text{source}} + Z - DO_{\text{sink, biomass}} - DO_{\text{sink, sediment}} \tag{A.9}$$

where $\Delta t = 24$ hours is the update time for all environmental variables. DO_{source} is given by an equation governing re-aeration from the surface (mg.L^{-1}.hr^{-1}) (Chapra, 1997; Schnoor, 1996, Sec 6.3):

$$DO_{\text{source}} = -K_v(DO - DO_u) \tag{A.10}$$

where DO_u (mg/L) is the concentration of oxygen in the upper water column at saturation. This is given by (Hyer et al., 1971, Eqn 12)

$$DO_u = 13.686 - 0.3466T + 0.0044972T^2 \tag{A.11}$$

where an upper water salinity of 10 psu has been assumed and T (Eqn A.3) is the temperature (°C). K_v (1/hr) is given by an equation similar to the O'Connor-Dobbins equation (Schnoor, 1996, Sec 6.3)

$$K_v = k_v \frac{\sqrt{U}}{D^{3/2}} \theta_v^{T-20} \tag{A.12}$$

and gives the dependence of re-aeration on temperature, T. k_v=0.003 (m/hr$^{1/2}$) is a constant (Borsuk et al., 2001b; Schnoor, 1996, Table 6.3), U is the mean tidal velocity taken to be 100 m/hr (Luettich Jr. et al., 1999), D (m) is the depth of the estuary, $\theta_v = 1.0$ (Borsuk et al., 2001b, Table 1).

Random mixing events, Z (mg.L^{-1}.hr^{-1}) in Eqn A.9, are modeled by transforming a Gaussian random field. The Gaussian field used to generate bottom salinity, X, is used (Appendix A.3.3), after it is transformed by:

$$Z = \begin{cases} 0 & \text{if } \sin(X) \leq 0 \\ DO_u \sin(X) & \text{otherwise.} \end{cases} \tag{A.13}$$

The rate at which oxygen is used depends on the total clam and background biomass, B_{total} (g/m^2) present on a triangle and the oxygen usage by the sediments. Oxygen utilization by crabs is ignored since crabs are mobile and crab biomass density per m^2 is much less than the combined clam and background biomass density. It is assumed that clam and background biomass can be combined into one term. The rate of oxygen usage (mg.L^{-1}.hr^{-1}) by the biomass on a triangle is similar to Hummel (1985a):

$$DO_{\text{sink, biomass}} = 0.167\, r_{\text{c,max}} \frac{B_{\text{total}}\, g(DO)}{D} f \tag{A.14}$$

where $r_{\text{c,max}}$ (1/hr) (Eqn A.17) is the clam's maximum rate of respiration, 0.167 converts the final rate of respiration to mg.L^{-1}.hr^{-1}, D is the average depth of the triangle, $g(DO)$ decreases linearly with DO for DO $\leq$ 4 mg/L (Eqn A.19) since clams (and it is assumed the background biomass) decrease their respiration rate under low oxygen conditions, and $f = f_{\text{c}}(T; \beta_{\text{c,resp}} = 0.17, T_{\text{c,max resp}} = 33, T_{\text{c,opt resp}} = 20)$ (Eqn A.18) alters the respiration rate of the biomass with temperature.

The oxygen used by the sediments (mg.L^{-1}.hr^{-1}) on the triangle is given by:

$$DO_{\text{sink, sediment}} = K_d\, \theta_d^{T-20}\, DO. \tag{A.15}$$

$K_d = 0.00575$ (1/hr) (Borsuk et al., 2001b, Table 1) is the sediment oxygen demand and $\theta_d = 1.13$ (Borsuk et al., 2001b, Table 1) controls how this rate changes with temperature.

For a triangle at a depth of 5 m, a DO of 4 (mg/L) and temperatures of 20, 25 and 30°C sediment oxygen demand is $\approx$ 0.023, 0.053, 0.078 (mg.L^{-1}.hr^{-1}), respectively and if the density of biomass on the triangle is 800 g/m^2, its oxygen demand is $\approx$ 0.009, 0.007 and

0.002 (mg.L^{-1}.hr^{-1}) respectively, since the biomass uses less oxygen at higher temperatures. The rate of re-aeration of the bottom waters depends on depth (Eqns A.10 & A.12) with deeper waters taking longer to re-aerate than shallower. Following mixing, deeper waters take longer to become hypoxic because more oxygen is stored above them. Finally, in Eqn (A.9), we also add the constraints that DO ≥ 0 and DO $\leq DO_u$.

A.4 Models for Clams and Background Prey

Adult clam densities typically range from 0-465 clam/m^2 in the middle Patuxent Estuary (McErlean, 1964). Most clams ($> 73\%$) occur in the upper 5 cm of sediment (< 1.0 cm in length), however the greatest fraction of biomass is composed of a few relatively large (> 1.0 cm length) clams at depths of 10 to 30 cm. In the Chesapeake, *Mya arenaria* accounted for 75.8% of the standing crop in sand and *Macoma* for 85.2% in mud.

To simplify model complexity, we only model a single bivalve (*Macoma balthica*, which we refer to as simply "clams"). In part, this simplification is forced by the lack of detailed life history information about *Macoma mitchelli* (but see Waller (1996)) and other benthic species inhabiting the Neuse. Clams and background prey are modeled spatially at the scale of the finest level triangles used to discretize the estuary (Appendix A.2). This enables hypoxia and crab predation to produce patches of clams and background prey as shown in the movies (See the online appendices). Clam and background prey density are assumed to be homogeneous across each fine-level triangle (Fig A.1).

A.4.1 Clam Growth Dynamics

Adult clams are generally less than 2.5 cm wide (McErlean, 1964), although a few may reach 3.0 cm (Bachelet, 1980). In northern climates, clams can live as long as 35 years (Bachelet, 1980), while 6-10 years is common in more southern climates (Gilbert, 1973). Clam growth is most rapid between April and June (1.9-3.7 mm/month) (Holland et al., 1987), slows in July and August and continues to decrease throughout the fall/winter. The variability in clam growth rates depends on temperature and possibly salinity resulting in southern clams growing faster than those further north. For Rand Harbor, Massachusetts, clams grew ≈ 1.0 and 0.7 cm in the first two years, respectively, before growth slowed considerably (Gilbert, 1973). A similar growth pattern has been observed in other locations (Bachelet, 1980; Commito, 1982). At temperate latitudes, the mass of bivalve molluscs generally declines during winter, declining more during warmer than colder winters (Honkoop & Beukema, 1997). Females reproduce when they are greater than 1 cm, or approximately 2.9 yrs for clams in northern climates like Maine (Commito, 1982) and at a younger age in warmer climates.

Our clam growth model closely follows the bivalve model proposed by Solidoro et al. (2000). We assume that clams on each triangle grow according to the same model with differences in growth rate occurring between triangles due to spatial differences in temperature and dissolved oxygen. Possible salinity effects are ignored (Holland et al., 1987). Because anthropogenic loading should increase algae, the primary food of clams (Hummel, 1985b), we assume that clam growth is not limited by food availability (Holland et al., 1980). Clam wet weight, $w_{\mathrm{c,w}}$ (g), is related to shell length, L_{c} (cm), by the allometric model

$$w_{\mathrm{c,w}} = \alpha_{\mathrm{c}} L_{\mathrm{c}}^{\beta_{\mathrm{c}}}, \tag{A.16}$$

where $\alpha_{\mathrm{c}} = 0.1$ g.cm$^{-\beta_{\mathrm{c}}}$ and $\beta_{\mathrm{c}} = 3.0$ (Gilbert, 1973; Bachelet, 1980, Table 2). The maximum size of clams in the Neuse is ≈ 2.5 cm (Bachelet, 1980, Table 7).

Clam growth rate is proportional to the difference in the grams of energy available for feeding and the energy used for respiration (Solidoro et al., 2000, Eqn 1):

$$\frac{\Delta w_{\mathrm{c,w}}}{\Delta t} = g(DO)\left(G_{\mathrm{c,max}}\, f_{c,G}\, w_{\mathrm{c,w}}^{2/3} - r_{\mathrm{c,max}}\, f_{c,r}\, w_{\mathrm{c,w}}\right). \tag{A.17}$$

The temperature and DO values used are constant over Δt and the values used are those from the start of the time interval. $f_{c,G} = f_{\mathrm{c}}(T; \beta_{\mathrm{c,grow}} = 0.2, T_{\mathrm{c,max\ grow}} = 31, T_{\mathrm{c,opt\ grow}} = 22)$ and $f_{c,r} = f_{\mathrm{c}}(T; \beta_{\mathrm{c,resp}} = 0.17, T_{\mathrm{c,max\ resp}} = 33, T_{\mathrm{c,opt\ resp}} = 20)$ are given by Eqn (A.18) and $g(DO)$ by Eqn (A.19). $f_{\mathrm{c}}(T; \cdot)$ is maximum at the optimal temperature and alters clam intake and respiration with bottom water temperature. The rate of clam growth at a given temperature and mass is shown in Fig A.4. f_{c} is given by:

$$f_{\mathrm{c}}(T; \beta, T_{\mathrm{max}}, T_{\mathrm{opt}}) = \left(\frac{T_{\mathrm{max}} - T}{T_{\mathrm{max}} - T_{\mathrm{opt}}}\right)^{\beta(T_{\mathrm{max}} - T_{\mathrm{opt}})} \exp\left(\beta(T - T_{\mathrm{max}})\right) \tag{A.18}$$

which is taken from Solidoro et al. (2000) and is similar in shape to that found by McMahon & Wilson (1981, Fig. 2).

Bivalves either conform to or regulate their rate of oxygen consumption independent of oxygen concentrations (Wang & Widdows, 1993). In *Macoma*, oxygen consumption decreased with decreasing DO concentration (McMahon & Wilson, 1981, Fig 5) and based on these results, we assume that this decrease in oxygen consumption represents an overall decrease in growth rate in Eqn (A.17) according to:

$$g(DO) = \begin{cases} 1 & \text{if DO} > 4 \text{ mg/l} \\ DO/4 & 0 \le \text{DO} \le 4. \end{cases} \tag{A.19}$$

Thus, $g(DO)$ decreases linearly with DO for DO ≤ 4 mg/L.

The wet weight of the clams in each of the 8 year classes for spring and fall recruitment on each triangle in the estuary are updated according to Eqn (A.17) every 24 hours. The maximum rate of respiration, $r_{\mathrm{c,max}}$=0.00034 (1/hour), is based on McMahon & Wilson (1981) and Hummel (1985a, Table 1). In Eqn (A.17), as a clam's mass increases its respiratory demands increase faster than its rate of food intake making it impossible for a clam to grow beyond a given mass. This fact was used to establish $G_{\mathrm{c,max}}$ at 0.00034 (g$^{1/3}$/hr).

A.4.2 Clam Mortality

Clams experience mortality due to temperature extremes, other causes not directly modeled, hypoxia, and crab predation. This section focuses on the first three while crab predation is discussed in Appendix A.5.6. Mortality due to the first three causes is updated every 24 hours (along with all the environmental variables) while the effects of crab predation on the number of clams in each age class are applied as the crabs forage. The cumulative proportion of clams dieing from the first three causes over Δt is the sum of the probabilities resulting from Eqns (A.20) and (A.21).

Mortality caused by temperature extremes and other causes (which in the parameterization below includes predation by fishes and other non-crab estuarine organisms) are modeled according to an exponential probability distribution (van der Meer et al., 2001) with hazard rate:

$$\lambda(T) = \begin{cases} 8\lambda_{\text{Base}} & \text{if clam} < 1 \text{ year} \\ \lambda_{\text{Base}} & \text{if clam} \geq 1 \text{ year} \end{cases} + \begin{cases} \lambda_{T_{\text{c,min resp}}} & \text{if } T < T_{\text{c,min resp}} = \text{-5 °C} \\ \lambda_{T_{\text{c,max resp}}} & \text{if } T > T_{\text{c,max resp}} = 33 \text{ °C} \\ 0 & \text{otherwise.} \end{cases} \tag{A.20}$$

$\lambda_{\text{Base}} = 1.2 \times 10^{-5}$ corresponding to 90% annual survivorship after the first year. Commito (1982) found a 75% annual survivorship under predation. Under no predation, 50% reductions in year 0+ clam densities have been reported (Holland et al., 1980) over 2 months. During winter, we would expect mortality to decrease. The high mortality during this early life stage is reflected in Eqn (A.20) with $8\lambda_{\text{Base}}$ corresponding to 43% annual survivorship.

The thermal tolerance of clams can be as low -5°C (Bourget, 1983) and as high as $\approx$ 35°C (Wilson, 1981). Kennedy & Mihursky (1971) found LC50 values of $\approx$ 33°C and that an increase of 1°C could mean the difference between 0% and 100% mortality. In the above hazard rate, if the temperature is less than $T_{\text{c,min resp}} = -5°$ C clams, survive on average for 2 hours and if temperature is greater than $T_{\text{c,max resp}} = 33$ they survive on average for 4 days.

Hypoxic exposure can also cause clam mortality. In the Calvert Cliffs region of Chesapeake Bay, hypoxia is severe enough that near total faunal depletion (molluscs, annelids, crustacea) occurs during the summer months due to low dissolved oxygen (Holland et al., 1977, 1987). Buzzelli et al. (2002) estimated that in the Neuse the clams *Macoma balthica* and *M. mitchelli*, which are the biomass dominants in the benthic assemblage, declined by 90-100% over 38% of the estuary in 1997. To model clam mortality due to hypoxic exposure, we use the logistic cumulative probability distribution function of times-to-death for a given fixed DO exposure (Borsuk et al., 2002):

$$F(t|DO) = \left(1 + \exp\left(-\frac{(t - (\lambda_a + \lambda_b\, DO))}{\lambda_c}\right)\right)^{-1}. \tag{A.21}$$

The most likely values of the parameters were $\lambda_a = 32.16$ (hr), $\lambda_b = 27.36$ (L.hr.mg^{-1}) and $\lambda_c = 9.6$ (hr), where t is the duration of hypoxia in hours. We are not aware of any studies examining how survival probabilities are altered by temperature or exposure to periodic hypoxic conditions. We assume that no clams will die at DO > 3 mg/L. To compute the number of clams dying under fluctuating DO, each triangle keeps track of the time at which its DO became ≤ 3 mg/L and the continuous contribution to the cumulative hazard is computed according to Borsuk et al. (2002, Eqns 7-13).

A.4.3 Clam Recruitment

Clams are iteroparous broadcast spawners, with males and females releasing gametes synchronously, typically between May to June although fall recruitment can also occur depending on how far south the clams are located (Gilbert, 1978; Harvey & Vincent, 1989). Release of sperm and eggs is likely triggered by temperature cues (7 to 14°C), spring tides and/or quantity of food available (Gilbert, 1978; Harvey & Vincent, 1989). After a few weeks of pelagic life, the larvae (≈ 300 μm) settle from the water column to the sediment (Bouma et al., 2001). Juvenile clams are capable of migration (Beukema & de Vlas, 1989), but this is unlikely to be an important factor in spatially structuring clam distribution.

Using a mesh size of 0.5 mm, Hines & Comtois (1985) reported 34,000 clams per m^2 (119 g/m^2 dry weight, 780 g/m^2 wet weight) in mud and 22,000 clams per m^2 (177 g/m^2 dry weight, 1150 g/m^2 wet weight) in sand at the mouth of the Rhode River, Maryland - similar to the biomass and larval densities reported for sites in Europe (Rosenberg et al., 1992; Bouma et al., 2001). In the Dutch Wadden Sea, recruit to egg ratio for clams varied between 0.0001 to 0.001 (Honkoop et al., 1998). Although 37% of year-to-year variation in recruit densities could be explained by inter-annual variation in winter temperature, only 7% was explained by variation in egg density. Thus, the number of adults and total spawned eggs are poor predictors of subsequent recruit abundance (Honkoop et al., 1998).

The model uses two discrete spawning events which occur on March 31 and August 31. At these times, female clams (assumed to be half of the population) with a shell length greater than 1 cm reproduce (Commito, 1982; Honkoop et al., 1998). The number of eggs produced per female is:

$$\#\ \text{eggs} = 10,000(L_c)^3 \quad \text{if } L_c > 1 \text{ cm.} \tag{A.22}$$

A mature female with a size of 1.5 cm (0.34 g wet wt) will produce approximately 34,000 eggs - within the range reported by Honkoop et al. (1998). The initial wet weight of recruited clams in the model is assumed to be 0.001 g (2.2 mm, Eqn A.16). Recruitment for the entire estuary is the sum of the fecundities for each female. The potential recruitment egg density, ρ_{ce} (#/m^2), is the total number of eggs divided by the area of the estuary and multiplied by a random estuary recruitment factor which is generated uniformly over the range 0.0001 to 0.001 (Honkoop et al., 1998). How the potential recruitment egg density is altered on each triangle by depth, current clam biomass and density is described below.

It is necessary to control the density of clam egg recruitment on each triangle because our model does not include all of the different predators and causes of mortality present in the actual estuary. In summary, fewer spat are assumed to settle on shallower (< 1.5 m deep) than deeper areas and recruitment is limited both by a triangle's current clam biomass density (Eqn A.23) and clam density (Eqn A.24).

Let $\gamma_{cD} = 1 - \exp(-D^2)$ be the depth factor limiting clam recruitment on shallow triangles and let ρ_{cB} (g/m^2) be the grams of clam biomass on the triangle and γ_{cB} the factor limiting clam recruitment on triangles with high clam biomass:

$$\gamma_{cB} = \begin{cases} 1 - \exp\left(-5\left(\frac{\rho_{cB,\text{recruit}} - \rho_{cB}}{\rho_{cB,\text{recruit}}}\right)\right) & \text{if } \rho_{cB} < \rho_{cB,\text{recruit}} \\ 0 & \text{otherwise} \end{cases} \tag{A.23}$$

which places an upper bound on the clam biomass density on each triangle: $\rho_{cB,\text{recruit}} = 850$ g/m^2 (Hines & Comtois, 1985).

Finally, let the density of clams already present on each triangle be given by $\rho_{\text{c,tri}}$ (#/m^2) and let $\rho_{cu} = 1300$ (#/m^2) (Holland et al., 1980) be an upper bound on clam density.

Accounting for depth, current clam biomass and clam density, the number of clams recruited to a triangle as a function of ρ_{ce}, (or potential recruitment egg density), is:

$$\text{recruit } (\#/\text{m}^2) = \begin{cases} \left((\rho_{cu} - \rho_{\text{c,tri}}) + \rho_{cu} \exp\left[- \left(\frac{\rho_{\text{c,tri}} + \rho_{ce}}{\rho_{\text{c,tri}}} \right)^2 \right] \right) \gamma_{cD}\, \gamma_{cB} & \text{if } \rho_{\text{c,tri}} < \rho_{cu} \ \& \ \rho_{cu} < \rho_{ce} \\ \rho_{ce}\, \gamma_{cD}\, \gamma_{cB} & \text{if } \rho_{\text{c,tri}} < \rho_{cu} \ \& \ \rho_{cu} \geq \rho_{ce} \\ \rho_{cu}\, \gamma_{cD}\, \gamma_{cB} \ \exp\left[- \left(\frac{\rho_{\text{c,tri}} + \rho_{ce}}{\rho_{\text{c,tri}}} \right)^2 \right] & \text{if } \rho_{\text{c,tri}} \geq \rho_{cu} \end{cases} \tag{A.24}$$

The first condition governs recruitment when clam density on the triangle, $\rho_{c,tri}$, is less than both the upper bound on clam density, ρ_{cu}, and the potential recruitment egg density, ρ_{ce}. The second condition applies when the potential egg density is less than the upper bound for clam density on a triangle. The last condition applies when the clam density already present on the triangle is greater than the upper bound for clam density on a triangle. In this last case, the density of clams recruited goes to zero rapidly as ρ_{ce} gets larger.

A.4.4 Background Prey

Background prey is a potential food source for crabs that cannot find sufficient clams. Background prey represents an aggregate of different possible crab prey (other benthic species, dead organisms, etc.) and is modeled at the scale of the finest triangles using a modified logistic growth model. Let N denote the number of grams of background biomass on a given triangle with area A (m^2). Changes in N (g) occur according to:

$$\Delta N = \left(1 - \frac{N/A}{K} \right) r_N\, f_b\, \tilde{N} A \Delta t - \alpha N \Delta t - \text{Hypoxia Mortality} - \text{Crab Predation.} \tag{A.25}$$

As with clams, this prey is updated every 24 hours (Δt) and its growth rate depends on temperature and also DO via $f_b = f_{\text{c}}\,(T; \beta_{\text{b,grow}} = 0.2, T_{\text{b,max grow}} = 35, T_{\text{b,opt grow}} = 26)$ (Eqn A.18). $r_N = 0.0008$ (1/hr) and controls the maximum rate of growth. $K = 400$ (g/m^2) is the carrying capacity for background prey on a triangle while $\tilde{N}$ (g/m^2) is the average density of the background prey calculated over the current triangle and its immediate neighbors and enables some spreading of background from patches of high density to low density. Background prey on each triangle experiences mortality due to other predators not included in this model at a rate governed by $\alpha = 0.0002$ (1/hr). Mortality due to hypoxia is calculated using Eqn (A.21) with the same parameters as for clams. The last term in Eqn (A.25) accounts for the number of grams consumed by the crabs over Δt (Appendix A.5.2).

A.5 Individual-Based Crab Model

Blue crabs have a complex life-cycle (Fig A.5) in which zoea must develop in the high salinity ocean waters before returning to the lower salinity waters of an estuary to complete their life-cycle. Growth in crabs can be very rapid, with sexual maturity reached in as short a time as 1 to 1.5 years. Conceptually, individual crab model consist of three primary parts. The first part involves algorithms which control crab movement, updating and crab-crab interactions (Appendices A.5.2-A.5.4). The second part of the model focuses on energy balance which encompasses crab feeding, egestion, metabolism, movement, molting and egg production (Appendices A.5.5-A.5.12). The final facet of the model deals with rules for crab spawning, larval development, recruitment back into the estuary, and sources of crab mortality (Appendices A.5.13-A.5.14).

Each individual crab maintains a set of state variables (energy balance, location, size, rate of movement, etc.) that are controlled and influenced by these sub-models. When a crab is updated (Appendix A.5.2), these state variables values are recomputed. This is accomplished by first determining whether the crab interacted with another crab and was killed or died from other causes (Appendix A.5.3 & A.5.14). If the updated crab did not die during the time period, it is then determined whether the crab has gained enough mass to start molting (Appendix A.5.11) which involves, among other things, altering the crab's metabolic rate until molting finishes. Next the crab's energy balance is computed by determining the amount of food ingested given the way it forages (Appendix A.5.6 & A.5.7), egested (Appendix A.5.8), metabolic costs under its current environmental conditions (Appendix A.5.9), and movement costs (Appendix A.5.10). Based on the crab's overall energy balance, the amount of excess energy is either devoted to growth (or loss if negative) if the crab is not an adult, while excess energy is devoted to reproduction if the crab is a mature female (Appendix A.5.12) and the crab spawns once it has produced sufficient eggs and the environmental conditions are adequate. The larvae develop and are instantiated into the model estuary upon reaching the equivalent of the 7th instar (Appendix A.5.13).

A.5.1 Crab State Variables

Crabs are individual objects that maintain a large number of state variables that change as the crab moves and interacts with its environment. These variables are grouped into classes which include general variables about the crab, reproductive variables, molting variables, metabolism variables, movement variables and life history information. We use *italicized text* when referring to one of these variables within the crab model.

- **General Variables:** *when instantiated (hr), current mass (g), current CW (cm), time when dies due to factors not modeled (hr).*
- **Reproduction Variables:** *sex (male or female), number of eggs currently carrying, maximum number of eggs it can carry before it must spawn, and mating status (not mated, mated, accumulating eggs, preparing to spawn, finished spawning).*
- **Molting Variables:** *instar, molt flag (not molting, preparing to molt, molting), mass next molt triggered, total energy required to molt, total energy expended molting.*
- **Metabolic Variables:** *eating status (not eating, eating or foraging), current stomach fullness (Eqn A.42), stomach volume (cm^3) (Eqn A.37), average quality of food in stomach (Eqn A.43), mass of food feeding on (g), quality of food feeding on.*
- **Movement Variables:** *Current location (x, y), current direction $\theta \in [0, 2\pi)$, rate of movement v (m/hr), time of last update, interaction flag (do nothing, flee, hit estuary*

boundary), pointer to triangle crab was on at the time of last update, the time and the crab which the given crab interacts with next.

A.5.2 Algorithm: Random Crab Updating

Unlike the environmental and habitat components of the model, crabs are updated on average once per hour using an algorithm (described below) that ensures non-sequential updating. Non-sequential updating of individuals in IBMs is essential to prevent spurious patterns and results (Schönfisch & de Roos, 1999). A priority queue (Sedgewick, 1992) plays a central role in our algorithm for scheduling the non-sequential updates by facilitating efficient insertions and removals ordered according to update time. There are two cases: no interaction (usually during winter), and interaction between crabs. Under the no interaction case, when a crab is updated all of the crab's state variables are updated and a new update time is generated according to an exponential distribution with mean 1 hr and crabs cycle through the priority queue in a random order so that after 1 and 3 hours, $\approx 63\%$ and $\approx 95\%$ of the crabs in the estuary will have been updated at least once. Given the rates at which ingestion and egestion occur, the mean update time cannot be increased much beyond 1 hour.

The second case involves crab-crab interactions that occur because a crab encounters conspecifics. Interactions result in even more frequent updates than under no-interactions and also make the above algorithm more complex because increased book-keeping is required to track previously scheduled interactions, enable crabs to be killed and removed from the model estuary without disrupting the inherent ordering of the priority queue.

Algorithmic Details A key assumption made in this algorithm is that over sufficiently small time intervals (minutes) only pairs of crabs interact and display aggression. The algorithm also relies on number of objects and data-structures to function. First, the priority queue stores what we call interaction objects which contain the times at which two crabs are scheduled to interact, pointers or references to the two interacting crabs, and a flag indicating whether or not this interaction should still occur or be canceled. This flag will be discussed further below. In addition to these interaction objects, each crab is stored in an interaction object in which the other crab it interacts with is itself at some future time greater than all other crab-crab interactions it is involved in. The reason for always including such an interaction object is that when a crab is killed, the killed crab is likely involved in other future interactions in the priority queue. As a result, one needs some way to know when a killed crab appears for the last time in the queue, and thus that the computer resources taken up by this crab object can now be freed. By always including a crab's interaction with itself at a time greater than all other interactions, this is easily determined.

Secondly, each individual crab maintains a set of pointers to all the interaction objects that it is potentially involved with. The reason for maintaining this set is because when a crab is updated, all subsequent interactions with other crabs can no longer be assumed to be valid. Thus, this set of pointers is used to change all the flags in the crab's other interaction objects to "cancel". As a result, when these interaction objects reach the front of the priority queue they are simply canceled.

The updating algorithm works as follows:

- Remove interaction object from priority queue. If not flagged as canceled, then proceed to update/interact the crabs. Otherwise, free up the interaction object.

- If the crabs are the same, and if the crab has been flagged as killed or dead then free-up the crab's computer resources. If not flagged as killed or dead, then flag any other interaction objects associated with the crab as "canceled" and delete the crab's set of pointers to the interaction object. Generate a new update time for the crab and determine if and when in the future it interacts with another crab.
  - If it could interact in the future (See Appendix A.5.3), place both crabs in an interaction object and add to the priority queue. Generate another update time for the crab greater than this (or any other) interaction times and update both crabs' interaction pointer sets.
  - If the crab doesn't interact with another crab, place it back in the priority queue and update its interaction pointer set.
- If the crabs are not the same, then let the two crabs interact and set the interaction objects pointed to by both crabs to "canceled" and delete the pointers to these interaction objects.
  - If a crab is killed, flag it as "killed". Update the other crab as described above.
  - For all other interaction outcomes, update both crabs singly as described above.

A.5.3 Algorithm: Interaction and Aggression Outcomes between Crabs

Crabs are highly cannibalistic with large crabs (14-16 cm carapace width) accounting for very high rates of juvenile mortality (40-90% in Chesapeake Hines & Ruiz (1995), >85% in Alabama Spitzer et al. (2003)), with somewhat lower rates farther north (Heck Jr & Coen, 1995). Juvenile crabs in turn prey on smaller crabs and megalopae (Moksnes et al., 1997). A variety of fish and birds are also known to consume blue crab, but in insignificant numbers relative to larger crabs (Hines & Ruiz, 1995; Hines, In Press). Blue crabs engage in aggressive and defensive behaviors to fend off other crabs from food or mates. In tank experiments, such behaviors occurred when two crabs were within 10 cm of each other (Jachowski, 1974). Larger individuals almost always dominate smaller ones (Dittel et al., 1995) and males typically dominate females (Jachowski, 1974). Many invertebrate and vertebrate species respond to threat or injury by autotomizing an appendage. Approximately 25% and 18% of the crabs sampled from Chesapeake Bay in 1986 and 1987, respectively, were missing one or more limbs, usually a cheliped (Smith, 1990). We do not model autotomy because limited levels of autotomy do not appear to alter crab behaviors (Jachowski, 1974) or life history (Smith & Hines, 1991; Smith, 1995).

In the model, we assume that a potential interacting crab can be chosen randomly based on the distance between the crab being updated and neighboring crabs. The set of neighboring crabs is found by aggregating the crabs located on the neighboring fine-level triangles within $d_{\text{max inter}}$=12 m (the *max interaction distance*) of the crab being updated. Crabs that are further than $d_{\text{max inter}}$ apart are assumed not to interact. Each crab stores the last crab it interacted with and this crab is excluded from the set of possible interactions. The distance between each neighboring crab, C, and the crab being updated, $d(C, C_{\text{update}})$, is computed and C is randomly designated as a potential interacting crab if $u < \sqrt{1 - \frac{d(C, C_{\text{update}})}{d_{\text{max inter}}}}$ where

u is a realization of a uniform random variable on $[0, 1]$. The potential interaction time of these two crabs is generated randomly over the smallest time interval until either crab was scheduled to be updated again (Appendix A.5.2). Over all potential interaction times, the pair of potentially interacting crabs with the smallest randomly generated update time is stored in the *priority queue* and in each crab's *interaction set*. As a result, crabs that are closer to each other have a greater chance of interacting.

A scheduled interaction will not occur if one of the crabs is updated because of an earlier scheduled update. If the interaction does occur, possible outcomes include that nothing happens to either crab, one crab is killed and nothing happens to the other, or one crab flees while nothing happens to the other. The actual outcome of the interaction depends on a large number of factors: gut fullness, whether one or both crabs are molting, the sexes of the interacting crabs, whether an interacting female is in her final molt, and the size difference between the crabs. The rules governing the outcome of interactions are not complex, but many different cases must be considered. These interaction rules are given below. A killed crab becomes food for the crab that killed it. If a *feeding* crab *flees*, its *mass of food feeding on* (Appendix A.5.6) is passed off to the attacking crab.

The interaction rules between two crabs, A and B are symmetric and so will only be described relative to Crab A. If the crabs are both molting, nothing happens to either of them. If crab A is molting then:

1. If A molting and male and B is not molting.
   - If the CW width of A is less than 1.4 times the CW of B, A dies and nothing happens to B.
   - If the CW width of A is greater than 1.4 times the CW of B. Nothing happens to A and B flees.
2. A molting, female and not on terminal molt, B is not molting.
   - Exactly as in the two cases in 1).
3. A molting, female and on terminal molt, B is not molting and male.
   - Nothing happens to A or B.
4. A molting, female and on terminal molt, B is not molting and female.
   - Exactly as in the two cases in 1).

Finally, we discuss the case when both crabs are not molting. The idea behind this rule is that crabs only attack other crabs and kill/eat them if their gut is almost empty and there are particular size differences between the two crabs. Let $c = 1 - \frac{V_{\text{stom}} - V_f}{V_{\text{stom}}}$, where V_f is the volume of food in the crab's stomach. c is between zero and 1 and denotes "gut emptiness". Let $\mu = 2$, $\sigma = 0.5$ and u be a realization of standard uniform random variable on $[0, 1]$. Let $\alpha_{\text{inter}} = 0.8$ and

$$\nu = \alpha_{\text{inter}} \exp\left(- \left(\frac{CW_A/CW_B - \mu}{\sigma} \right)^2 \right). \tag{A.26}$$

Then,

- If $c_A > 0.95$, then
  - if $u \leq \nu$, Crab B killed by Crab A.
  - else B flees, nothing happens to A.
- If $c_A \leq 0.95$ then B flees.

For $c_A > 0.95$ for Crab A, if both crabs are the same size, then there is only a small chance that B is killed. When A is twice as big as B, B is killed with probability 0.8, and when A is 3 times as big as B, B has a low probability of being killed since it is less likely that A would bother with such small prey.

A.5.4 Algorithm: Movement

Many crustaceans are tolerant of hypoxic exposure and can regulate oxygen consumption at low oxygen concentrations (McMahon, 2001). However, both the impacts of hypoxia and a crab's reaction to it are stage specific. Adult crabs avoid hypoxic water (Lowery & Tate, 1986; Pihl et al., 1991; Das & Stickle, 1994). Juvenile crabs (20-25 mm carapace width, CW) prefer oxygen concentrations of 4.5 to 5.8 mg/L, but have a reduced ability to detect low oxygen and to find and remain in optimal oxygen conditions (Das & Stickle, 1994). Crabs exposed to normoxia grow faster, have a higher feeding rate, molt more and have a shorter intermolt interval than those exposed to low oxygen conditions (Das & Stickle, 1993). Adult males tend to spend their lives in lower salinity water located in the upper part of the estuary. Prior to mating, females are distributed throughout the estuary, but following mating remain in higher salinity waters near the mouth of the estuary.

Individual crabs in this model are assumed to be moving continuously with a rate, $v \geq 0$ (m/hr), at an angle $\theta \in [0, 2\pi)$ relative to the horizontal axis of the estuary. Movement is determined by the crab's local environment or the finest level triangle containing the crab. Since crabs move continuously in space, determining this fine level triangle is accomplished using the nested conforming triangulation of the estuary (Fig A.1). After determining the coarsest-level triangle containing the crab with an iterative search, one then searches within the triangles that each coarser level triangle is divided into (Fig A.1) and one repeats this process down the nested triangulation levels. The average computational cost of finding the finest-level triangle containing the crab using such an algorithm is much less than if we were to exhaustively search over all finest-level triangles. Such nested triangulations also play a central role in adaptive multigrid algorithms used to numerically solve partial differential equations (e.g., Braess, 1997) and will be useful if more detailed and mathematically complex models (e.g., a partial differential equation model for DO) are ever required.

Unlike the above algorithm, movement of individuals in IBMs is typically done by dividing the spatial domain into small cells with individuals moving between neighboring cells when updated. Such movement algorithms, however, have limitations relative to the one outlined above (Tischendorf, 1997). First, the size of the grid is limited by memory capacity and computational time required to iterate over the entire grid. Second, the fixed spatial structure implies equal resolution for both landscape features and individual movements. Finally, individuals can only move in complete cell units and are limited in movement angles. For such a movement algorithm to work, the distance between cells must be small relative to the individual's actual movement rates and a balance must be found between computational tractability (number of cells that can be stored in memory) and the time resolution of the model. The smaller each individual cell, the smaller the time resolution over which the model can be advanced, but the greater the model's computational demands.

The crab's new direction of movement, θ_{new}, is arrived at by generating a new random change in direction based on a variety of factors, including oxygen concentration, salinity, depth, whether the crab is fleeing as a result of an interaction or if the crab has hit the boundary of the estuary. θ_{new} is kept with $[0, 2\pi)$.

If the crab is not *fleeing* and it has not *hit the estuary boundary*, then θ_{new} is generated randomly based on trying to maximize or minimize environment variables. The environment variables are not all of equal importance in determining a crab's direction of motion. In the list below, conditions further down in the list over-ride earlier ones. Let $u(\psi)$ denote a realization of a uniform random variable generated over the interval $[\psi - \pi/4, \psi + \pi/4]$ and let θ_c denote the current direction of the crab. Let θ_p denote the direction in which the particular environment variable is maximum/minimum (depending on the context) and is computed based on the values of the variable at the three nodes defining the triangle of the crab's current triangle in the case of salinity and depth and using the neighboring set of triangles for DO.

- **Base Case** θ_{new} is uniformly distributed over $[0, 2\pi)$.
- **Salinity** Two salinity thresholds are set based on the mean salinity at $d_s = 0.5$ and $d_s = 0.7$ using Eqn (A.6) (Appendix A.3.3). The first value defines a threshold for the juveniles ($v_{j,sal}$) while the second defines a threshold for sexually mature females ($v_{f,sal}$).
  - **Juvenile** Crab's CW < 5 cm and the salinity of its environment is $> v_{j,sal}$, then $\theta_{\mathrm{new}} = u(\theta_p)$ where θ_p is toward lower salinity water.
  - **Non-Juvenile Male** Crab's CW ≥ 5 cm, male and salinity $> v_{f,sal}$, then $\theta_{\mathrm{new}} = u(\theta_p)$ where θ_p is toward lower salinity water.
  - **Non-Juvenile Female** Crab's CW ≥ 5 cm, female, and salinity $< v_{f,sal}$, then $\theta_{\mathrm{new}} = u(\theta_p)$ where θ_p is toward higher salinity water.
- **Depth**
  - **Juvenile** CW ≤ 5 cm and crab depth ≥ 1.5 m, then $\theta_{\mathrm{new}} = u(\theta_p)$ where θ_p is toward shallower water.
  - **Non-Juvenile** CW > 5 cm and crab depth < 1.5 m, then $\theta_{\mathrm{new}} = u(\theta_p)$ where θ_p is toward deeper water.
- **DO**
  - **Moderate DO** Surrounding DO $\in [3, 4)$ and if a uniform random number generated over the range $[0, 1]$ is $> DO - 3$, then $\theta_{\mathrm{new}} = u(\theta_p)$ towards higher dissolved

oxygen. Thus, the closer the DO is to 3, the greater the chance that the crab's direction of movement will be influenced by its DO environment

  - **Low DO** If crab's DO < 3, then $\theta_{\text{new}} = u(\theta_p)$ towards higher dissolved oxygen.

- **Flee or Hit Estuary Boundary** $\theta_{\text{new}} = \theta_c - \pi + u(\theta_c)$.

A crab's maximum rate of movement, $v_{\max}$, for a 200 g crab is ≈ 720 (m/hr) (Houlihan et al., 1985; Wolcott & Hines, 1990; Clark et al., 1999). In the model, the maximum rate of movement decreases with decreasing crab size. The new rate of crab movement, v (m/hr), depends on whether the crab is eating or molting, the temperature of the crab's environment, whether the crab has lost weight because it is starved, whether it is fleeing from another crab, moving out of an hypoxic patch, or moving away from or into higher or lower salinity water. The factor decrease in the crab's maximum rate of movement, γ_{met}, depends on how the temperature of the crab's environment differs from $T_{\text{met opt}}$ and whether the crab lost weight due to starvation:

$$\gamma_{\text{met}} = \left(\frac{G}{G_{\max}}\right)^2 f \tag{A.27}$$

where G is the current mass of the crab, $G_{\max}$ the maximum mass ever attained and $f = f_{\text{Temp}}(T; Q_{\text{met}} = 2.5, T_{\text{max met}} = 35, T_{\text{opt met}} = 26)$ is given by Eqn (A.39).

Let $\alpha_{\text{max move}} = 300^{1-\beta_{\text{move}}}$ $(\text{g}^{1-\beta_{\text{move}}})$. The actual rate of crab movement, v (m/hr), depends on whether the crab is eating or molting and environmental conditions:

$$v = \begin{cases} 0: & \text{is } \textit{eating} \text{ or } \textit{molting} \\ v_{\max}\,\gamma_{\text{met}}\,\alpha_{\text{max move}}\,z\,G^{\beta_{\text{move}}-1}: & \text{all other cases} \end{cases} \tag{A.28}$$

where z is a realization from Beta$(b_1, b_2 = 20)$ random variable. The value of b_1 is given by:

$$b_1 = \begin{cases} 2 & : \quad \text{If Salinity conditions not met} \\ 4 & : \quad \text{If DO} < 3 \text{ mg/L, or Fleeing} \\ 1 & : \quad \text{Otherwise} \end{cases} \tag{A.29}$$

Fig A.6 shows the density functions for the velocity of crab movement for a 200 g crab when the crab is either fleeing low DO, another crab, trying to find more optimal salinity conditions or simply diffusing about the estuary.

A.5.5 Crab Energy Balance: Overview

The energy balance of crabs, like clams, is modeled using grams wet weight. Let the mass of the crab at time t (including stomach contents, but excluding eggs) be given by G (g) and the amount of food in the stomach of the crab by G_{stom} (g). Mass balance dictates that:

$$\frac{\delta G}{\delta t} = G_{\text{ingest}} - G_{\text{egest}} - G_{(\text{resp + excrete})} - G_{\text{move}} - G_{\text{molt}} - G_{\text{repro}}. \tag{A.30}$$

That is, the rate of change in the mass of a crab over each update time, δt, is governed by the change in the mass of food ingested minus the mass egested, in addition to the mass expended for respiration and excretion, movement, molting, and reproduction. How each of these terms is modeled is described below. The way in which crabs forage and feed (Appendix A.5.6) provides the necessary background information for understanding how ingestion (Appendix A.5.7) and egestion (Appendix A.5.8) are modeled.

A.5.6 Energy Balance: Foraging and Finding Clams or Background Prey

Blue crabs are highly omnivorous, feeding on molluscs (both bivalves and gastropods), fish, small benthic infauna, algae, vascular plants and conspecifics - depending on prey availability (Laughlin, 1982; Eggleston, 1990). A summary of previous diet studies done on the genus *Callinectes* noted that molluscs (primarily soft shelled clams) and crustaceans account for between 41% and 71% of a crab's diet, with molluscs accounting for between 21% and 45% (Mantelatto & Christofoletti, 2001). *Macoma balthica* and *Macoma mitchelli* - the dominant bivalves in the Neuse estuary - thus form the dominant component of a crab's diet (Sullivan & Gaskill, 1998). Crabs, clams and the background prey have different caloric contents: crabs 1000 cal/g wet (Cummins & Wuycheck, 1971), clams 500 cal/g wet (Cummins & Wuycheck, 1971; Szaniawska et al., 1986), background prey assumed to be 350 cal/g wet.

Model crabs feed on clams, background prey or killed crabs (Appendix A.5.3). The average caloric content of the food a crab fed on between updates is found using a feeding algorithm. The crab's *eating status* is determined based on gut fullness, and is set to *foraging* (meaning the crab can move) if it previously was *not eating*, its stomach is $<$ 10% full and it is *not molting*. If a crab killed another crab (Appendix A.5.3), it becomes food for the attacking crab. If this is insufficient to satiate the attacking crab, it attempts to find clams and if insufficient clams are found then low caloric content background prey are fed on. The average caloric content of all food fed on, q_{feed}, is computed as a mass-weighted average. The algorithm for feeding on clams involves the following steps that are discussed in greater detail below: determining the number of clam searches, determining the average probability of finding clams on each search, determining whether an individual crab actually fed, and if so which clams it fed on given the environmental variables and clam size distribution on the triangle.

The number of searches that a crab could undertake over the interval δt since its last update is generated randomly according to a Poisson distribution with mean $6\delta t$. Thus, over a one hour period a foraging crab would on average search for clams six times. Each fine-level triangle stores clams according to increasing size which enables a binary search to be conducted to find the range of clam sizes small enough for the crab to eat. The criteria used is that the shell length of the clam divided by the crab's CW must be less than 1/3. Once the range of forageable clam sizes is known, the probability that a crab finds suitable clams is calculated based on the density of forageable clams $\rho_{\text{c}[,]}$ (#/m^2) according to:

$$\text{Probability finds clams} = 1 - \exp\left(-\left(\rho_{\text{c}[,]}\ \gamma_{\text{c,encounter}}\right)^3\right). \tag{A.31}$$

$\gamma_{\text{c,encounter}} = 1/75$ (m^2/#) governs how the probability of finding a clam decreases as $\rho_{\text{c}[,]}$ decreases. Using the third power means that unless the density of clams is less than $1/\gamma_{\text{c,encounter}}$ (#/m^2), crab's will likely find clams.

An individual crab feeds if a realization from a uniform random variable, u, is less than the probability given by Eqn (A.31). This is used to reflect the reality that as clam density decreases, the probability of an individual crab being successful in finding clams decreases. The purpose of this is to afford clams a low density refuge while distributing found clams to individual crabs. Thus, if a crab feeds the number of clams consumed is just the expected value or the number of times it searched multiplied by the probability of finding clams. This is rounded to the largest integer value and is given by:

$$\text{\# Clams Found} = \lceil (\text{Probability Finds Clams})(\text{\# Searches}) \rceil. \tag{A.32}$$

The number of clams found are selected from the clam age classes on the triangle. The number of clams actually taken will either be the number of clams to be found (Eqn A.32) or less than this number if the *mass of food feeding on* is sufficient to fill the crab's stomach.

Bigger clams are buried deeper in the sediments than smaller clams. Thus, clams from each forageable age class, i, on the triangle are selected randomly using weighting factors which account for the mass, $w_{(c,w)_i}$; number of clams, η_i, in that age class; and DO on the triangle. The weighting factor, ϕ_i, for forageable age class i is given by

$$\phi_i = \eta_i \exp\left(-\gamma_{\text{clam}} w_{(c,w)_i}\right) \tag{A.33}$$

The weighting factors are constructed so that if the number of clams is the same across all age classes, clams of smaller mass will have larger ϕ_i values than larger clams. With $\gamma_{\text{clam}} > 0$ which occurs when DO ≥ 1 mg/L (Eqn A.34), the larger the mass of the clam the smaller will be its weighting factor and likelihood of being preyed upon.

Short low oxygen durations that are not severe enough to produce mortality can cause clams to extend their siphons farther to reach higher oxygen concentrations (Taylor & Eggleston, 2000; Tallqvist, 2001) in principle increasing the possibility of crab predation. This is accounted for using:

$$\gamma_{\text{clam}} = \begin{cases} 0 & \text{if DO} < 1 \\ \gamma_{\text{clam, def}}(1 - \exp(-(DO - 1)) & \text{if DO} \geq 1 \end{cases} \tag{A.34}$$

where $\gamma_{\text{clam, def}}$ is the default factor for a clam's depth refuge. It should be noted that the actual effect of γ_{clam} was subsequently found to be rather small due to crab avoidance of water with DO < 3 mg/L, and thus the actual rate of clam predation was no higher under hypoxic than normoxic conditions, agreeing with empirical findings (Seitz et al., 2003a).

If at the end of the above clam feeding algorithm a crab cannot find sufficient clams to fill its stomach more than 50% full and if the *mass of food feeding on* is less than 50% of the potential grams of food it could feed on over the time interval if food were widely abundant (Eqn A.38), the crab then attempts to feed on background prey.

$$\text{Probability finds background} = 1 - \exp\left(-\left(\gamma_{\text{b,encounter}} \frac{N}{A}\right)^{2.5}\right) \tag{A.35}$$

where $\gamma_{\text{b,encounter}} = 1/100$ ($\text{m}^2/\#$) governs how the probability of finding background prey increases with the density of background prey, N/A (Eqn A.25). If a realization from a uniform random variable, u, is less than the probability it finds background prey, the crab feeds on the background provided the number of grams of background to be consumed is actually present on the triangle.

The mass of background prey a crab finds is exactly the difference between the mass required to fill its stomach 50% full and the *mass of food feeding on* found in the previous part of the feeding algorithm. Thus, if a crab is forced to feed on background prey, its stomach will never be more than 50% full.

A.5.7 Energy Balance: Ingestion

The above feeding algorithm gives the number of grams of food the crab found since it was last updated. However, the *mass of food feeding on* is not the same as the amount of food ingested into a crab's stomach. One reason for this distinction is if the crab is feeding on another crab it may not ingest an entire crab before it is satiated and moves on.

A crab continues to feed until either its stomach becomes full or it consumes all the *mass of food feeding on*. In the first case, *eating status* is set to *not eating*, *mass of food feeding on* is set to zero and any remaining food is returned to the estuary as part of the lower quality background prey on that triangle. In the second case, if the stomach is $<$ 95% full, *eating status* is changed from *eating* to *foraging*, meaning the crab can move around the estuary.

Computing the mass of food ingested requires models of a crab's stomach size and ingestion rate. The allometric relationship used between a crab's CW and mass, G, is (Olmi III & Bishop, 1983; Pullen & Trent, 1970; Cadman & Weinstein, 1985; Newcombe et al., 1949):

$$G = \alpha_{\mathrm{G}} * CW^{\beta_{\mathrm{G}}}. \tag{A.36}$$

Based on these studies, β_{G} is 2.7 and α_{G} is 0.14 g/cm$^{\beta_{\mathrm{G}}}$. A crab's stomach volume, V_{stom} (cm^3), is given by:

$$V_{\mathrm{stom}} = \alpha_{\mathrm{stom}} CW^{\beta_{\mathrm{stom}}}. \tag{A.37}$$

In small, starved crabs, the log of the mass of fresh meat consumed per gram of crab per day decreased with the log of the crab's wet weight with a slope value of $\approx$ -0.55 (Wallace, 1973). If the wet weight of the crab is given by Eqn (A.36) and β_{G} is 2.7, this suggests that β_{stom} is ≈ 2. α_{stom} is set at 0.0265 (cm).

The volume of food in a crab's stomach is given by $V_f = G_{\mathrm{stom}}/\rho_f$ (cm^3) where the density of the food, $\rho_f = 1.5$ (g/cm^3), is assumed constant for all food types. The rate at which food is ingested into the stomach from the *mass of food feeding on* depends on stomach fullness, crab size and temperature:

$$G_{\mathrm{ingest}} = \overbrace{\left(\frac{V_{\mathrm{stom}} - V_f}{V_{\mathrm{stom}}}\right)^{1/4}}^{\text{Stomach Fullness}} \overbrace{\alpha_{\mathrm{ingest}} \mathrm{CW}^{\beta_{\mathrm{ingest}}}}^{\text{Size}} \overbrace{f_{\text{ingest, temp}}}^{\text{Temperature}}. \tag{A.38}$$

The first term in Eqn (A.38) implies that the maximum rate at which food can be ingested will decrease to zero as the crab's stomach becomes full. The second term ensures that larger crabs can ingest food at a greater rate, while the last term describes how the rate of food ingestion is altered by temperature. $f_{\text{ingest, temp}} = f_{\text{Temp}}(T; Q_{\text{ingest}} = 5, T_{\text{max ingest}} = 33, T_{\text{opt ingest}} = 25)$ is based on a model proposed for yellow perch (Kitchell & Stewart, 1977):

$$\begin{aligned} f_{\text{Temp}}(T; Q_m, T_m, T_o) &= \left(\frac{T_m - T}{T_m - T_o}\right)^x \exp\left(x - x\frac{T_m - T}{T_m - T_o}\right) \qquad (A.39) \\ x &= \frac{w^2\left(1 + \sqrt{1 + 40/y}\right)^2}{400} \\ w &= (\log Q_m)(T_m - T_o) \\ y &= (\log Q_m)\,(T_m - T_o - 2). \end{aligned}$$

$T^{\circ}_{\text{max ingest}}$C is the maximum temperature at which crabs feed while $T_{\text{opt ingest}}$ is the temperature giving maximum feeding rate (Eqn A.39, Fig A.7). At 25°C , crabs with a CW of 15 cm (an empty stomach volume of ≈ 6 cm^3) require approximately 15 minutes to fill their stomachs.

A.5.8 Energy Balance: Egestion

There are two components to egestion: egestion from a crab's stomach and egestion from the crab itself. The stomach is emptied due to egestion at a rate which depends on a crab's size and the temperature of its environment:

$$G_{\text{egest stom}} = 1_{[V_f/V_{\text{stom}}>0]}\,\rho_f\,\alpha_{\text{egest}} CW^{\beta_{\text{egest}}} f_{\text{ingest, temp}}. \qquad (A.40)$$

The indicator function $1_{[V_f/V_{\text{stom}}>0]}$ ensures that egestion can only occur if the stomach contains food. α_{egest} and β_{egest} are set at 0.004 (cm$^{3-\beta_{\text{egest}}}$.hr^{-1}) and 2.0, respectively, based roughly on gut evacuation times (McGaw & Reiber, 2000). By specifying the temperature dependence with $f_{\text{ingest,temp}}$, we assume that temperature alters ingestion (Fig A.8) and egestion similarly.

The rate a crab egests mass, G_{egest}, (g/hr) is a fraction of the rate at which food is egested from the crab's stomach:

$$G_{\text{egest}} = (1 - \gamma_{\text{absorption}}\, q_{\text{stom}})\, G_{\text{egest stom}} \qquad (A.41)$$

where q_{stom} is the average food quality of the food in the crab's stomach (Eqn A.43), $\gamma_{\text{absorption}}$ is the absorption coefficient, set to 0.6 (Guerin & Stickle, 1992).

The mass of food in the stomach, G_{stom} (g), following ingestion and egestion is computed as:

$$G_{\text{stom new}} = \begin{cases} G_{\text{stom old}} + (G_{\text{ingest}} - G_{\text{egest stom}})\delta t & : G_{\text{stom old}} + G_{\text{ingest}}\delta t > G_{\text{egest stom}}\delta t \\ 0 & : G_{\text{stom old}} + G_{\text{ingest}}\delta t \le G_{\text{egest stom}}\delta t \\ \rho_f V_{\text{stom}} & : G_{\text{stom old}} + (G_{\text{ingest}} - G_{\text{egest stom}})\delta t > \rho_f V_{\text{stom}} \end{cases} \qquad (A.42)$$

where δt is the size of the time step since the crab was last updated.

If $G_{\text{stom new}} > 0$, the new *stomach food quality*, q_{stom} which is dimensionless and always between 0 and 1, is given by:

$$q_{\text{stom new}} = \frac{q_{\text{stom old}} G_{\text{stom old}} - q_{\text{stom old}} G_{\text{egest stom}}\delta t + q_{\text{feed}} G_{\text{ingest}}\delta t}{G_{\text{stom new}}} \qquad (A.43)$$

where q_{feed} is the food quality of the food the crab is ingesting. If $G_{\text{stom new}} = 0$ then $q_{\text{stom}} = 0$. $q_{\text{stom}} = 1$ if the crab is feeding on crabs. Since the caloric content of clams is 1/2 that of crabs (Appendix A.5.6) the food quality of clams is set at 0.5 and background at 0.35.

A.5.9 Energy Balance: Respiration and Excretion

The costs of respiration (g/hr) depend on a crab's size and the temperature of its environment while excretion costs are modeled as a fixed fraction of respiration costs:

$$G_{(\text{resp + excrete})} = (1.0 + \gamma_{\text{excretion}})\, \alpha_{\text{min met}}\, G^{\beta_{\text{met}}}\, f_{\text{Temp}} \tag{A.44}$$

where $\gamma_{\text{excretion}}$ is set at 0.05 (Guerin & Stickle, 1992, Tables 2 & 3), $\alpha_{\text{min met}} = 0.00166$ ($\text{g}^{1-\beta_{\text{met}}}$/hr) (Houlihan et al., 1985; Booth & McMahon, 1992), and $\beta_{\text{met}} = 2/3$ (Laird & Haefner Jr, 1976; Houlihan et al., 1985) governs how the rate of energy expenditure increases with increasing crab mass, G (g). Metabolic rate has been shown to increase four-fold between ≈ 10 and 33°C (McGaw & Reiber, 2000). The function $f_{\text{Temp}} = f_{\text{Temp}}(T; Q_{\text{met}} = 2.5, T_{\text{max met}} = 35, T_{\text{opt met}} = 26)$ is given by Eqn (A.39). Between 13 and 28 °C , different sized crabs utilize their mass at $\approx 6.6 \times 10^{-5}$ to $\approx 1.26 \times 10^{-3}$ (g wet wt)/(g wet wt hr) (Leffler, 1972; Laird & Haefner Jr, 1976; Crisp, 1984; Booth & McMahon, 1992). See Fig A.9 for plots of the costs of respiration and excretion per g of crab mass as a function of mass and temperature.

A.5.10 Energy Balance: Movement

Houlihan et al. (1985) measured the energetics of swimming for juvenile (≈ 17 g) and medium sized (≈ 42 g) crabs in sea water at 22° C. Base metabolism for these two sizes was $\approx 5.6 \times 10^{-4}$ and 2.8×10^{-4} (g wet wt)/(g wet wt hr). Metabolism increased linearly with increases in swimming speed for both sizes. At 720 m/hr, crabs of both sizes use ≈ 5 times as much energy swimming as they do resting.

In the model, the cost of transport per g of body weight depends on the mass, G (g), of the crab and its speed of movement, v (m/hr) (Eqn A.28):

$$G_{\text{move}} = \alpha_{\text{move}} G^{\beta_{\text{move}}}\, v \tag{A.45}$$

where $\beta_{\text{move}} \approx 1/3$ (Houlihan et al., 1985), and $\alpha_{\text{move}} = 0.00004$ ($\text{g}^{1-\beta_{\text{move}}}.\text{m}^{-1}$). The above equation implies that larger crabs use proportionately less energy for movement than smaller crabs (Fig A.10). Under the above parameter values, the ratio of the crab's maximum rate of mass usage due energy expenditure for movement relative to the crab's maximum metabolic rate at $T_{\text{opt met}} = 26$°C is ≈ 3.5 and the ratio of energy usage for movement plus respiration and excretion to respiration and excretion is ≈ 4.5, agreeing with the results of Booth & McMahon (1992).

A.5.11 Energy Balance: Molting

Molting requires that a crab expend a great deal of energy generating a new exoskeleton - peak energy expenditure occurs immediately after shedding (deFur, 1990) at a rate comparable in magnitude to that of exercising crabs in high salinity water (Booth & McMahon, 1992). Shedding of the old exoskeleton for 10.1 to 12.7 cm CW crabs is done within two to three hours (van Engle, 1958); it takes approximately 9-12 hours for the shell to acquire a papery or leathery texture; and another 12-24 hours for the shell to fully harden (van Engle, 1958; Freeman et al., 1987). During molting, CW increases on average by 15 to 35% over temperatures between 14° to 32° C and salinity of 7.5 to 26 psu (Tagatz, 1968). Crabs molt more frequently at higher temperatures (leading to greater daily rates of CW increase) but the percentage increase in CW per molt is smaller (Leffler, 1972). Crabs 1.3 to 2.5 cm CW molt every 10 to 15 days, while $>$ 10 cm CW crabs molt every 20 to 50 days (van Engle, 1958; Ryer et al., 1990). Molting does not occur during November through April. The average CW of sexually mature female crabs ranges between 7.5 and 20 cm with a mean of 14.4 cm (Fisher, 1999) or $\approx$ 200 g and males are larger than females (e.g., Olmi III & Bishop, 1983).

In the model, molting is triggered when a crab's mass, G, becomes greater than the *mass when molting is triggered* causing *molt flag* to be set to *preparing to molt.* The duration of molting depends on the amount of energy (g) that the crab must expend to molt and the rate at which it can expend this energy. When molting starts, the crab cannot eat (*eating status = not eating*) nor does it move. The total energy a crab must expend to molt depends on its size:

$$G_{\text{total to molt}} = \alpha_{\text{molt}} CW^{\beta_{\text{molt}}}. \tag{A.46}$$

For $\alpha = 0.02$ g/cm$^{\beta_{\text{molt}}}$ with $\beta_{\text{molt}} = 2$, a 15 cm CW crab will use ≈ 4.5 g to molt.

The rate at which the crab molts depends on the crab's metabolic rate which governs the rate of mass use due to energy expenditure during molting, G_{molt} (g/hr):

$$G_{\text{molt}} = \alpha_{\text{max met}}\, G^{\beta_{\text{met}}}\, \exp\left(-\frac{1}{2}\left(\frac{G_{\text{total molted}} - 1/2 G_{\text{total to molt}}}{\sigma_{\text{molt}}\, G_{\text{total to molt}}}\right)^2\right) f_{\text{Temp}}. \tag{A.47}$$

$\alpha_{\text{max met}}$=0.00678 (hr^{-1}.g$^{\beta_{\text{met}}-1}$) (Booth & McMahon, 1992, Table 1) & (Houlihan et al., 1985, Fig 1). Based on the equation, larger crabs expend energy at a faster rate. $G_{\text{total to molt}}$ is given by Eqn (A.46), $G_{\text{total molted}}$ is the number or grams of energy that the crab has already expended molting, $\sigma_{\text{molt}} = 0.25$ governs the rate of mass use from energy expenditure as molting progresses. f_{Temp} is the same as the term in Eqn (A.44) and accounts for a crab's metabolic rate at different temperatures. G_{molt} is shown in Fig A.11 at a temperature of $T_{\text{opt met}} = 26$°C as a function of CW and $G_{\text{total molted}}$. A crab with a 15 cm CW will take $\approx$ 1.25 days to fully molt.

As a crab molts, $G_{\text{total molted}}$ is incremented and the crab stops molting when $G_{\text{total molted}} = G_{\text{total to molt}}$. The *molt flag* is then set to *not molting* and the crab's state variables are updated, including the crab's *current CW*, *mass next molt triggered*, *mating status* and *stomach volume.*

The proportion increase of the crab's CW at molting depends on the temperature of the crab's environment and is based on model proposed by Smith (1997). The further the temperature is away from the crab's optimal metabolic temperature, $T_{\text{opt met}}$, the smaller the average percent increase. The proportion increase in CW ranges from $p_{\text{cw l}} = 0.24$ to $p_{\text{cw u}} = 0.32$. The actual proportion increase is generated randomly. Let u be a realization of a uniform RV on $[0,1]$,

$$\gamma = \begin{cases} \frac{(T-T_{\text{min met}})}{(T_{\text{opt met}}-T_{\text{min met}})} & \text{if } T_{\text{min met}} \leq T \leq T_{\text{opt met}} \\ \frac{(T_{\text{max met}}-T)}{(T_{\text{max met}}-T_{\text{opt met}})} & \text{if } T_{\text{opt met}} < T \leq T_{\text{max met}}, \end{cases} \tag{A.48}$$

and $x = u\gamma$. Let $y = (1 - CW/19)^{0.45}$ if CW $\leq$ 19 cm and 0 otherwise. y is used to decrease the changes in CW per molt as the crab's CW gets closer to 19 cm. The random increase in CW is given by:

$$CW_{\text{new}} = (1 + p_{\text{cw,l}} + (p_{\text{cw,u}} - p_{\text{cw,l}})\, x\, y)\, CW_{\text{old}}. \tag{A.49}$$

where $p_{\text{cw,l}}$ is the lower proportion of CW increase and $p_{\text{cw,u}}$ is the upper proportion increase.

The new *mass when molting triggered* is given by applying Eqn (A.36) to CW_{new} (Eqn A.49) and the crab's new *stomach volume* is given by Eqn (A.37). In the model, male crabs cease molting once they reach the 20th instar. If a crab is female and is reaching its 18th molt, it mates with a male provided a male with an instar greater than 18 is present within 5 times the *maximum interaction distance* (See Appendix A.5.3). If the female mates, its *mating status* is set to *mated*. If a suitable male is not present, the female will not mate, but will attempt to mate again the next time she molts. Following molting, the crab's *eating status* is set to *foraging* and the crab is able to move again.

A.5.12 Energy Balance: Egg Production and Spawning

Crab mating generally occurs from May through October (van Engle, 1958). When a female is approaching sexual maturity, a male crab will carry the female beneath him until she molts and will not cannibalize her when she molts. Following shedding, mating lasts from 5 to 12 hours. Females mate once and store sperm to fertilize all subsequent batches of eggs. Two to nine months may elapse between mating and spawning (van Engle, 1958). If mating occurs in May, the first egg mass may be laid in August. Females that mate in August and September are unlikely to spawn until the following May or June. Females can spawn throughout the entire summer and may spawn more than once. Spawning is rapid and is completed in $\approx$ 2 hours (van Engle, 1958). The number of eggs produced per female ranges from 500,000 to 8,000,000 with bigger females producing more eggs (Prager et al., 1990). It is not known whether bigger females produce higher quality eggs. Spawned eggs are carried on the abdomen of the female for $\approx$ 2 weeks until the larvae emerge. Larval release occurs at least two months after mating, during early May through September (van Engle, 1958). Newly hatched larva are carried out into nearshore ocean waters where they progress through seven or eight zoea stages and are recruited back into an estuary upon reaching the megalops stage (Epifanio, 1995).

In the model, after a female *mates*, it has the capacity to start producing eggs. The *mating status* for the crab is set to *accumulating eggs* and the number of eggs which the female must produce before it spawns is generated (Prager et al., 1990):

$$\text{Number Eggs}/10^6 = -2.248 + 0.377 * CW + e \tag{A.50}$$

where e is distributed as a normal RV with mean 0 and SD = 1.39 and CW is in cm. The number of eggs to be generated is updated each time the crab spawns.

It is assumed that females only generate eggs if their energy balance is positive ($\delta G/\delta t > 0$ in Eqn A.30) and if the crab's mass is greater than 75% of its maximum mass, $G_{\max}$ (g), the crab ever attained. If the crab's mass is below this threshold, all excess energy is put into regaining this lost mass until the crab reaches 75% of $G_{\max}$ at which point the proportion of excess energy put into eggs increases linearly from 0 at 75% to 1 at the $G_{\max}$. This condition ensures that starved reproductive crabs will first regain lost mass before putting energy into reproduction. If a crab's ovaries are full, the crab is unable to spawn and the rate of food ingestion is greater than the crab's energy costs, then the crab's rate of egestion is increased so that $\delta G/\delta t = 0$.

It is assumed that each egg involves a fixed investment of energy. The precise energy content of blue crab eggs is not known. For the crab *Thalamita crenata* (Latreille), the energy content of its eggs are $\approx$ 0.0454 cal/egg (or 0.19 J/egg) (Kannupandi et al., 1999) with a wet weight of $\approx$20.47 μg per egg. Blue crab eggs are $\approx$0.25 mm in diameter (Churchill Jr., 1917-1918). We assume that if a mature female blue crab releases $\approx 2.6 \times 10^6$ eggs (Prager et al., 1990), these eggs would have a wet weight of $\approx$ 53 g and have a total energy content of $\approx$ 118,000 cal (494,000 J). Thus, the number of eggs produced per gram of excess energy is $\approx 22,000$ eggs.

In the model, crabs may produce eggs during the winter and summer. Once the number of eggs produced by the crab reaches the number needed in Eqn (A.50), its *mating status* is changed from *accumulating eggs* to *preparing to spawn* and it no longer accumulates eggs. The crab spawns if the temperature (Eqn A.3) is above $T_{\text{min spawn}} = 19°\text{C}$. If the temperature is above $T_{\text{max spawn}}$ the crab spawns, but all its eggs will suffer mortality in the maturation pot (Appendix A.5.13). Once a crab spawns, its eggs are added to the maturation pot (Appendix A.5.13), the number of eggs that the crab must generate before it can spawn again is generated according to Eqn (A.50) and the *mating status* of the crab is set back to *accumulating eggs.*

A.5.13 Rules: Larval Development and Recruitment

In addition to computing a crab's energy balance, another important component of the model involves development, recruitment and initialization of crabs into the model estuary. Development of spawned crab eggs occurs in the maturation pot object representing the ocean. All eggs released over a single day by all female crabs in the estuary are stored in a single "egg pot". The maturation pot is comprised of a sequential, linked list of pots each containing the number of larvae/juvenile crabs and their collective development stage. Once a day, the larvae/young crabs in this list are updated and growth and mortality applied based on the average temperature for that day. Based on the development information for blue crabs (van Engle, 1958; van den Avyle, 1984; O'Leary Amsler & George, 1984; Etherington & Eggleston, 2000), it is assumed that crabs take anywhere from 80 to 145 days to go from spawned egg to 7th instar - the stage when the crabs are moved from the egg pots and instantiated into the estuary. Crabs are instantiated at the 7th instar to avoid the computational costs of modeling large numbers of juvenile crabs which have very short lifespans.

It is assumed that the rate at which the crabs progress through development depends solely on average temperature. The development rate of larvae/crabs in each egg pot is taken to be linear with mean temperature, T (Eqn A.4), according to $aT + b$ where $a = (1 - \gamma_{\text{maturation}})/(T_{\text{max spawn}} - T_{\text{min spawn}})$ and $b = 1 - aT_{\text{max spawn}}$. $\gamma_{\text{maturation}} = 0.55$ is a constant chosen so that at a temperature of $T_{\text{min spawn}} = 19°\text{C}$, development to 7th instar takes 145 days and at $T_{\text{max spawn}} = 29°\text{C}$ it takes 80 days.

Larvae/crabs in an egg pot die at a constant rate where the proportion surviving after a time interval t is $\exp(-\lambda_{\text{mat}}t)$ and $\lambda_{\text{mat}} = 5 \times 10^{-3}$ (1/hr). Thus, the longer the development the greater the mortality. Over an 80 d development, the proportion of the larvae/crabs surviving is 1×10^{-4} while over 145 d it is only 5.6×10^{-8}. If the mean temperature given by Eqn (A.4) is outside the range $[T_{\text{min spawn}}, T_{\text{max spawn}}]$, all the larvae/crabs in the egg pots die.

The degree to which megalopae return to a particular estuary is unknown and dispersal between estuaries is likely. However, the large distance between major estuaries in the Mid Atlantic Bight and the coherence between spawning and recruitment events suggests that larvae often return to their parent estuary (Garvine et al., 1997). North Atlantic estuaries show constant low levels of daily settlement punctuated by significant, episodic peaks that can account for $> 50\%$ of the annual settlement at a site (van Montfrans et al., 1995). Variables such as wind vectors, radiant energy and surface temperature are thought to be important predictors of recruitment (Tang, 1985; Epifanio, 1995; Rugolo et al., 1998).

Thus, the proportion of 7th instar crabs recruited into the model estuary is generated randomly and is negatively correlated with the current density of crabs in the estuary and positively correlated with the number crabs produced by the egg pots. Let u be a realization of a uniform RV on $[0, 1]$ and let $\vartheta = \text{Crab Density}/\rho_{\text{max}}$ $((\#/\text{m}^2)/(\#/\text{m}^2))$. The maximum density of 7th to 20th instar crabs in the estuary is assumed to be no larger than $\rho_{\text{max}} = 0.4$ $(\#/\text{m}^2)$. The proportion of the 7th instar crabs instantiated from the egg pots for a given day is u^{ϑ}. Thus, if the crab density is less than ρ_{max} $(\#/\ \text{m}^2)$ a larger proportion are instantiated then when the density is greater than ρ_{max}. This reflects the fact that the higher the crab density in the estuary, the smaller the proportion of recruits surviving past the 7th instar.

Instantiated crabs are randomly placed in the estuary. Let u_x and u_y denote realizations from a uniform random variable over $[0, 1]$ and let d_x and d_y denote the horizontal and vertical dimensions of the rectangle containing the part of the estuary being modeled. Under a wind driven mechanism of recruitment, it is likely that higher densities of megalopae and juvenile crabs will be found toward the mouth of the estuary. The initial location of an instantiated crab is given by $(d_x\sqrt{u_x}, d_y u_y)$ provided this location is contained in the estuary.

A crab's sex is specified randomly based on a Bernoulli random variable where the probability of *male* is dependent on the sex ratio (assumed to be 50%). Both initial CW and mass contain a random component. The initial CW of the instantiated 7th instar crab is uniformly distributed over 1.05 to 1.65 cm while the initial mass of the crab, G_{init}, is given by applying Eqn (A.36) to $CW_{\text{init}}/(1+1/2u)$ where u is a realization from a uniform random variable over $[0, 1]$. Thus, the initial mass of the crab is set below the mass at which molting would be triggered. The crab's initial stomach volume is given by Eqn (A.37).

A.5.14 Rules: Sources of Mortality

Mean annual natural mortality rate is ≈ 0.375 (Rugolo et al., 1998; Eggleston, 1998) and only about one out of every million eggs survives to become an adult (van Engle, 1958).

Although crabs can live as long as 8 years, the average age in the Chesapeake population is ≈ 1.5 yrs and $\approx 97\%$ of all individuals are less than 3 yrs of age (Rugolo et al., 1998).

In the model, a crab dies either because of aggression from other crabs, temperature extremes, starvation, a lack of oxygen, or when it reaches its life expectancy. Rules governing crab death as a result of interactions between crabs were discussed in Appendix A.5.3. If the temperature at the crab's location goes below 5°C or above 35°C (the min and max temperatures for the crab's metabolic processes (Tagatz, 1969, Table 1)) the crab dies immediately due to thermal stress. A crab dies of starvation if its mass drops below 40% of its maximum weight, $G_{\max}$. Likewise, a crab dies due to a lack of oxygen if the DO in the environment encountered by the crab is continuously below 1 mg/L for more than 3 days. The criteria for death due to hypoxia are kept simple because in the actual estuary, crabs will likely swim up to the oxygen rich surface waters if the bottom waters become hypoxic (Das & Stickle, 1994). This condition is included as a way to ensure that the crab movement algorithm is sufficient for getting crabs out of hypoxic waters in a timely fashion. Lastly, crabs may die due to other causes not explicitly modeled. The life expectancy of crabs (assuming no predation) is assumed to follow a Beta distribution. The life expectancy of a crab (assuming the do not die from specific model causes) is generated when the crab is first instantiated into the estuary (Appendix A.5.13). Let $X \sim \text{Beta}(m_1 = 3.0, m_2 = 1.5)$ then the *time when dies due to other causes* is given by $Y = 8X$. Thus, we assume crabs don't live beyond 8 years.

A.6 Scaling of the Estuary

In the unscaled model estuary, a density of 0.1 crabs/m^2 represents $\approx 2.2 \times 10^8$ crabs. Although parallel computers make it possible to model this number of crabs, a reduction in the computational demands can be achieved by scaling the estuary. In scaling down the size of the estuary, two things are considered. First, the size of the fine-level triangles (Appendix A.3) must be sufficiently small to provide the degree of spatial resolution required to observe desired changes in the spatial distribution of crabs, clams and background prey. Secondly, the number of crabs in the estuary must be sufficiently large that the probability of a fine-level triangle being unoccupied by chance is small. These two criteria work against each other. On the one hand, increasing the number of fine-level triangles (decreasing their size or area) will lead to greater spatial resolution in clam and background biomass distribution. Alternatively, if the number of crabs in the estuary is kept constant, increasing the number of fine-level triangles will increase the spatial variability in crab density and biomass since there will be a greater chance that each triangle contains none or only a single crab.

The number of refinement levels and average unscaled area of the triangles were listed in Appendix A.3 with the finest level consisting of 1079 triangles. Based on a uniform distribution of crabs over the estuary, > 2000 crabs are required to ensure that the chance of a triangle being empty by chance is less than 20%. The dimensions of the estuary are scaled by a factor of 100 so that the area of the scaled estuary becomes $\approx 22,000$ m^2 and 2000 crabs corresponds to an average crab density of ≈ 0.09 crabs/m^2. Thus, in the scaled estuary each individual crab can be thought of as representing a cohort of similar crabs (say in size and spatial location) in the unscaled estuary. Provided one does not aggregate to the extremes, the behavior of individuals in the scaled estuary will adequately represent the behaviors occurring in the unscaled estuary. Given that the scaled estuary is a miniature model of the unscaled estuary, we also scale down the velocity at which crabs move and the *maximum interaction distance* over which crabs interact. In this way, it is as if the crabs in the scaled estuary are moving about with similar probabilities of encountering each other or the estuary boundary as in the unscaled estuary. However, each crab's energy usage is calculated as if it were moving about at the unscaled rates of movement.

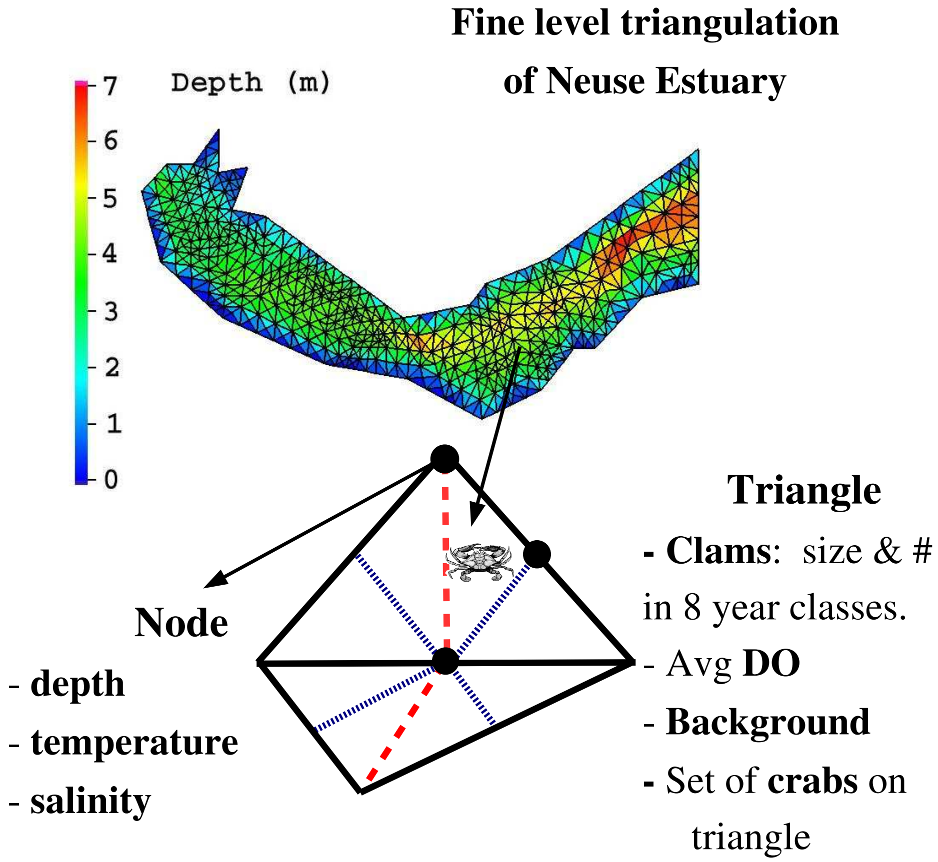

Fig. A.1: Information and variables stored on each fine-level triangle in the model estuary. Node variables defining the triangle store the depth (m), temperature (°C) and bottom water salinity (psu). Each triangle stores the background biomass (g), DO (mg/L) and a set of pointers to the crabs present on it along with the average mass (g) and number of clams in each of 8 year classes. The nested conforming triangulation allows individual crabs to be located within a fine-level triangle by recursively applying a procedure that can determine if a given crab is located within a given triangle or not. The black lines show the coarse triangles, the red lines show the finer triangles these coarse triangles are divided into, and similarly for the blue lines.

Fig. A.2: The Neuse River originates north of Durham, NC has a watershed area of 16,102 km^2 (North Carolina Department of Environment, Health and Natural Resources, 1993) and travels ≈ 320 km through the central Piedmont to the coastal plain. The estuary has a mean width of 6.5 km, a length of 70 km, average depth of 3.5 m and maximum depth of 7 m (Selberg et al., 2001). Like many estuaries on the East Coast of the USA, the Neuse has experienced rapid development in its watershed during the last 50 years and as a result the Neuse receives substantial nutrient loading. These problems are exacerbated by its relatively long flushing time (Luettich Jr. et al., 1999) and low average discharge rates (Kim, 1990). The red box highlights the part of the Neuse focused on in the model.

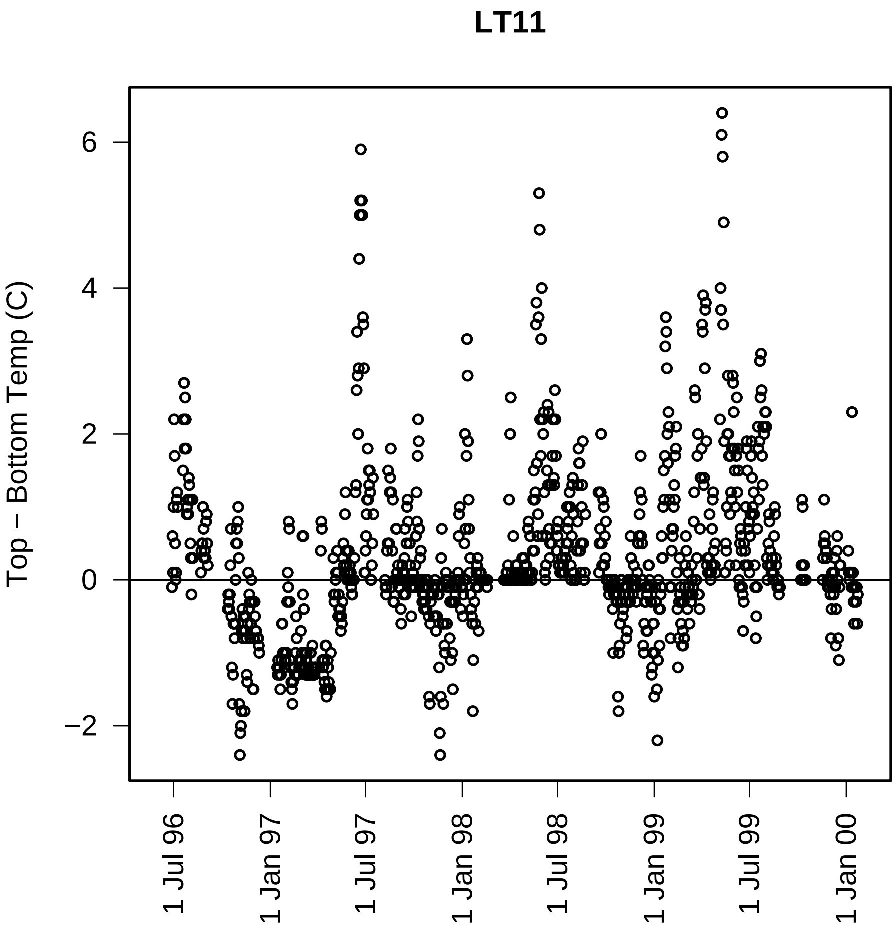

Fig. A.3: Plot of daily differences in top and bottom water temperatures from site LT11 in the Neuse River Estuary. Data from USGS.

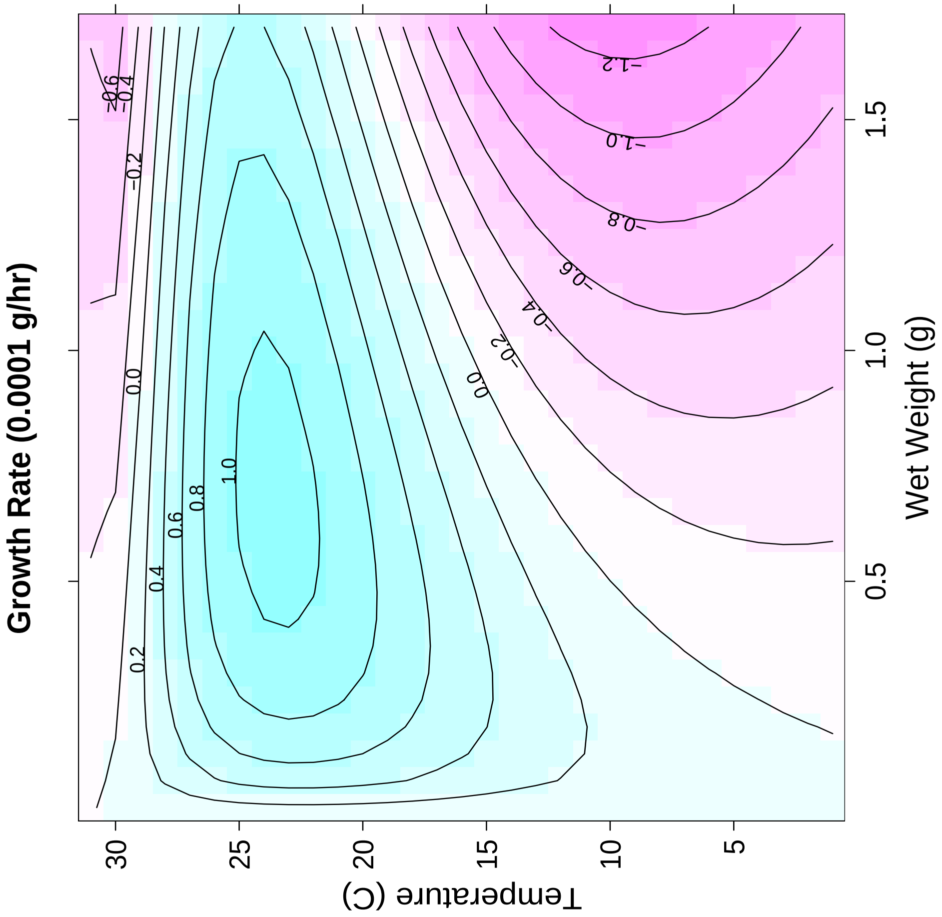

Fig. A.4: Clam growth rate at a given mass and temperature for DO > 4 mg/L.

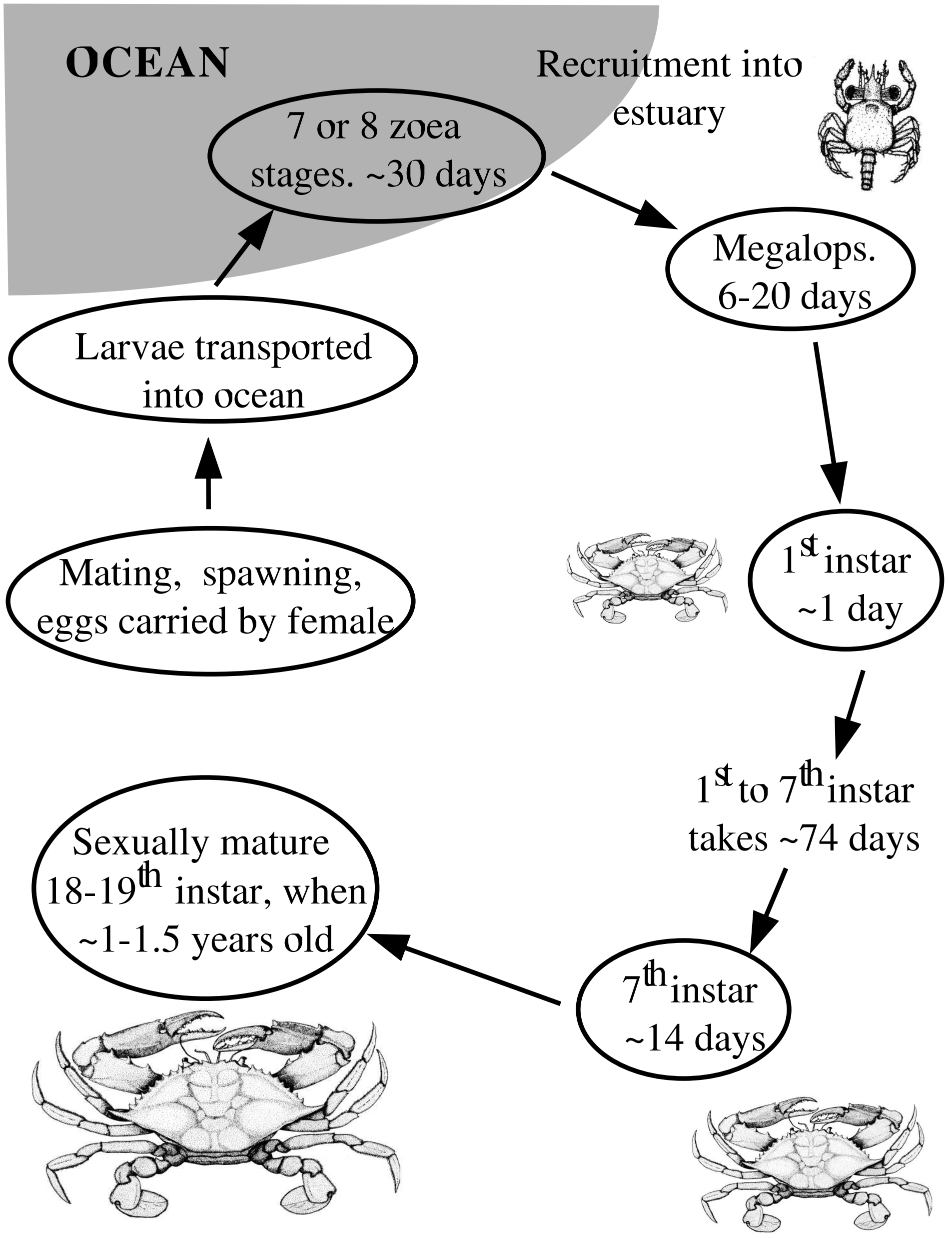

Fig. A.5: The blue crab has a complex life-cycle. The zoea stages are spent in the ocean. Megalops are recruited back into the estuary where crabs spend the rest of their lives. The body plan of an adult crab is evident upon reaching the first instar.

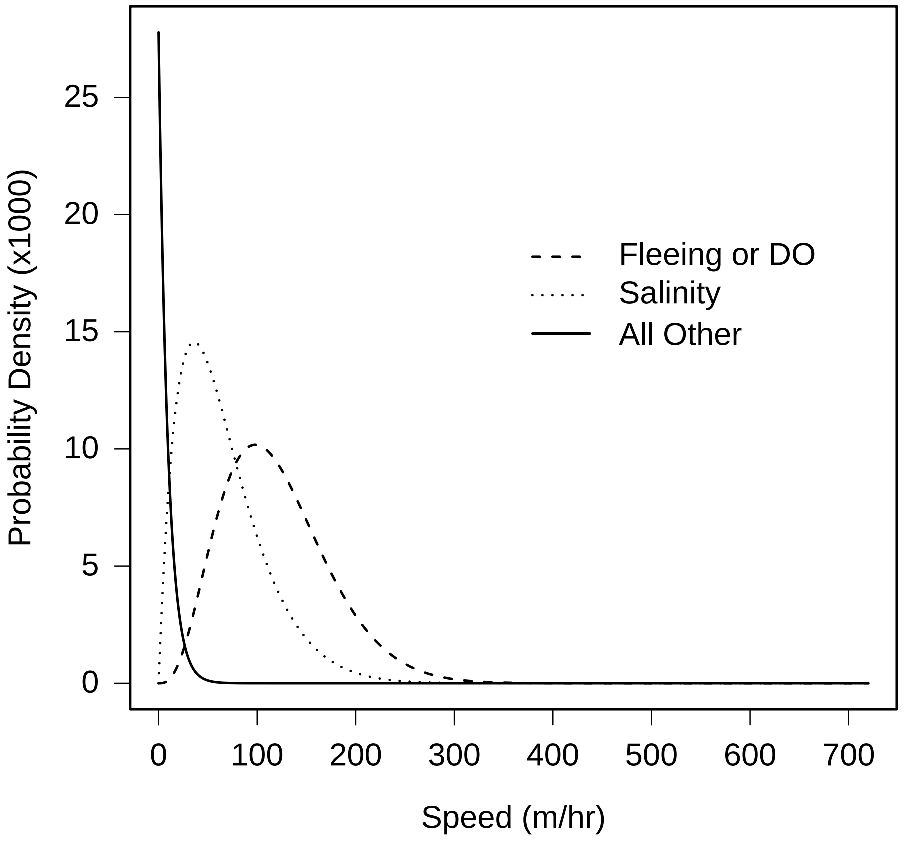

Fig. A.6: Movement distribution for a 200 g crab at a temperature of $T_{\text{opt met}} = 26°\text{C}$ under three scenarios: fleeing another crab or moving away from low DO, optimizing salinity, or all other cases (Eqn A.28).

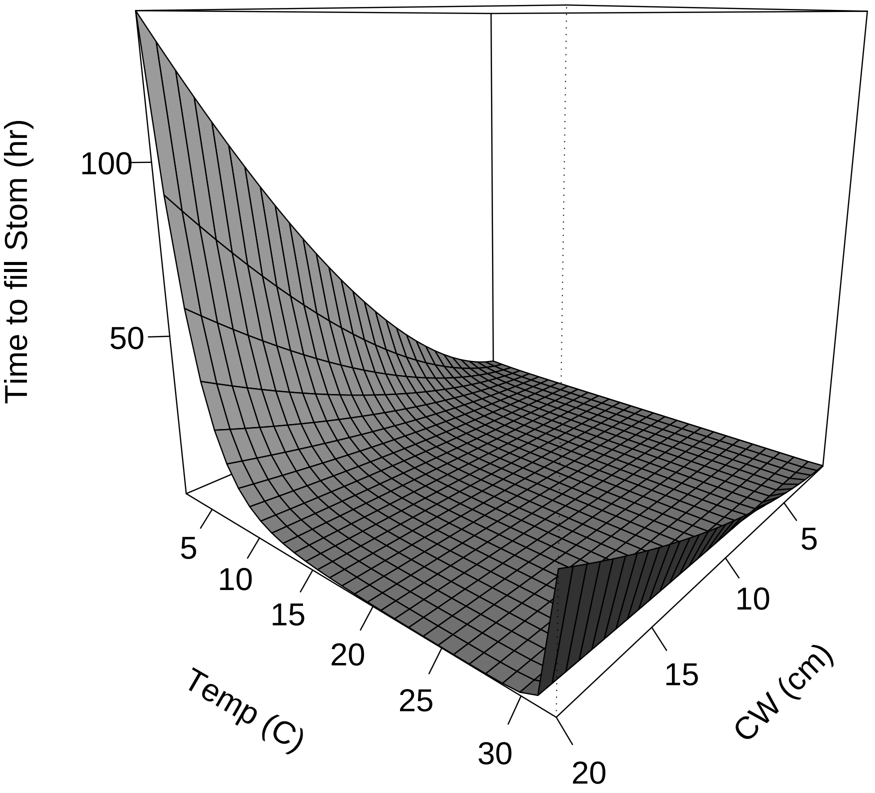

Fig. A.7: Time for a completely empty crab stomach to fill due to ingestion as a function of CW (cm) and temperature (°C). The time is computed based on Eqns (A.37) and (A.38). Larger crabs have to spend more time feeding than smaller crabs.

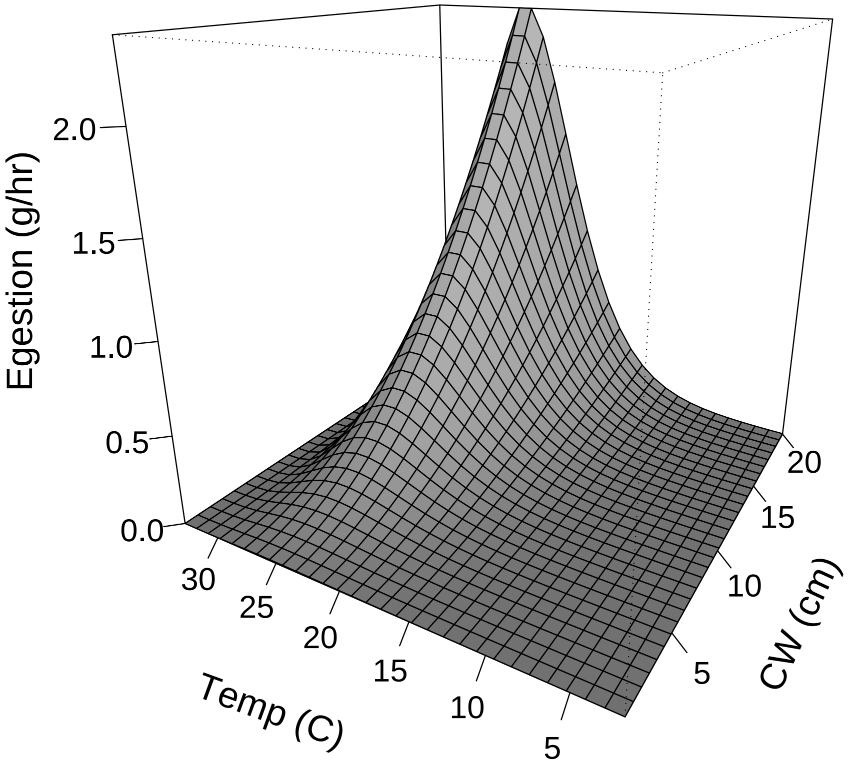

Fig. A.8: Rate of egestion (g/hr) from the stomach of different sized crabs vs temperature (Eqn A.40).

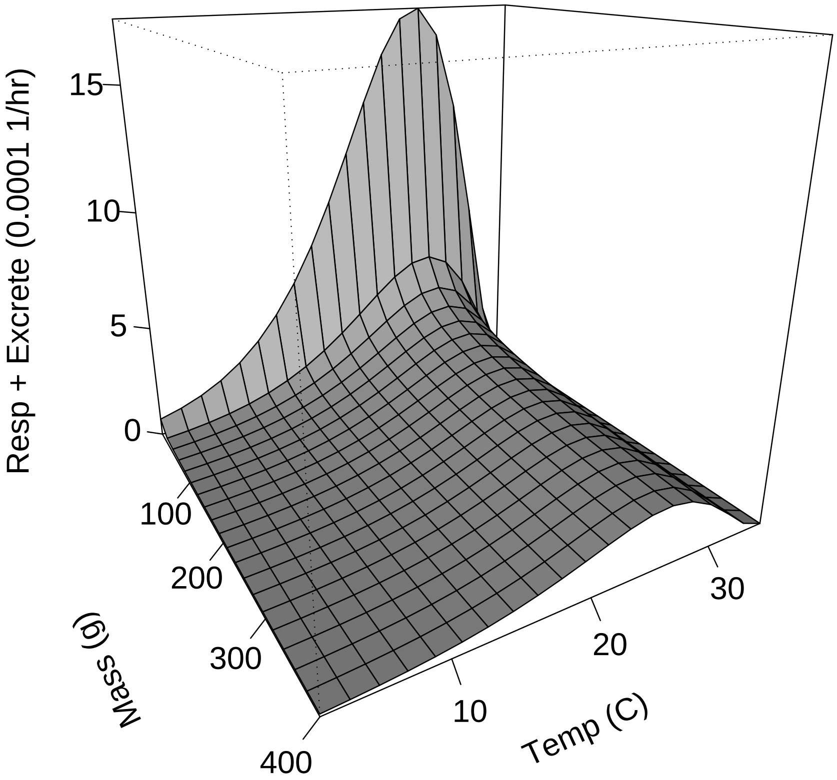

Fig. A.9: Energy usage per g of crab mass (10^{-4} g.g^{-1}.hr^{-1}) for respiration and excretion for different sizes and temperatures.

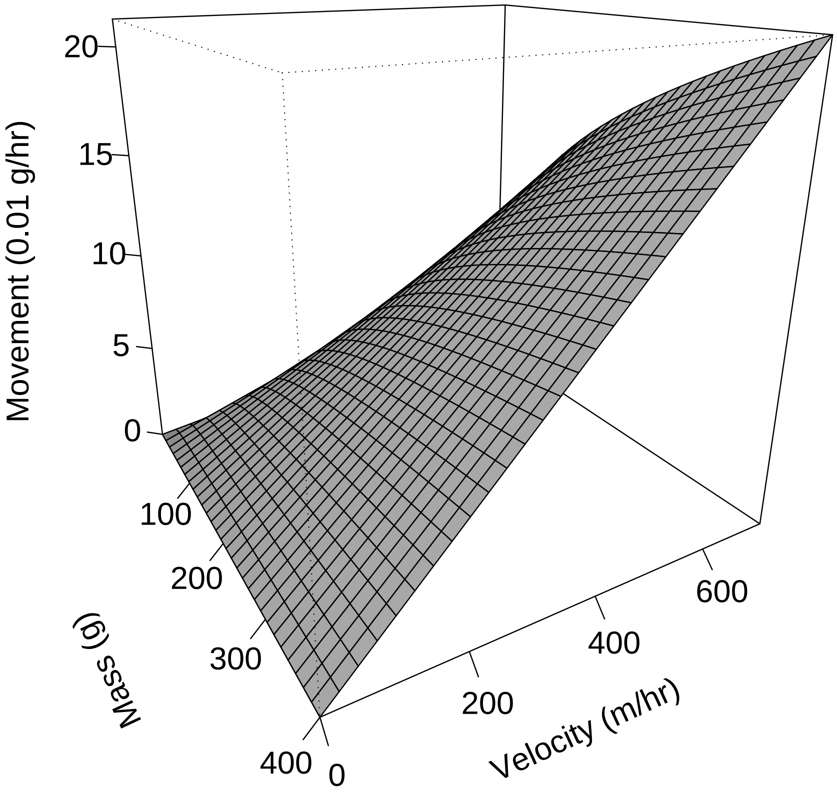

Fig. A.10: Energy usage in grams per mass of crab (0.01 g/hr) for crabs moving at different velocities (Eqn A.45).

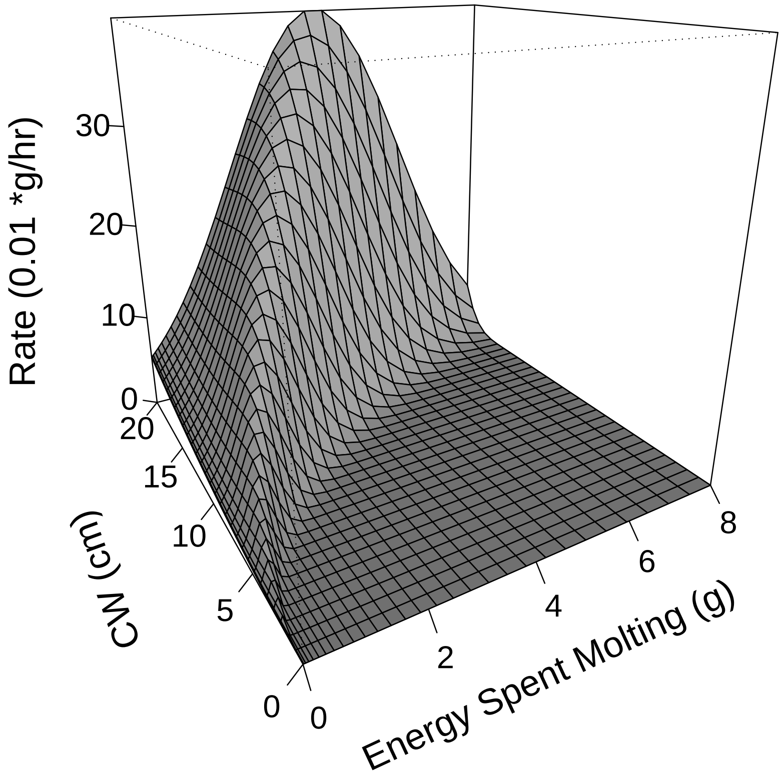

Fig. A.11: Rate (0.01 g/hr) at which crabs expend energy as they molt as a function of the total energy required to molt (g) and the CW (cm) of the crab. Temperature is at $T_{\text{opt met}} = 26^\circ$ C.

B Model Assessment

We begin by briefly summarizing the methodology used for model assessment (Appendix B.1). Most of the assessment results presented are focused at the middle level of the overall model hierarchy (Fig 1). Since the environmental variables are central to all other model behavior, we start by assessing the environmental variables (Appendix B.2), then clams and background prey (Appendix B.3) and finally how crabs respond to both environmental conditions and prey availability (Appendix B.4). Finally, we consider how crab population dynamics were affected by altering the clam model in ways suggested during review of this manuscript (Appendix B.5).

Model parameter values used throughout this section (unless otherwise noted) are summarized in Table C.1. Assessment results presented are conducted using a maximum hypoxic extent of 45% and a Short hypoxic duration as described in the Methods. All statistical analysis was done with the statistical package R (Ihaka & Gentleman, 1996) (`http://cran.r-project.org`). The MPG movies were created using the programs GMV by Frank Ortega at Los Alamos National Laboratory (`http://www-xdiv.lanl.gov/XCM/gmv/GMVHome.html`) and Mplayer (`http://www.mplayerhq.hu/`). All simulations were run on a Dell Precision 340 Workstation with a 1.7 Ghz processor running Red Hat Linux 9.0. Each 40 year simulation took $\approx$ 24-40 hours.

B.1 Overview of Assessment Methodology

Models are connected to our theoretical understanding of system operation via a set of morphisms or relationships that link the model and represented system (Zeigler et al., 2000). The aim of model assessment is to establish the strength of these morphisms via a process of model verification, validation and a more general critique of the entire modeling process. This section highlights a portion of the assessment carried out on this model.

The first step in the model assessment process we refer to as *model verification* and is concerned with ensuring that the model has been built correctly relative to the model design document (Balci, 1994; Zeigler et al., 2000). The primary aim of this step is to eliminate implementation errors. This involves checking the actual implementation against the design specification, a summary of which is given in Appendix A. In addition, the model was constructed to facilitate highly detailed tracking of individuals. Each time the crab is updated (on average once per hour) all of a crab's state variables and its local environmental variables can be exported. This information enabled us to analyze whether or not the rules specified in the model design were actually occurring in the situations they were supposed to. Both these steps formed the basis of the initial model assessment, but we have included little of this low level assessment here because it was solely concerned with ensuring that the model accurately represents the model design document (Appendix A). Thus, each low-level component of the model has been assessed and is functioning as described.

The next step in assessment is *model validation* and is concerned with building the right model. This involves substantiating that the behavior of the model is "close enough" to the behavior of the source system so that it is impossible to distinguish the behavior of the systems in the applicable experimental frames (Balci, 1994; Zeigler et al., 2000). An *experimental frame* is a specification of the conditions under which both the source system and model are to be observed or experimented with. Specifying the experimental frames ensures a fair comparison between the output of the two systems. Examples of experimental frames are given below. The concept of an experimental frame extends to situations where little empirical information is available. The literature can be consulted for further guidance (e.g., Balci, 1994; Kleijnen, 1995; Rykiel Jr., 1996; Balci, 1997; Yilmaz & Balci, 1997; Zeigler et al., 2000). At this stage, assessment of emergent properties such as the time it takes a crab to reach sexual maturity are of particular importance since such times are not hard-wired into the model, but emerge based on the interaction of a crab's development and energy balance rules in conjunction with the environment it encounters.

The larger aim in documenting the model implementation and assessment is to facilitate the larger process of model critique. This allows others (especially those not involved in developing the model) to understand the modeling decisions made and their implications.

B.2 Environmental Variables

The environmental variables are central to the population dynamics of all organisms in this model. For example, temperature alters metabolism and growth rates, salinity and DO play important roles in spatially structuring the crab population while hypoxia causes clam and background prey mortality. The environment variables were assessed without crabs present in the estuary. Most of the assessment criteria used are highly qualitative in nature because data sets which would enable more quantitative criteria to be used were not available. Relevant MPG movies are provided in the online appendices.

B.2.1 Temperature and Salinity

Behaviors that should be displayed by the model with respect to temperature include (Luettich Jr. et al., 1999; Selberg et al., 2001): that the magnitude of variation in temperature across the estuary at any given time should range between 1-5°C ; smaller variation in temperature over the estuary during winter; inversion of temperature with season (deeper areas cooler in summer and warmer in winter than shallow areas). For salinity, the behaviors desired included (Luettich Jr. et al., 1999; Selberg et al., 2001): seasonal component to variation; wide variation in salinity across the estuary (generally within 0 to 5 psu at the west end of the estuary and between 5 to 21 psu on the east end); and salinity should generally be greater in deeper waters. The only experimental conditions shared by the model and estuary are the time course over which the above criteria are to hold.

With respect to the qualitative behaviors desired, temperature and salinity in the model agreed with those reported for the Neuse. Both the Neuse and the model (see movies) display temperature inversions with season. Deeper areas were $\approx$ 3°C cooler in summer and $\approx$ 3°C warmer in winter than shallow areas. Maximum temperature was approximately 30°C with the largest variation ($\approx$ 5°C) in September. Over a year, salinity was generally 0 to 5 psu at the west end of the estuary and between 5 to 21 psu on the east end. Over the estuary, salinity ranged between 0 to $\approx$ 10 psu during winter and between $\approx$ 5 to $\approx$ 20 psu during summer with deeper areas always more saline than shallower.

B.2.2 DO

In the model, the concentration of DO is generated based on temperature, depth and salinity (Appendix A.3.4). Thus, we need to ensure that under similar temperature and salinity inputs to both systems, and with similar quantities of clam and background prey biomass, DO behaves similarly in the two systems. Validation of the DO, clam and background prey models was done iteratively since these models depend on each other. The particular behaviors focused on for validation include: seasonal component to DO variation; lower DOs in summer ranging from 0 to 8 and 0 to 12 (mg/L) in the winter; percent of estuary experiencing hypoxia at any time should be within $\approx 0\%$ to $\approx 50\%$ during July through October, depending on the year; the length of time areas of moderate depth remain continuously hypoxic should last anywhere from one day to two weeks.

The duration, extent and seasonal fluctuations in hypoxia agreed with those reported for the Neuse (Selberg et al., 2001, Table 3) (Buzzelli et al., 2002, Table 2). Shallow portions of the model estuary (depth < 2 m) were never hypoxic and the median time the deepest areas remained hypoxic was ≈ 9 days (Fig B.1). The empirically measured durations of hypoxia at stations LT9 and LT11 in the Neuse over years 1989 to 1999 are given in Fig B.2. However, the large amount of missing data in these time series biases the durations, making them appear shorter than they actually are. We conclude that the ranges displayed in both Figs B.1 and B.2 are in general agreement. The maximum percentage of the estuary hypoxic at any given time during summer ranged between 40% and 60% (Fig B.3), agreeing with empirical measurements. For the model estuary, DO in summer ranged from 0 to 8 and 0 to 12 (mg/L) in the winter and mirrored changes in temperature.

B.3 Clams and Background Prey

The models of clam and background prey were initially assessed without any crabs present in the model estuary so the dynamics could be observed without the confounding influence of crab predation. These biotic components have more facets that must be assessed than the environmental variables (e.g., rates of growth, density and biomass). In the experimental frames used, the environmental variables must satisfy the experimental frames specified above. This ensures that the inputs to the two systems are similar.

B.3.1 Clams - Growth, Spawning, Density and Biomass

The rate at which clams grow is dependent on the environmental variables the clam experiences (Appendix A.4.1). In the model, clams spawn at fixed times provided they are larger than a minimum size threshold. Thus, overall clam recruitment is indirectly dependent on the environmental variables. The particular criteria used included the daily rate of clam growth; time to reach sexual maturity; average clam density in the estuary; average clam biomass and the spatial variation in clam biomass.

Simulations indicated that 20 years was an adequate burn-in time for clams and background prey (Fig B.4). Distinct annual cycles were present even without predation. Clam growth rates agreed with those reported by Nichols & Thompson (1982) and are generally < 0.002 (g/day) over the first 2 years following recruitment (Fig B.5) and showed no difference with depth. Further, model clams lost mass during winter, agreeing with Honkoop

& Beukema (1997). Clams spawned at the beginning of May reached sexual maturity (a size ≥ 1 cm) anywhere from November to the following March while clams spawned at the beginning of September reached maturity between February and March of the next year. This is in agreement with studies done in Chesapeake Bay (Holland et al., 1987, Fig 7).

There was no difference in the model's spring and fall recruitment densities. For the model, average clam density without predation was 1000 clams/m^2. Given the differences in the mesh-sizes of screens used to filter sediments for clams, comparing this density to empirical findings is difficult. Under predation, Seitz et al. (2003b) reported densities up to 500 per m^2 using a 1 mm mesh, while in upper Chesapeake bay, recruitment densities of $>$ 0.5 mm clams at particular sampling times were as high as 30,000 per m^2 in the absence of predation and 6500 per m^2 with predation (Holland et al., 1980).

In the model average clam biomass was ≈ 750 (g/m^2) and average background biomass was 240 (g/m^2). In Chesapeake Bay under predation, total biomass in mud and sand habitats was 119 and 177 (g dry/m^2) or ≈ 720 and 1100 (g wet/m^2) with clams accounting for at least 76% of the total biomass (Hines & Comtois, 1985) (i.e., clams ≈ 547 or 840 (g wet/m^2) and background biomass ≈ 173 & 254 (g wet/m^2)). The highest clam biomass density in the model occurred at depths between 1 and 4 m, with clam biomass decreasing rapidly for depths less than 1 m or greater than 4 m. The lower biomass in the deeper parts of the estuary is caused by clam die-off due to hypoxia and not limitations in recruitment since maximum clam density in the model occurred in the deepest parts of the estuary. The movies indicate that clam and background biomass decreased towards the mouth of the estuary where hypoxia was generally more severe.

B.3.2 Sensitivity of Clam and Background Prey to Hypoxia under Predation

Both clams and background experienced mortality due to hypoxia according to Eqn (A.21) in which the most influential parameters are λ_b and λ_c. Because this equation was determined using expert elicitation techniques, it seemed necessary to determine the extent to which both prey could be affected by a misspecification of these parameters. Thus, separate simulations were run in which each parameter was varied based on these parameter's posterior distributions (Borsuk et al., 2002): $\lambda_b = 1.24$, 1.14, 1.04 (L.hr.mg^{-1}) and $\lambda_c = 0.425$, 0.4, 0.375 (hr). The results indicated that decreasing λ_b from the default value decreased clam biomass by ≈ 40 (g/m^2) and decreased background prey by ≈ 20 (g/m^2). Decreasing λ_c had a smaller, but similar effects to λ_b. It is concluded that over the range of uncertainty in these parameters, the effects of a misspecification would be relatively minor on the overall levels of prey biomass.

B.4 Crabs

Having established that the environment variables, clams and background prey are behaving reasonably relative to what is known empirically, we now examine particular life-history attributes of the model crabs. As before, the particular assessment conditions established above become the experimental conditions that must be met between the two systems so that the behaviors of crabs can be meaningfully compared.

Blue crabs have even more behaviors that need to be assessed than clams or the background prey. The groups of criteria focused on include individual crab growth and molting; spawning and recruitment; movement, density and spatial distribution; rates of aggression and starvation; and finally the sensitivity of rates of aggression to the particular model assumptions made. All of these behaviors depend on the way in which a crab interacts and responds to its local environmental variables, prey, and other crabs. For example, properties like the time to reach sexual maturity are the result of the interaction between algorithms governing crab feeding, metabolism, molting, and movement - all of which are affected by the crab's environment.

B.4.1 Growth & Molting

Except for the qualitative description in Appendix A.5.11 (which we will not repeat here) few quantitative criteria can be specified to assess the model's rates of crab growth. Crab growth is the result of interaction between rules governing crab feeding, energy balance, metabolism, molting and environmental conditions. 7th instar model crabs were typically instantiated in early August and reached instar 12 by early September, although many did not reach this stage till the following April. A model crab's energetics were such that 1 gram of food intake (with an average food quality of ≈ 400 cal/g) was required for a crab to gain ≈ 0.15 g of mass. Molting generally ceased during November to April, although a few of the larger crabs (instar 19 & 20) molted during March (Fig B.6). Cessation of molting during winter results in two distinct relationships between CW versus intermolt period (Fig B.7), and age versus CW (Fig B.8). A 15 instar crab added ≈ 15 g between molts, while an 18th instar crab added ≈ 50 g. A 10 cm CW crab added between 1.5 and 1.8 cm to its CW when it molted. The empirical cumulative distribution function for the time to sexual maturity indicated it took approximately 1 year for a crab to go from the 7th to 18th instar (Fig C.5). Crabs reaching the 18th instar did so over a range of months (typically June to October, Fig B.9). At temperatures between 22 and 30 °C molting took between 24 and 44 hours (Fig B.10). Crabs generally spent $\ll 5$ hours continuously foraging during summer and went through long periods (> 50 hours) during October through April when they did not eat because of their low metabolic rate.

B.4.2 Spawning and Recruitment

The criteria used to assess spawning and recruitment behaviors is summarized in Appendices A.5.12 & A.5.13 and is not repeated here. Crab spawning behavior emerges because individual crabs were able to reach sexual maturity under the rules governing their growth and development under the particular environmental conditions encountered.

Most spawning by model crabs occurred in late April and tapered off towards September. No spawning occurred between October and early April. Crabs spawned at similar rates over temperatures of 20 and 28°C . The vast majority of spawning occurred close to the mouth of the model estuary. Crabs spawned in water whose salinity ranged from ≈ 10 to 20 psu. The average inter-spawning period was 2.1 months and almost all mature female crabs spawned between 1 and 2 times per year. The earliest times crabs were instantiated into the model estuary was mid July and the latest was the end of September.

B.4.3 Movement

The detailed paths of a male and female model crab over their entire lifetime show that they move in a quasi-continuous manner (Fig B.11). As a result of the dependence of movement rate on temperature, the median and range of velocities of crab movement increased during summer, peaking in July at a median of $\approx$ 15 m/hr - within the range reported in Appendix A.5.4. Crabs also responded quickly to changes in the location of low DO (Fig B.12) resulting in high crab densities on the edges of hypoxic regions and almost no crab biomass in low DO areas.

B.4.4 Density and Distribution

The density of crabs in the Rhode River, a sub-estuary of Chesapeake Bay, ranged between ≈ 0.01 and 0.1 crabs per m^2 during 1991 to 1993, but has been as high as 0.5 crabs per m^2 on other years (Clark et al., 1999). The vast majority of such crabs are juveniles (Orth & van Montfrans, 1987). In the model, the maximum density ($\#/m^2$) of 7 to 12 instar crabs varied between ≈ 0.3 to 0.25 and decreased to ≈ 0 shortly before 7th instar crabs were instantiated into the estuary (Fig B.13). The average density of 13 to 17 instar crabs in the model was ≈ 0.027 while 18+ density was ≈ 0.017 ($\#/m^2$). Recent studies also suggest that areas of low salinity and unstructured habitats can contain high densities of juvenile crabs (Lipcius et al., 2005; Posey et al., 2005).

Crab density and distribution in the model emerges primarily based on crab cannibalism and avoidance of hypoxia. The distribution of different instar crabs across the estuary (Fig B.14) showed that the movement algorithm (Appendix A.5.4) did result in a higher density of mature female crabs towards the mouth of the estuary (Appendix A.5.4). Small crabs were located in shallower waters on the edge of the estuary while large crabs were located at intermediate depths during summer and moved back into the deeper parts of the estuary during fall.

B.4.5 Mortality - Aggression & Starvation

Crab survival and population-level rates of mortality are primarily dependent on algorithms governing crab aggression and movement in response to environmental conditions. The average mortality rate ($\#.m^{-2}.hr^{-1}$) over the entire estuary due to aggression by other crabs was $\approx$ 0 between December to April, but increased with crab density both at the fine-level triangle and estuary scales during other times. 92.7% of all mortality was caused by aggression and only 6.9% was caused by starvation of small instar crabs that occurred primarily during February-March and August-September. The relative size of the attacking crab was always larger than the size of the killed crab, on average at least 1.7 times or more larger (Fig B.15). Other minor causes of death were asphyxiation due to a crab's inability to escape low DO waters (Appendix A.5.14) and crab's reaching their life expectancy.

B.4.6 Sensitivity of Crab-Crab Interactions

Appendix A.5.3 describes how interactions between crabs are modeled. Given that little is known empirically about crab-crab interactions, a sensitivity analysis was conducted to determine the importance of the assumptions made. One part of the algorithm utilizes a *maximum interaction distance* (Appendix A.5.3). Since this parameter has the largest impact on the rate of crab cannibalism, three interaction distances are considered in Scenario III in the paper. The other possibilities considered here include shifting the function in Eqn (A.26) to the Left and Right from the Default position ($\mu = 1.5, 2.0, 2.5$), changing the width of the function by altering σ to 0.4, 0.5 & 0.6 and changing the overall height of the function by setting α_{inter} to 0.7, 0.8 & 0.9.

Shifting the function Left or Right (i.e., changing the ratio of crab sizes at which death due to aggression is most likely) had the largest effect of the two possibilities considered. Shifting Left (crabs 1.5 times smaller experience maximum mortality due to aggression) lead to a higher overall survival than shifting Right (Fig B.16). This counter-intuitive result is caused by differences in the density of 7-12 instar crabs leading to differences in survival, as discussed in the paper. Changing the width or height of the function had little influence on survival, gut fullness or average food quality of 18+ crab densities.

B.5 Sensitivity of Crab Dynamics to Clam Model Assumptions

During review of this manuscript, it was pointed out that northern *Macoma balthica* populations differ from those located further south. Given that the parameterization of the clam model was largely based on these northern populations, it was unclear how the model results would change if the clam model more closely reflected southern populations. The three primary concerns raised were: 1) the life-history characteristics of the clams in the Neuse River system differed from those used in the model (higher growth rates, larger size at maturity, and spawning occurred earlier in spring and later in fall than specified), 2) clam densities in the model were at the high end and crab densities at the low end of those observed empirically, and 3) clam recruitment was too low in shallow parts of the estuary. To assess the impacts of these factors, separate simulation studies were done for each of these three cases (detailed below) in addition to the case where all three factors were changed together.

B.5.1 Altering Clam Growth Rates, Size at Maturity, and Spawning Times

Clam growth rate was altered so that clams achieved sexual maturity (2 cm) after ≈ 1 year and reached 3.25 cm shell length after ≈ 3 years. Clam spawning times were also altered from the ends of March and August to the ends of February and October and only clams > 2 cm were able to reproduce (previously, was > 1 cm). All other aspects were kept the same.

Clam biomass increased by a factor of 2.5 to 842 g/m^2 from 334 g/m^2 under the original model parameterization. Background prey remained the same. Crab densities for 7-12, 13-17 and 18+ instars were 0.1396, 0.0228 and 0.0181 (#/m^2) respectively (originally 0.111, 0.0265 and 0.0145 #/m^2 Table 1) while average gut fullness for the same instar classes was 0.41, 0.48 and 0.49 respectively (originally 0.438, 0.478 and 0.492). Since a bigger clam contains more biomass than a smaller clam, food limitation is thus more likely under the original model parameterization than the modified parameterization.

B.5.2 Altering Clam Densities

Since clam densities in the model are at the high end of those found in nature, we conducted a sensitivity analysis to determine how crab population dynamics might be affected if just clam density was lowered - all other factors kept the same. In the altered model, clam density was 657 (originally 864 #/m^2, Table C.2) while biomass dropped to 243 from 334 (g/m^2). Crab densities decreased for 7-12 and 13-17 instars (0.1068 and 0.0203 versus 0.1106 and 0.0256 #/m^2 originally) while 18+ densities increased to 0.0175 from 0.0145 (#/m^2). Gut fullness was $\approx$ 20% lower (around 0.36 compared to 0.44) and egg production per mature female decreased to 1519 from 1828 (#/# hr) in the original model.

For the model, clam densities are for ALL clams in the estuary. Thus, that model densities are higher than estuary densities is not surprising given that clams below the mesh size used to sieve sediments are missed (Appendix B.3.1). Certainly, if the density of clams were further reduced, food limitation would likely result. However, it is not clam density per se that is important, but clam density across the different clam size ranges which is better reflected by clam biomass.

B.5.3 Altering Clam Recruitment in Shallow Waters

The rules governing clam recruitment (Appendix A.4.3) include a factor, given by $\gamma_{cD} = 1 - \exp(-D^2)$, limiting recruitment in shallower parts of the estuary. This factor enters into the overall recruitment level computed using Equation (A.24). To address the concern that clam recruitment is actually higher in shallower parts of the estuary, we set $\gamma_{cD} = 1$ independent of depth. With this change, clam biomass increased to 384 (g/m^2) (originally 334 g/m^2 Table 1) while density decreased slightly to 827 (#/m^2) (originally 864 #/m^2). Overall crab density for 7-12, 13-17 and 18+ instars increased slightly (0.1266, 0.0217, and 0.0204 #/m^2 respectively) relative to the original parameterization (0.1106, 0.0256, and 0.0145 #/m^2 respectively). The increased 7-12 crab density lowered background biomass to 127 (g/m^2) from the original 146 (g/m^2). There were no indications that crab gut fullness or egg production were impacted by these changes.

In summary, allowing greater clam recruitment on the shallower parts of the estuary increased overall crab densities and rates of recruitment. Thus, the effect of the original parameterization is that a greater proportion of clams in the estuary are being exposed to hypoxia than occurs in nature, leading to lower clam biomass, thereby increasing the possibility of food limitation, and decreasing the importance of cannibalism.

B.5.4 Altering All Clam Factors Together

To assess the combined impact of all model changes for the cases above, the above changes were made jointly and clam density was decreased even further than in Appendix B.5.2. Clam biomass was originally 334 (g/m^2), (Table C.2) while after the these modifications increased to 715 (g/m^2) even though clam density was decreased to 388 (#/m^2) compared to 893 (#/m^2) originally. The net result was that adult crab density increased to 0.0200 from 0.0145 (#/m^2). Crabs showed no evidence of food limitation (gut fullness $>$ 0.44 for all instar classes and egg production per mature female was 2297 #/# hr). These values were all greater than those obtained under the original 45% Short case (Table C.2). Thus, the combined effect of the misspecifications in the clam model for the Neuse River estuary had no effect on the larger conclusion reached - namely that crab population dynamics are primarily controlled by cannibalism and not food limitation.

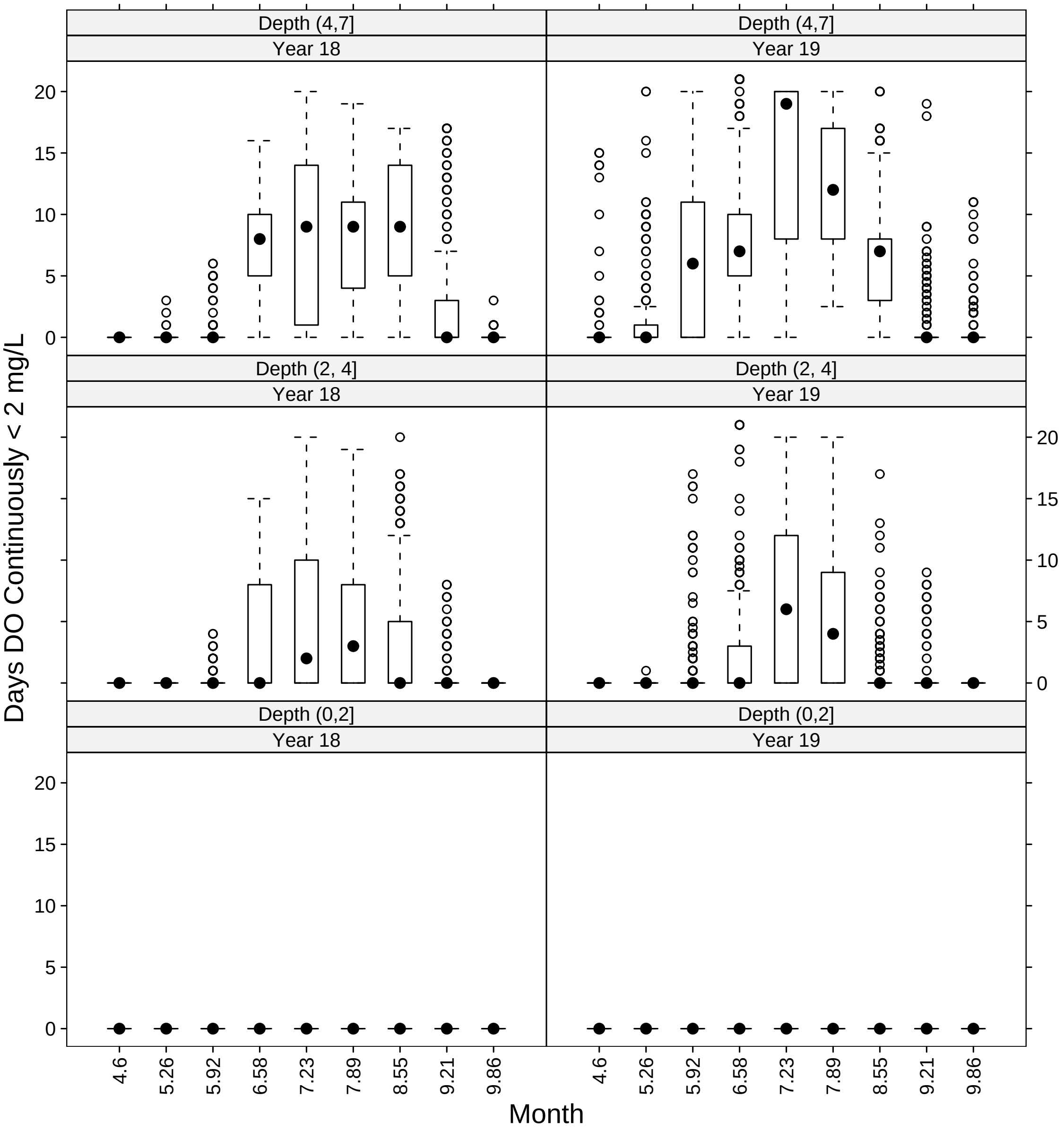

Fig. B.1: The number of consecutive days locations remain hypoxic (DO < 2 mg/L) under the model during years 18 and 19. 20 day consecutive non-overlapping windows are used. Results are shown for all fine-level triangles in the estuary, conditioned on depth and year.

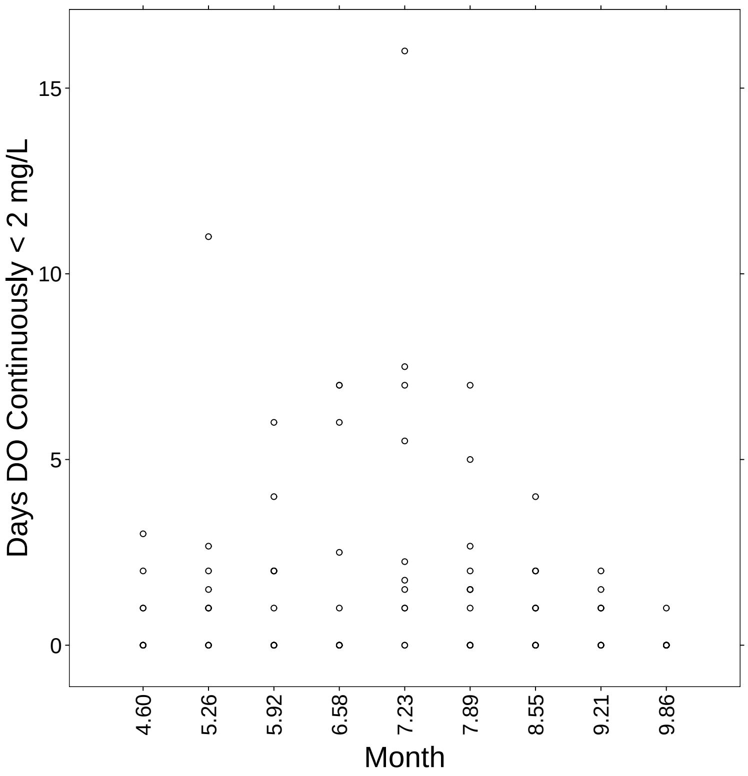

Fig. B.2: Durations of hypoxia (DO < 2 mg/L) at measurement sites LT9 and LT11 in the Neuse over years 1989 to 1999. As in Fig B.1, durations are calculated over consecutive, non-overlapping 20 day intervals. The large amount of missing data in this dataset results in a bias towards shorter hypoxic durations. Unlike Fig B.1 which is done over two years over the entire estuary, this figure is for two sampling sites over multiple years.

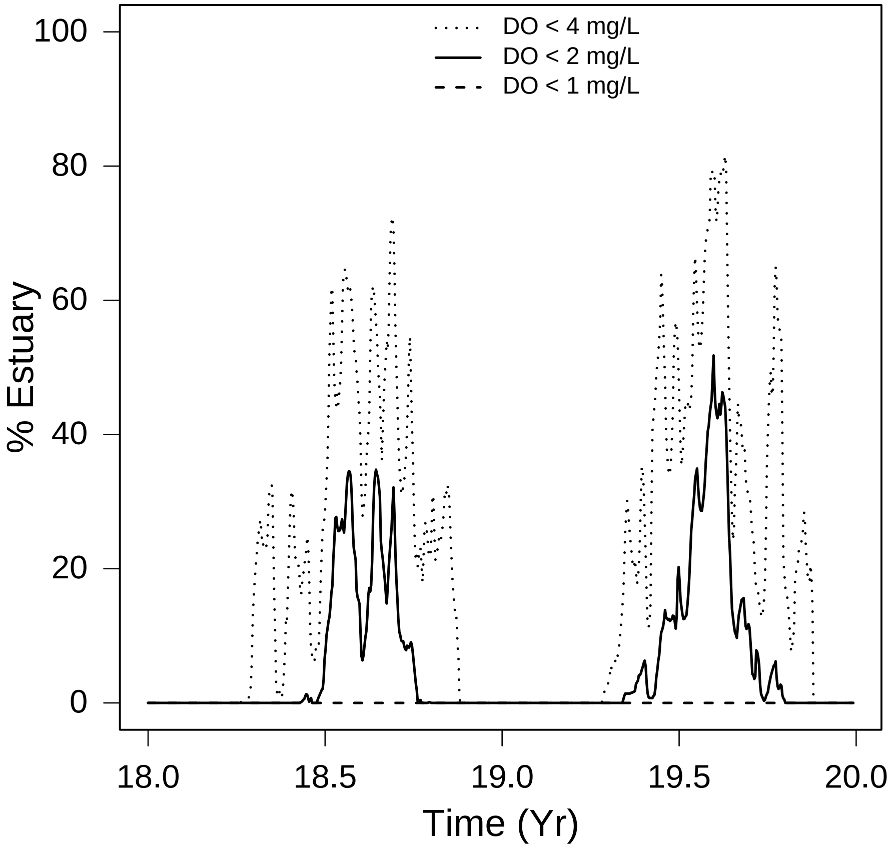

Fig. B.3: Percent of the entire estuary with a DO (mg/L) concentration falling within the given intervals over years 18 and 19.

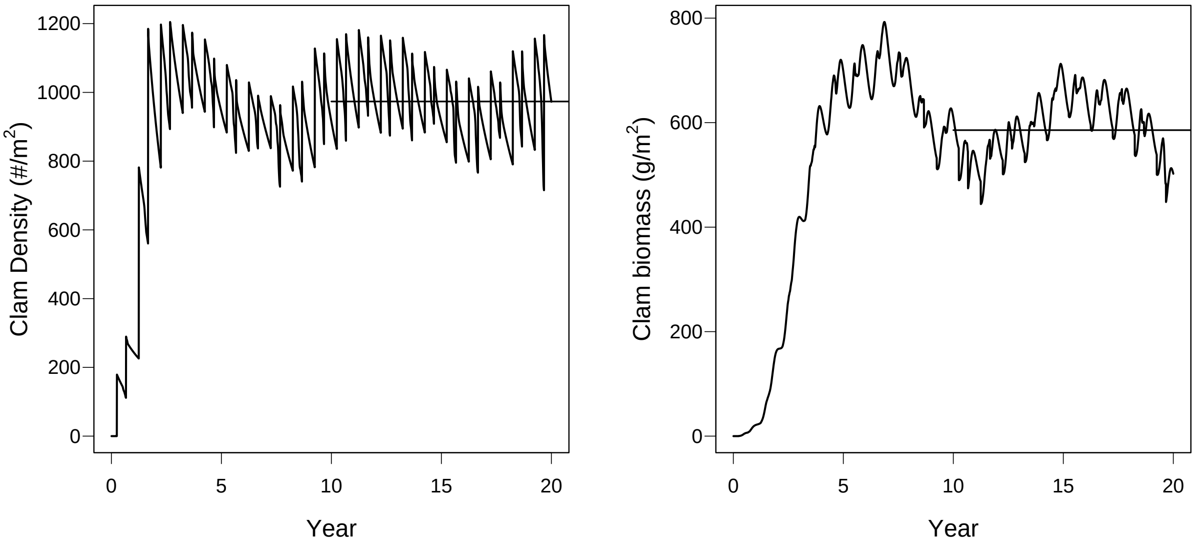

(a) Clam Density (#/m^2)

(b) Clam Biomass (g/m^2)

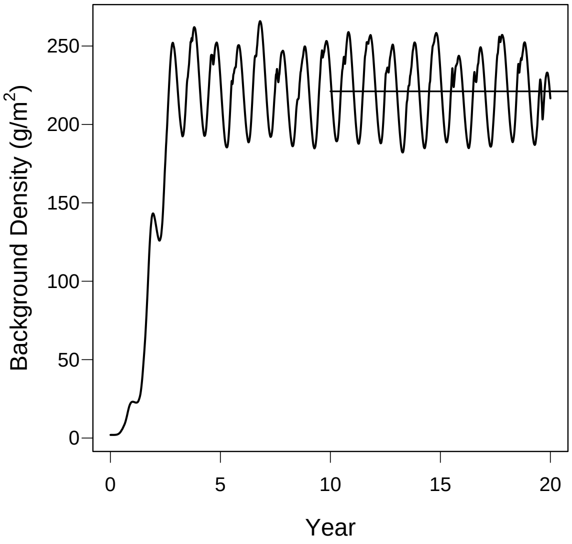

(c) Background Biomass (g/m^2)

Fig. B.4: Fig (a): Clam density over time (#/m^2). Fig (b): Clam biomass density over time (g/m^2). Fig (c): Background prey density (g/m^2) over time. All three variables appear to have stabilized after 20 years. Horizontal lines represent the average computed after year 10.

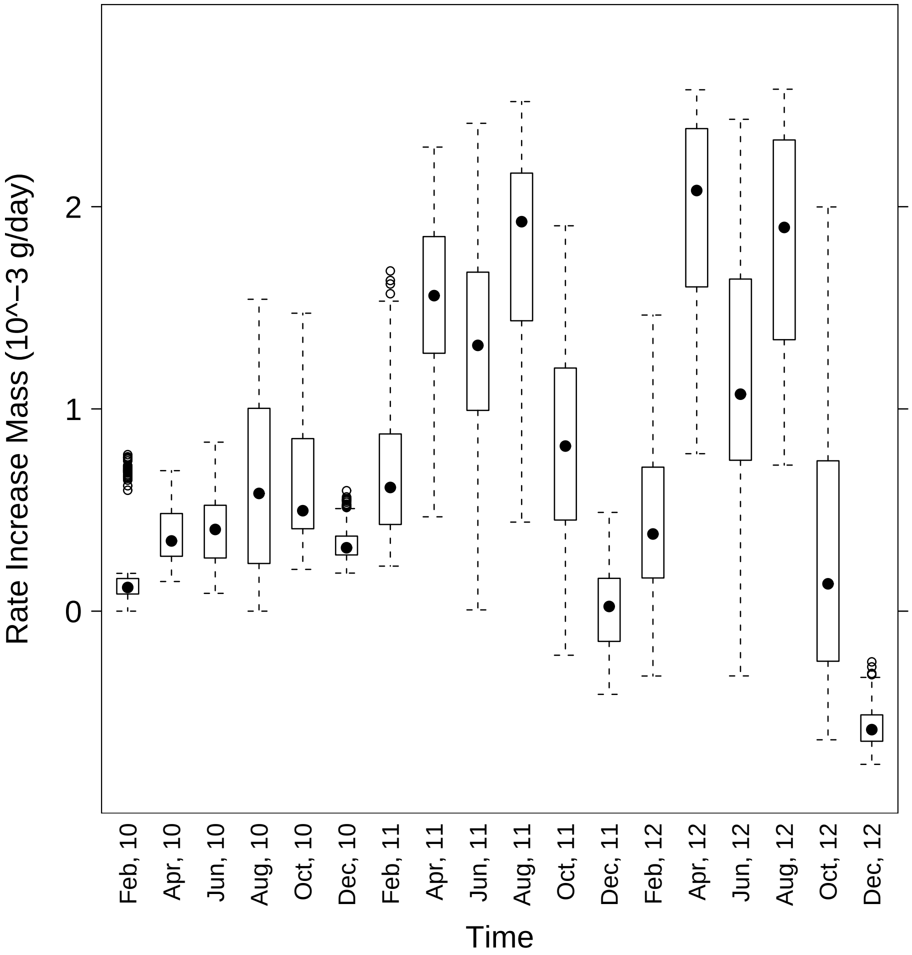

Fig. B.5: Rate of growth (g wet/day) of clams spawned in the spring and fall of year 10 over the subsequent 2.5 years. Clams are followed on 40 randomly selected fine-level triangles. The rate of growth slows considerably during the clam's first winter and they may loose mass during their second winter. The large variability in growth rates during summer results from the different depths temperatures and DO of the triangles.

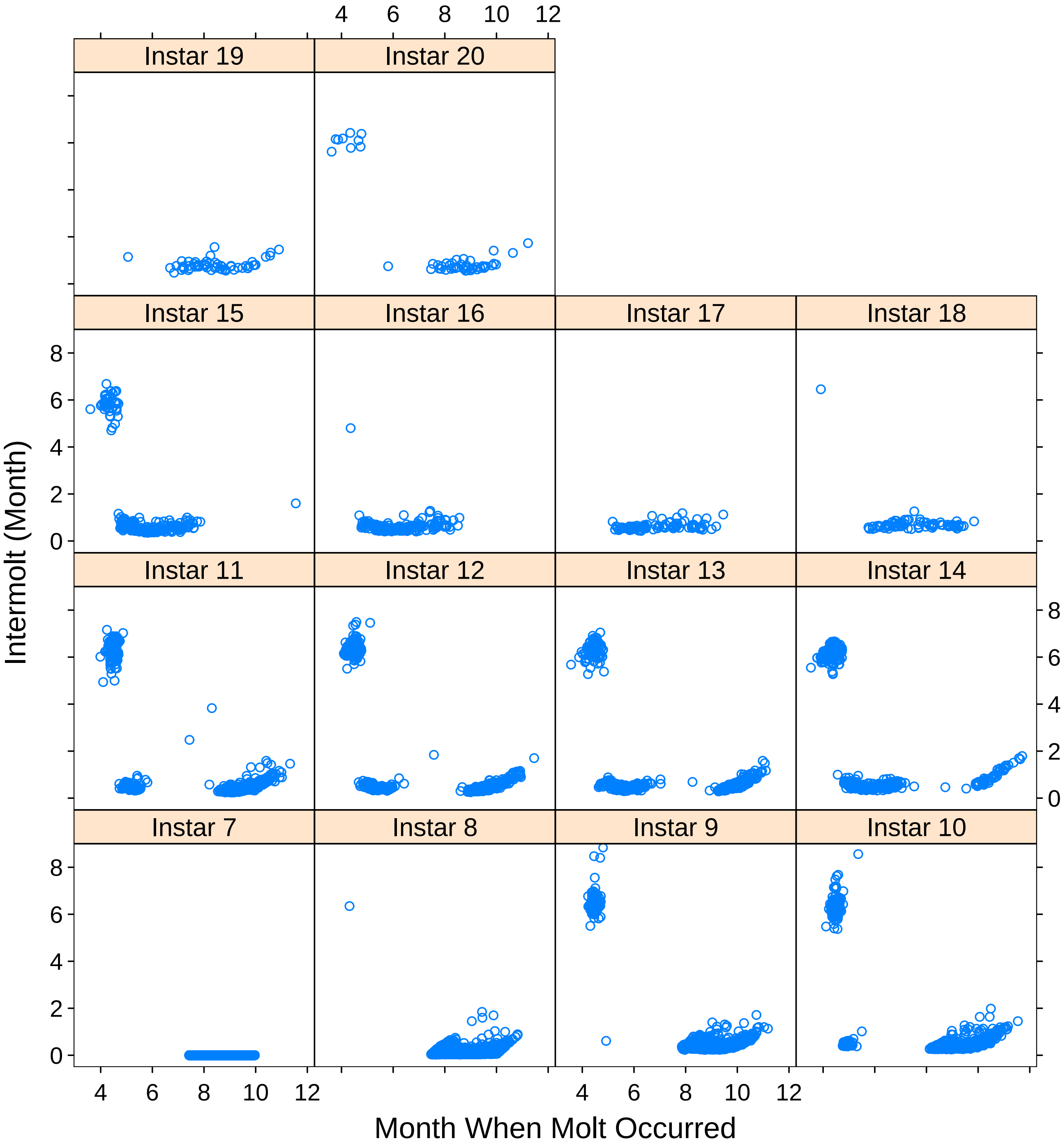

Fig. B.6: Length of time between successive molts by the month when the subsequent molt occurs and the instar of the molting crab. E.g., Instar 8 represents the time to go from instars 7 to 8.

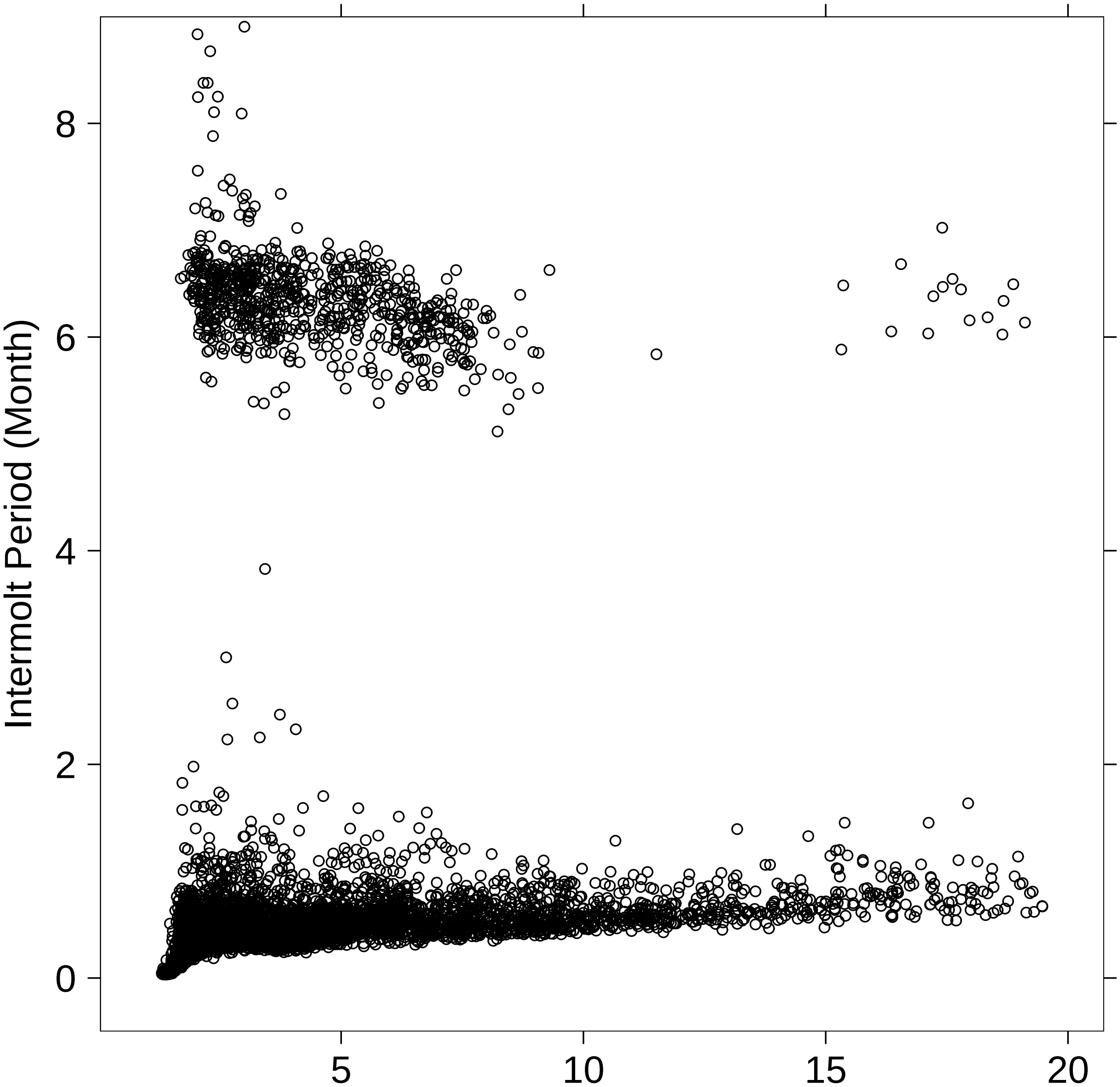

Fig. B.7: Length of time between successive molts by the CW of the molting crab.

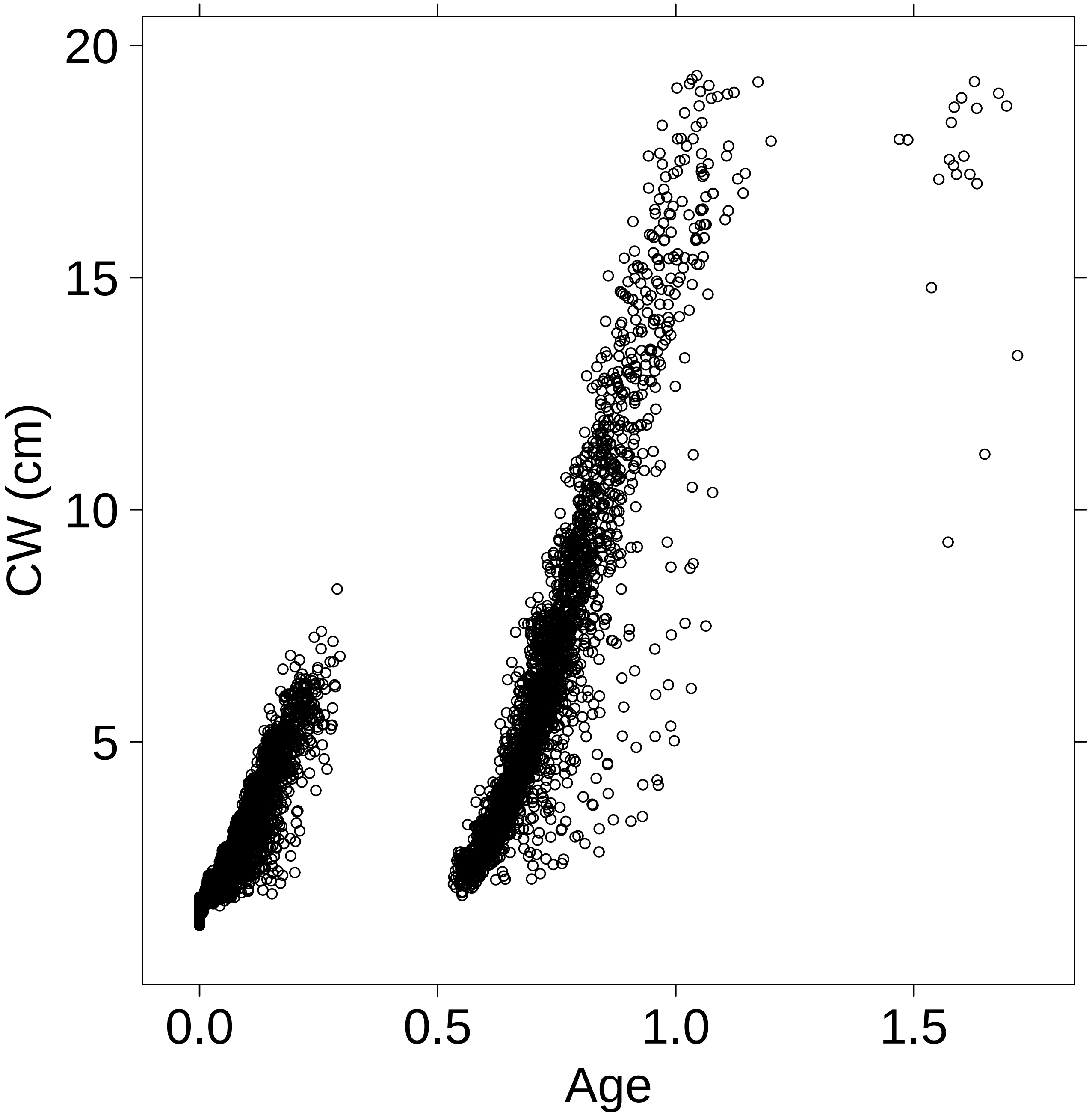

Fig. B.8: Crab age on CW

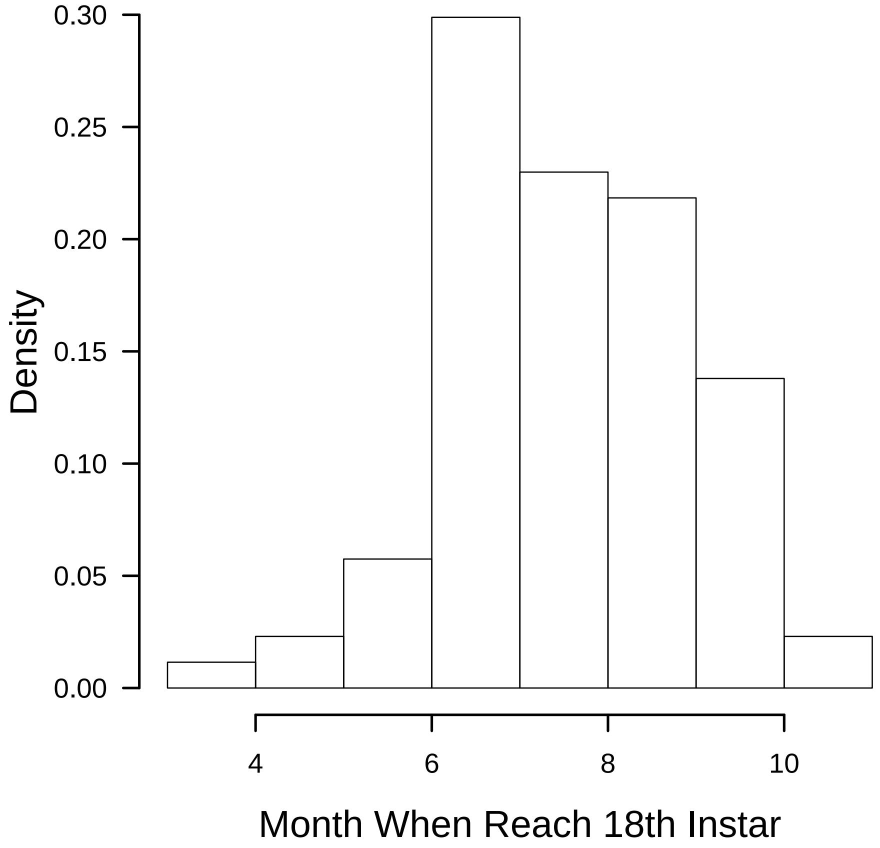

Fig. B.9: Distribution of month (April to October) when crabs reached the 18th instar.

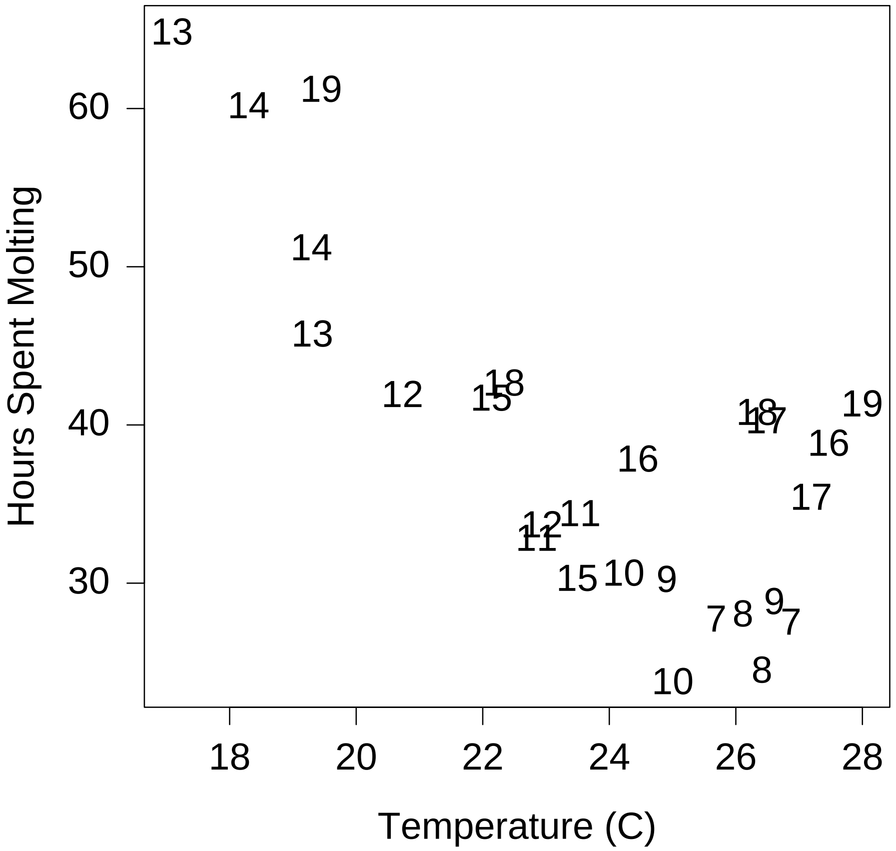

Fig. B.10: Amount of time two crabs took to molt at different instars (the numbers shown on the plot) and temperatures. The plot is based on the detailed life histories of two randomly selected crabs.

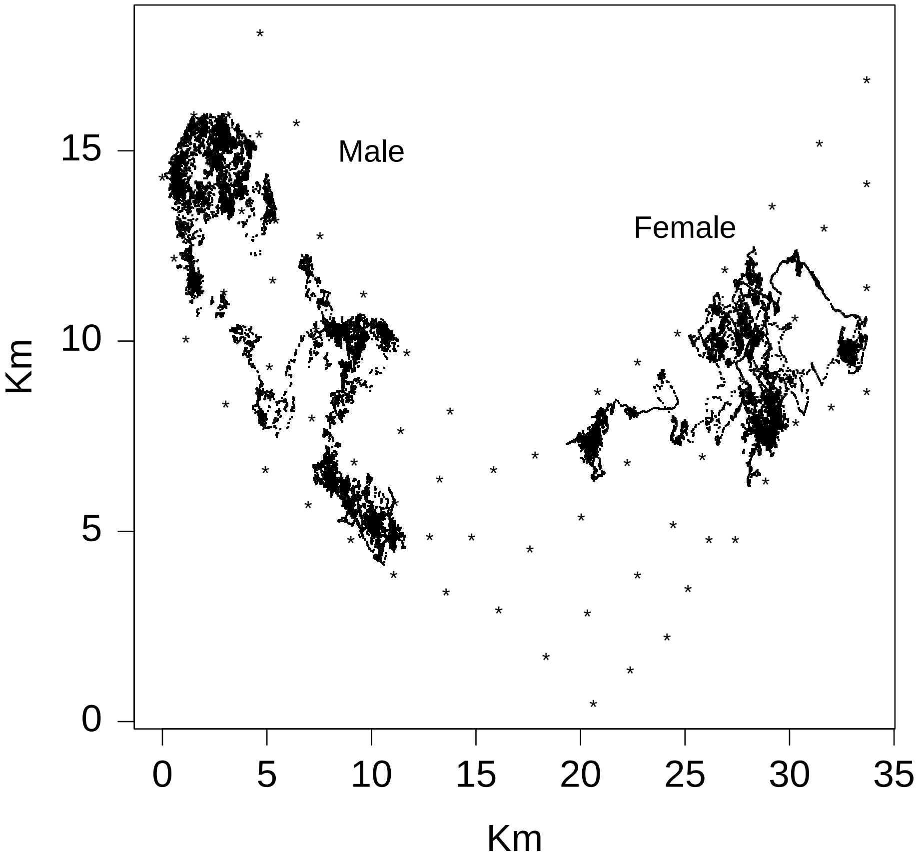

Fig. B.11: Paths of a male and female crab in the estuary over their lifetime.

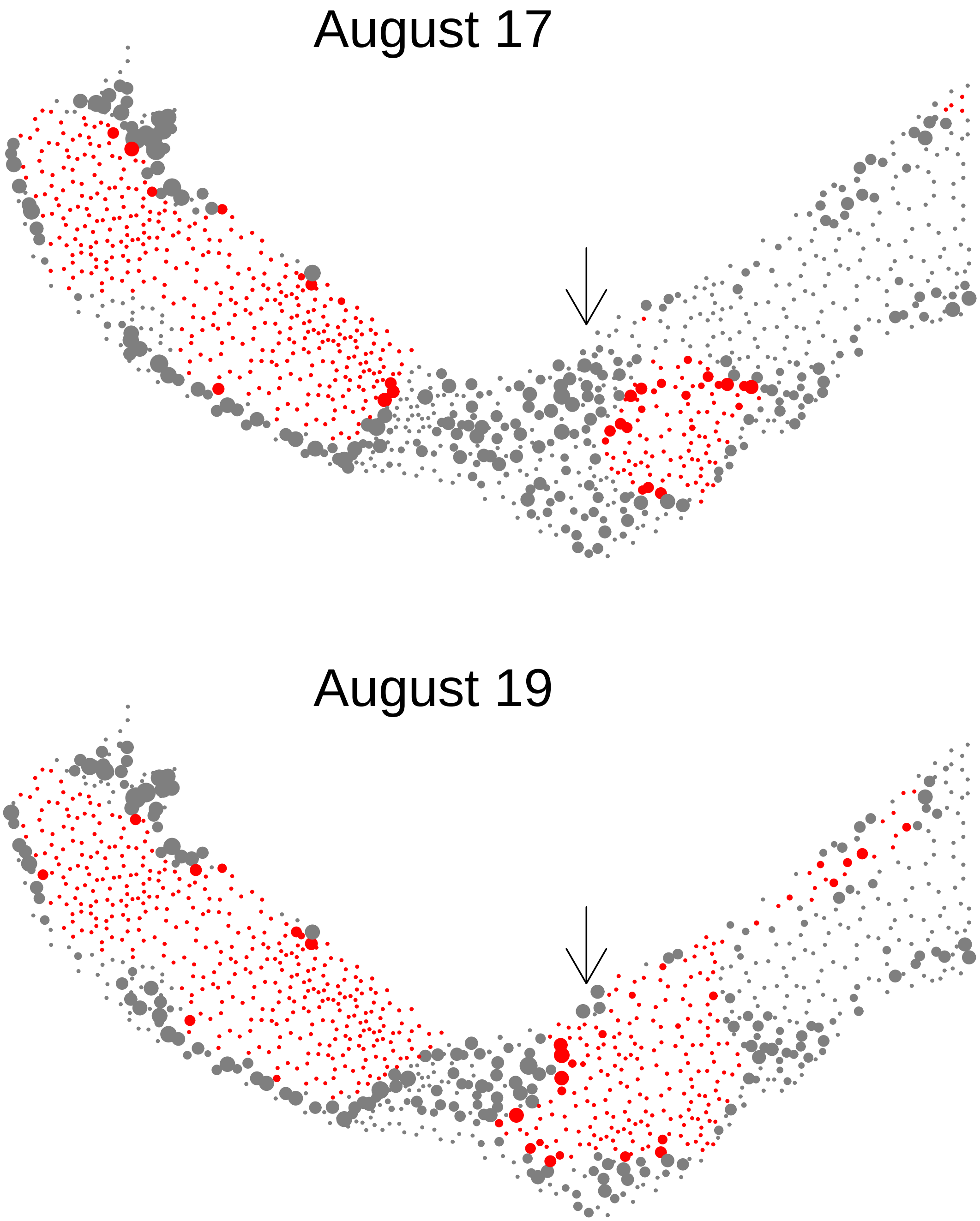

August 17

August 19

Fig. B.12: Each point represents a single fine-level triangle in the estuary. The size of the point represents the amount of crab biomass (g/m^2) on that triangle. The larger the point, the more biomass present. Red points indicate locations in the estuary experiencing a DO < 3 mg/L. Gray points indicate DO ≥ 3. The arrows highlight the changes that occurred in crab biomass as a result of changing DO over August 17 to 19.

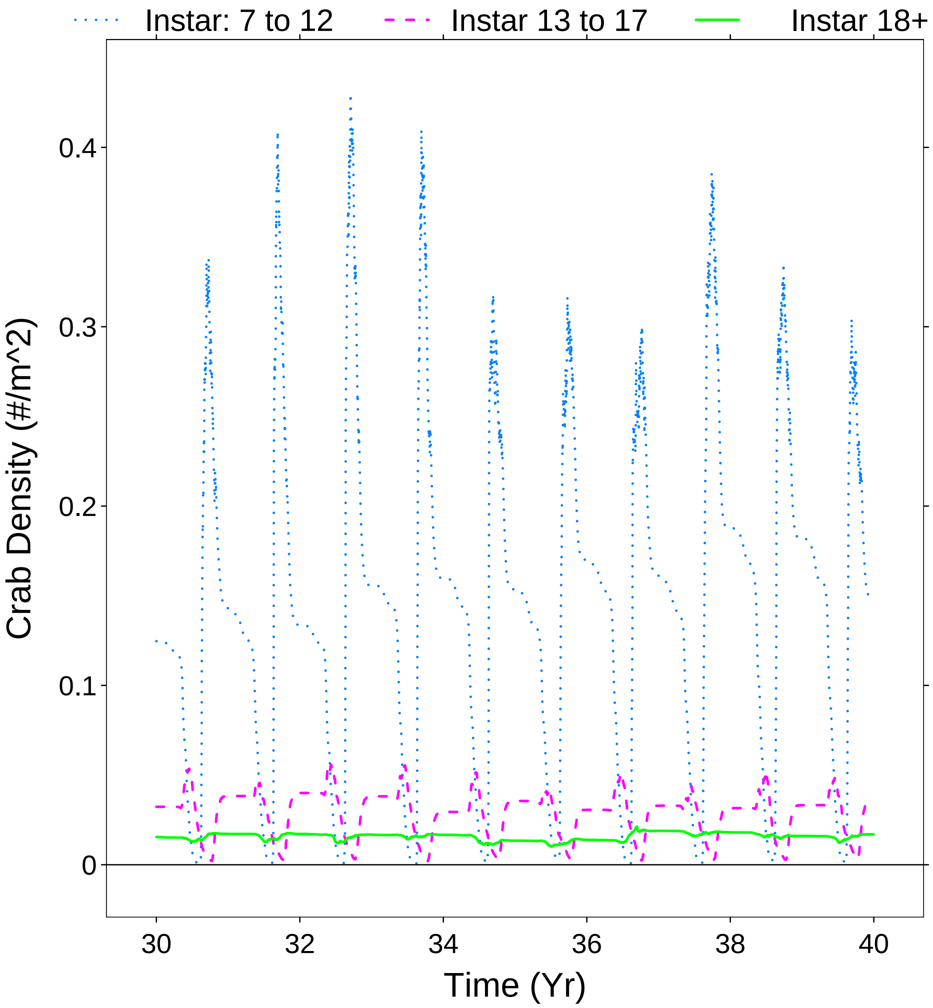

Fig. B.13: Time series of density (#/m^2) for 7-12, 13-17 and 18+ instar classes of crabs during years 30 to 39 over the entire estuary.

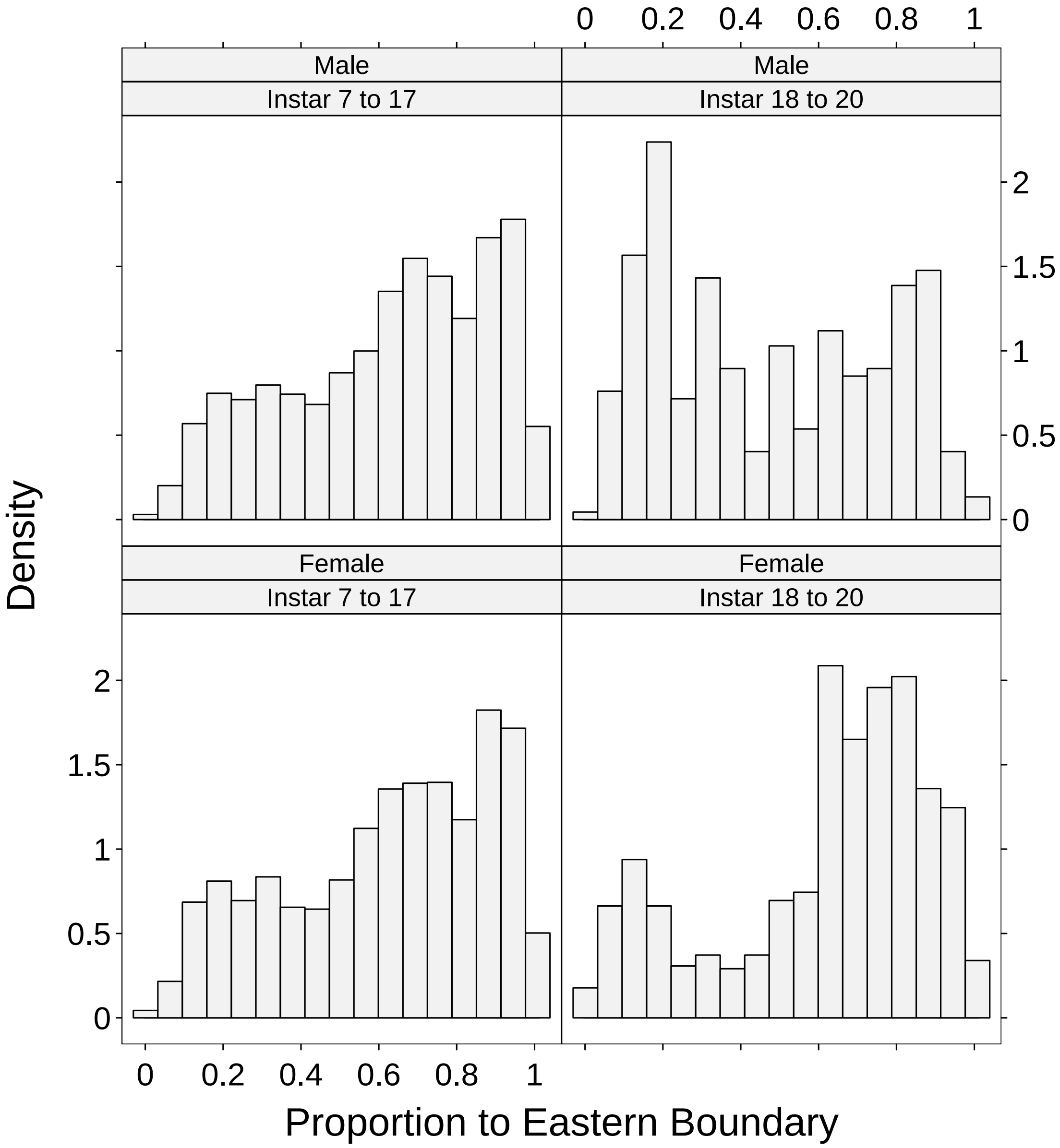

Fig. B.14: Density of crabs vs proportional distance to the eastern boundary of the estuary conditional on the sex and instar of the crab.

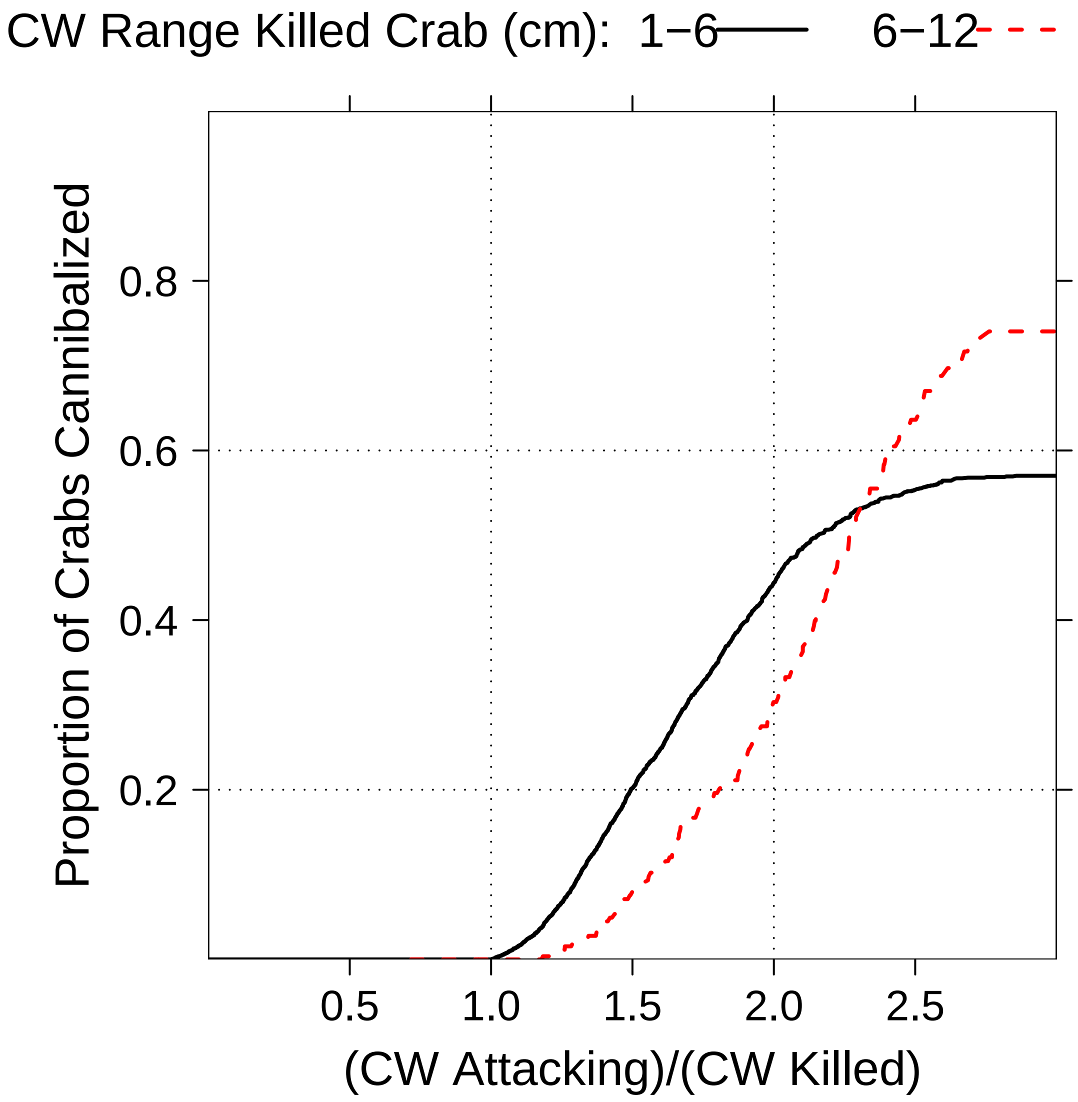

Fig. B.15: Proportion of two different size classes of crabs killed (CW 1-6 cm, and 6-12 cm) relative to the ratio of how much larger the attacking crab was. A smaller proportion of 1-6 cm CW crabs were cannibalized than 6-12 instar crabs - the other major cause of mortality for these small juvenile crabs being starvation. Second, the crabs killing the 1-6 cm CW crabs were on average a factor of ≈ 1.7 larger while for 6-12 cm CW crabs the attacking crabs were on average larger by a factor of at least 2. In neither case was a large proportion cannibalized by similar sized conspecifics.

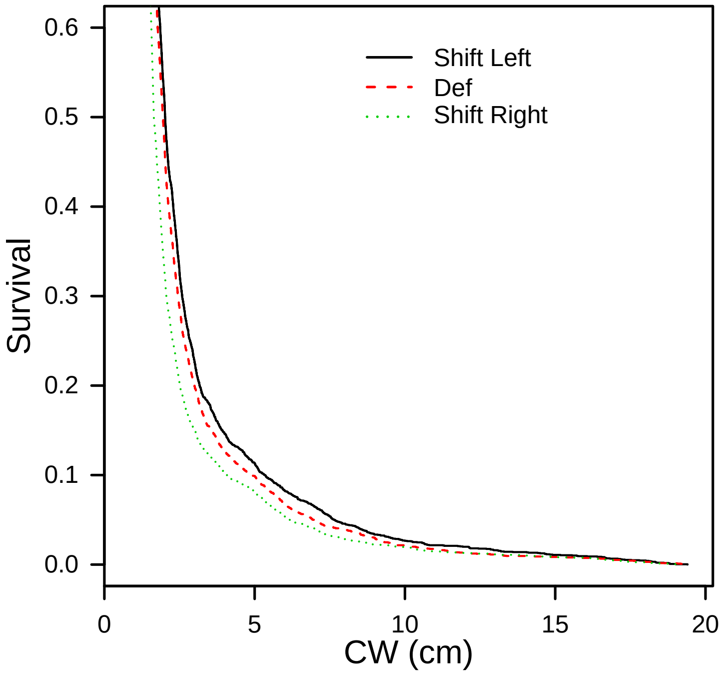

Fig. B.16: Effect on crab survival of altering the ratio of crab sizes at which death due to aggression is most likely (see Appendix B.4.6). Left, Def & Right correspond to $\mu = 1.5, 2.0, 2.5$.

C Model Parameters and Additional Results

Table C.1: Names, units, descriptions, values and references for the list of variables used in the crab model.

Symbol	**Units**	**Description**	**Value**	**References**
3D Random Fields				
# of Mesh Levels		Total number of refinements done of the coarse grid	4	Appendix A.3.
N_x		Number of discretization points used for generating field in the x direction	64	Appendix A.3.1
N_y		Number of discretization points used for generating field in the y direction	32	Appendix A.3.1
N_t		Number of discretization points used for generating field in the t direction	256	Appendix A.3.1
η		Filter used on the Gaussian Random Field		Eqn (A.1)
$\sigma_{x,S}$	m	SD of filter in x direction used for generating salinity field	1000	Appendix A.3.3
$\sigma_{y,S}$	m	SD of filter in y direction used for generating salinity field	800	Appendix A.3.3
$\sigma_{t,S}$	hr	SD of filter in t direction used for generating salinity field	48	Appendix A.3.3
$\sigma_{x,T}$	m	SD of filter in x direction used for generating temperature field	1000	Appendix A.3.2

continued on next page

Symbol	**Units**	**Description**	**Value**	**References**
$\sigma_{y,T}$	m	SD of filter in y direction used for generating temperature field	800	Appendix A.3.2
$\sigma_{t,T}$	hr	SD of filter in t direction used for generating temperature field	48	Appendix A.3.2
$\xi(x, \sigma)$		Component of the filter η		Eqn (A.2)
Variables Associated with Habitat				
$d(x, y)$	m	Distance from the western most point of the estuary		Appendix A.3.2
$d_{\max}$	m	Maximum distance from the western most point of the estuary		Appendix A.3.2
d_s		Proportion of distance from the western most point of the estuary	$d(x, y)/d_{\max}$	Appendix A.3.2
$D(x, y)$	m	Depth of estuary at location		Appendix A.3
DO	mg/L	Concentration of oxygen in bottom water of estuary	Eqn (A.9)	Borsuk et al. (2001b, Eqn 21)
DO_u	mg/L	Concentration of oxygen in upper water column at saturation	Eqn (A.11)	Hyer et al. (1971, Eqn 12)
K_d	1/hr	Rate constant for oxygen demand by sediment Eqn (A.15)	5.75E-3	Based on Borsuk et al. (2001b,a)
θ_d	x^{-T}	Constant representing level of temperature dependency. Eqn (A.15)	1.13	Borsuk et al. (2001b, Table 1)

continued on next page

Symbol	Units	Description	Value	References
k_v	m/hr$^{1/2}$	Constant for vertical oxygen exchange from surface, Eqn (A.12)	0.003	Based on Borsuk et al. (2001b); Schnoor (1996, Table 6.3)
K_v	1/hr	Governs vertical oxygen exchange. Eqn (A.10) & (A.12)		Schnoor (1996, Sec 6.3)
θ_v	x^{-T}	Constant representing level of temperature dependence. Eqn (A.12)	1.0	Borsuk et al. (2001b, Table 1)
S_{bot}	psu	Bottom salinity	Eqn (A.6)	Appendix A.3.3
S_{deep}	psu	Maximum salinity	Eqn (A.7)	Appendix A.3.3
T	° C	Temperature	Eqn (A.3)	Appendix A.3.2
T_{depth}	° C	Temperature	Eqn (A.5)	Appendix A.3.2
T_{mean}	° C	Temperature	Eqn (A.4)	Appendix A.3.2
U	m/hr	Mean tidal velocity Eqn (A.12)	100	Luettich Jr. et al. (1999)
Clam Variables				
α_{c}	g/cm^3	Scaling parameter relating clam length, L_{c}, to wet weight, $w_{\text{c,w}}$. Eqn (A.16)	0.1	Gilbert (1973); Bachelet (1980, Table 2)
β_{c}		Power relating clam length L_{c}, to wet weight, $w_{\text{c,w}}$. Eqn (A.16)	3.0	Gilbert (1973); Bachelet (1980, Table 2)
$\beta_{\text{c,grow}}$	°C^{-1}	Coeff. of temperature growth. Eqn (A.17)	0.2	Solidoro et al. (2000)

continued on next page

Symbol	**Units**	**Description**	**Value**	**References**
$\beta_{\mathrm{c,resp}}$	$^\circ\mathrm{C}^{-1}$	Coeff. of temperature respiration. Eqn (A.17)	0.17	Solidoro et al. (2000)
Δt	hr	Time between updates of clams	24	
$f_{c,G}$		Temperature dependence of clam growth	Eqn (A.18)	Solidoro et al. (2000)
$f_{c,r}$		Temperature dependence of clam respiration	Eqns (A.17)	Solidoro et al. (2000)
$G_{\mathrm{c,max}}$	$\mathrm{g}^{1/3}/\mathrm{hr}$	Maximum growth rate for clam on a wet weight basis Eqn (A.17).	4.3E-4	Based on Solidoro et al. (2000, Table 2)
$g(DO)$		Proportion decrease in metabolism due to DO	Eqn (A.19)	McMahon & Wilson (1981)
γ_{cB}		Clam biomass factor influencing recruitment	Eqn (A.23)	
γ_{cD}		Triangle depth factor influencing recruitment	App A.4.3	
Initial mass	g	Initial mass of recruited clam	0.001	
L_{c}	cm	Length of clam shell		Eqn (A.16)
λ_a	hr	Parameter Eqn (A.20), CDF of times till death at fixed DO	32.16	Borsuk et al. (2002)
λ_b	L hr/mg	Parameter Eqn (A.20), CDF of times till death at fixed DO	27.36	Borsuk et al. (2002)
λ_c	hr	Parameter Eqn (A.20), CDF of times till death at fixed DO	9.6	Borsuk et al. (2002)

continued on next page

Symbol	Units	Description	Value	References
λ_{Base}	hr^{-1}	Mortality rate without predation Eqn (A.20)	1.2E-5	Commito (1982); van der Meer et al. (2001)
$\lambda_{T_{\text{c,min resp}}}$	hr^{-1}	Mortality rate for clams in water less than -5°C . Eqn (A.20)	0.2	
$\lambda_{T_{\text{c,max resp}}}$	hr^{-1}	Mortality rate for clams in water greater than $T_{\text{c,max resp}}$ ° C. Eqn (A.20)	1.04E-2	
$r_{\text{c,max}}$	1/hr	Maximum respiration rate for clam on a wet weight basis Eqn (A.17)	3.5E-4	Based on McMahon & Wilson (1981); Hummel (1985a, Table 1)
ρ_{cB}	g/m^2	Grams of clam biomass on a given fine-level triangle		Eqn (A.23)
$\rho_{cB,\text{recruit}}$	g/m^2	Upper bound on clam biomass on a given fine-level triangle Eqn (A.23)	850	Hines & Comtois (1985)
ρ_{ce}	$\#/\text{m}^2$	Potential recruitment egg density		Appendix A.4.3
$\rho_{\text{c,tri}}$	$\#/\text{m}^2$	Clam density on a fine-level triangle		Eqn (A.24)
ρ_{cu}	$\#/\text{m}^2$	Upper bound on clam density on a given triangle Eqn (A.24)	1300	Holland et al. (1980)
T	°C	Temperature of clam.		
$T_{\text{c,max grow}}$	°C	Max temperature for growth. Eqn (A.17)	31	
$T_{\text{c,max resp}}$	°C	Max. temperature for respiration. Eqn (A.17)	33	Kennedy & Mihursky (1971); Wilson (1981)

continued on next page

Symbol	**Units**	**Description**	**Value**	**References**
$T_{\text{c,min resp}}$	°C	Min. temperature for respiration. Eqn (A.17)	-5	Bourget (1983)
$T_{\text{c,opt grow}}$	°C	Optimal temperature for growth. Eqn (A.17)	22	Solidoro et al. (2000)
$T_{\text{c,opt resp}}$	°C	Optimal temperature for respiration. Eqn (A.17)	20	Bensch et al. (1992)
$w_{\text{c,w}}$	g	Clam's wet weight.		Eqn (A.16) & (A.17)
		Background Food		
A	m^2	Area of fine-level triangle	Eqn (A.25)	
α	1/hr	Base mortality rate of background	2E-4	
$\beta_{\text{b,grow}}$	°C^{-1}	Coeff. of temperature growth. Eqn (A.25)	0.2	
$f_b(T;\cdot)$		Temperature dependence of growth of background food Eqn (A.25)	$f_c(T;\cdot)$	Eqn (A.18)
N	g	Number of grams of background food on a fine-level triangle		Eqn (A.25)
$\tilde{N}$	g	Average density of background food just on triangle and neighbors		Eqn (A.25)
K	g/m^2	Carrying capacity of background	400	Eqn (A.25)
ρ_b	g/m^2	Density of background food on triangle	N/A	

continued on next page

Symbol	**Units**	**Description**	**Value**	**References**
r_N	1/hr	Max growth rate of background	8E-4	Eqn (A.25)
Δt	hr	Time between updates of background	24	Eqn (A.25)
$T_{\text{b,max grow}}$	°C	Max temperature for growth. Eqn (A.25)	35	
$T_{\text{b,opt grow}}$	°C	Optimal temperature for growth. Eqn (A.25)	26	
		Crab Variables		
α_{egest}	$\frac{\text{cm}^{3-\beta_{\text{egest}}}}{\text{hr}}$	Parameter in Eqn (A.40).	0.004	
α_{ingest}	$\frac{\text{g}^{1-\beta_{\text{ingest}}}}{\text{hr}}$	Parameter relating size of crab to ingestion rate. Eqn (A.38)	30.0	
α_{G}	$\text{g/cm}^{\beta_{\text{G}}}$	Scale parameter in Eqn (A.36) relating CW to wet weight	0.14	Olmi III & Bishop (1983); Pullen & Trent (1970); Cadman & Weinstein (1985); Newcombe et al. (1949)
$\alpha_{\text{max move}}$	$\text{g}^{1-\beta_{\text{move}}}$	Scalar governing maximum rate of movement Eqn (A.28)	$300^{1-\beta_{\text{move}}}$	
$\alpha_{\text{max,met}}$	$\frac{g^{1-\beta_{\text{met}}}}{\text{hr}}$	Maximum base respiration parameter. Eqn (A.44)	0.00678	Booth & McMahon (1992, Table 1) & Houlihan et al. (1985, Fig 1).
$\alpha_{\text{min,met}}$	$\frac{\text{g}^{1-\beta_{\text{met}}}}{\text{hr}}$	Minimum base respiration rate. Eqn (A.44)	0.00166	Booth & McMahon (1992, Table 1)& Houlihan et al. (1985, Fig 1).
α_{molt}	$\text{g/cm}^{\beta_{\text{molt}}}$	Scalar relating CW to total grams to molt. Eqn (A.46)	2E-2	

continued on next page

Symbol	**Units**	**Description**	**Value**	**References**
α_{move}	$\frac{\text{g}^{1-\beta_{\text{move}}}}{\text{m hr}}$	Scalar relating mass and movement rate to energy expenditure. Eqn (A.45)	4E-5	Houlihan et al. (1985, Fig 1)
α_{stom}	cm	Scaling parameter for stomach volume in Eqn (A.37)	0.0255	Based on McGaw & Reiber (2000)
β_{egest}		Parameter in Eqn (A.40).	2.0	
β_{ingest}		Parameter relating size of crab to ingestion rate. Eqn (A.38)	0.25	
β_{G}		Power relating CW to wet weight in Eqn (A.36)	2.7	Olmi III & Bishop (1983); Pullen & Trent (1970); Cadman & Weinstein (1985); Newcombe et al. (1949)
β_{met}		How metabolic demand increases with weight. Eqn (A.44)	2/3	Houlihan et al. (1985)
β_{molt}		Power relating CW to total grams crab must expend to molt. Eqn (A.46)	2	
β_{move}		Power relating mass to rate of energy usage for movement. Eqn (A.45)	0.33	Houlihan et al. (1985)
β_{stom}		Power of CW for computing stomach volume Eqn (A.37)	2.0	See Appendix A.5.6
b_1		First parameter of movement distribution. App. A.5.4	1	
b_2		Second parameter of movement distribution. App. A.5.4	40	

continued on next page

Symbol	Units	Description	Value	References
CW	cm	Carapace width		
$CW_{\text{init, lower}}$	cm	Lower range of CW at 7th instar. Appendix A.5.13	1.05	Newcombe et al. (1949, Table IV)
$CW_{\text{init, width}}$	cm	Width of CW instantiation range at. Appendix A.5.13	0.6	
$d_{\text{max inter}}$	m	Maximum distance between crabs when they may interact	12	Appendix A.5.3
δt	hr	Random time interval between a crab's updates		Appendix A.5.2
Energy_{egg}	cal	Energy content of a single crab egg.	0.0454	Kannupandi et al. (1999)
η_i	#	Number of clams in age class i	Eqn (A.33)	
$f_{\text{Temp}}(T;\cdot)$		Function governing metabolism on temperature	Eqn (A.39)	
$f_{\text{ingest, temp}}$		Particular parameterization of $f_{\text{Temp}}(T;\cdot)$	Eqn (A.38)	
G	g	Wet weight of crab.	Eqn (A.30)	
G_{egest}	g/hr	Grams egested from the crab	Eqn (A.41)	
$G_{\text{egest stom}}$	g/hr	Grams egested from the stomach	Eqn (A.40)	
G_{ingest}	g/hr	Grams ingested into the crab's stomach.	Eqn (A.38)	
$G_{\text{mass next molt}}$	g	Mass when next molting will be triggered. Eqn (A.36)		

continued on next page

Symbol	**Units**	**Description**	**Value**	**References**
G_{molt}	g/hr	Grams expended molting over δt	Eqn (A.47)	
G_{move}	g/hr	Grams used solely by crab moving	Eqn (A.45)	
G_{repro}	g/hr	Grams put into reproduction	Appendix A.5.12	
$G_{\text{resp+excrete}}$	g/hr	Respiration and excretion costs	Eqn (A.44)	
G_{stom}	g	Grams of food in stomach	Eqn (A.42)	
$G_{\text{total to molt}}$	g	Total grams crab expends to molt	Eqn (A.47)	
$G_{\text{total molted}}$	g	Grams expended molting.	Eqn (A.47)	
$\gamma_{\text{absorbtion}}$		Absorption coefficient. Eqn (A.41)	0.6	Guerin & Stickle (1992, Tables 2&3)
γ_{clam}		Change in weighting factor caused by DO $<$ 1 mg/L Eqn (A.34)		Appendix A.5.6
$\gamma_{\text{clam,def}}$		Default weighting factor for clam depth refuge Eqn (A.34)	1.0	
$\gamma_{\text{c,encounter}}$	$\text{m}^2/\#$ clams	Constant in Eqn (A.31)	1/75	
$\gamma_{\text{b,encounter}}$	$\text{m}^2/\#$	Governs probability of finding background food	Eqn (A.35)	
$\gamma_{\text{excretion}}$		Excretion as a proportion of respiration costs	0.05	Guerin & Stickle (1992, Tables 2&3)

continued on next page

Symbol	**Units**	**Description**	**Value**	**References**
$\gamma_{\text{maturation}}$		Constant governing rate crab development in maturation pot. See App. A.5.13	0.55	
$\gamma_{\text{mov}}(T)$		Gives dependence of rate of movement on temperature.	Eqn (A.27)	
λ_{mat}	1/hr	Mortality rate for crabs in maturation pot. App. A.5.13	5E-3	
$\lambda_{\text{update max}}$	hr^{-1}	Parameter governing crab's update times	1.0	
m_1		First parameter for crab's lifetime distribution. App. A.5.14	3.0	
m_2		Second parameter for crab's lifetime distribution. App. A.5.14	1.5	
Max Age	hr	App. A.5.14	70080	Rugolo et al. (1998)
ϕ_i		Weighting factor governing crab's foraging ability on clams	Eqn (A.33)	
$p_{\text{cw,l}}$		Lower bound for proportion increase in CW. Eqn (A.49)	0.24	Tagatz (1968, Table 2)
$p_{\text{cw, u}}$		Upper bound for proportion increase in CW. Eqn (A.49)	0.32	Tagatz (1968, Table 2)
Q_{egest}		Slope for temperature dependence of egestion in Eqn (A.40)	5	
Q_{ingest}		Slope for temperature dependence of intake in Eqn (A.38)	5	

continued on next page

Symbol	**Units**	**Description**	**Value**	**References**
Q_{met}		Slope for temperature dependence of metabolism	2.5	Booth & McMahon (1992)
q_{feed}		Quality of food feeding on		
q_{stom}		Quality of food in stomach	Eqn (A.43)	
$\rho_{\mathrm{c}[,]}$	$\#/\mathrm{m}^2$	Density of clams within crab's forageable size range		Eqn (A.31)
ρ_{energy}	cal/g wet wt	Energy density of crab	1000	Cummins & Wuycheck (1971, Table 2, p 25)
ρ_f	$\mathrm{g/cm}^3$	Density of food in stomach	1.5	
ρ_{c}	$\#/\mathrm{m}^2$	Density clams on triangle		App. A.4 & A.5.6
ρ_b	$\mathrm{g/m}^2$	Density of background food on triangle	Eqn (A.35)	
ρ_{max}	$\#/\mathrm{m}^2$	Upper bound on the density of crabs in the estuary	0.4	Appendix A.5.13
Scale factor		Factor by which the estuary is scaled Appendix A.6	100	
Sex Ratio		Proportion of male crab's instantiated into the estuary.	0.5	
σ_{molt}	$\mathrm{g}^{-1/2}$	Parameter governing rate of energy expenditure as molting progresses. Eqn (A.47)	0.15	
θ_{new}	rad	Direction of crab movement, kept between $[0, 2\pi)$.		
$T_{\mathrm{max\ egest}}$	°C	Maximum temperature for crab egestion. Eqn (A.40)	33	

continued on next page

Symbol	**Units**	**Description**	**Value**	**References**
$T_{\text{max ingest}}$	°C	Maximum temperature for crab ingestion. Eqn (A.38)	33	
$T_{\text{max met}}$	°C	Maximum temperature for metabolic processes	35	Tagatz (1969, Table 1)
$T_{\text{max spawn}}$	°C	Maximum temperature for crab spawning	29	van den Avyle (1984)
$T_{\text{min spawn}}$	°C	Minimum temperature for crab spawning	19	van den Avyle (1984)
$T_{\text{min met}}$	°C	Minimum temperature for metabolic processes	2	Tagatz (1969, Table 1)
$T_{\text{opt egest}}$	°C	Optimal temperature for crab egestion. Eqn (A.40)	25	
$T_{\text{opt ingest}}$	°C	Optimal temperature for crab ingestion. Eqn (A.38)	25	
$T_{\text{opt met}}$	°C	Optimal temperature for metabolic processes	26	
v_{max}	m/hr	Maximum rate of crab movement. Eqn (A.28)	720	Clark et al. (1999); Houlihan et al. (1985)
v	m/hr	Actual rate of crab movement.	Eqn (A.28)	
V_{stom}	cm^3	Volume of Crab's Stomach.	Eqn (A.37)	
V_f	cm^3	Volume of food in crab's stomach.	G_{stom}/ρ_f	
X		Gaussian Random Field		App. A.3 & A.3.1
Z		Random mixing term for DO		Eqns (A.13) & (A.9)

Table C.2: Estuary wide summaries of hypoxic extent crossed with duration. Additional variables are given in Table 1. For all variables except **Recruit 7, 12 & 18**, the mean and (SD) were calculated for the daily model exports for years 30 through 39 between June 1 and September 30 (n=1220). **Recruit 7, 12 & 18** were calculated over the entire 10 year period. The variable **Max % Hypoxic** is the maximum percentage of the estuary hypoxic per year averaged over the 10 years.

	Max Extent Hypoxia											
	≈ 15%			**≈ 30%**			**≈ 45%**			**≈ 60%**		
Hypoxic Dur	**Short**	**Long**	**Fixed**	**Short**	**Long**	**Fixed**	**Short**	**Long**	**Fixed**	**Short**	**Long**	**Fixed**
Max % Hypoxic	17.7 (6.5)	18 (6.5)	15.6 (0.1)	28.1 (7.2)	27 (7.4)	32.8 (0.1)	44.9 (7.2)	41.7 (7.7)	45.1 (0.1)	61.9 (6.2)	58.3 (6.4)	58.8 (0)
% Hypoxic	5.7 (5.3)	6.9 (5.9)	7.3 (5.7)	10.7 (7.7)	12.5 (8.4)	18.9 (9.8)	20.9 (11.3)	22.9 (11.4)	31.1 (12.7)	36.9 (13)	37.8 (12.6)	45.2 (12.7)
DO (mg/L)	5.5 (0.7)	5.4 (0.7)	3.5 (0.2)	5.2 (0.8)	5.1 (0.8)	3.1 (0.3)	4.8 (0.8)	4.8 (0.8)	2.9 (0.3)	4.1 (0.9)	4.1 (0.9)	2.6 (0.3)
Hypoxic Edge (10^{-2} m/m^2)	1.12 (0.85)	1.33 (0.91)	1.59 (1.08)	1.82 (1.07)	2.06 (1.11)	2.7 (0.97)	3.04 (1.28)	3.25 (1.27)	3.71 (1.04)	4.13 (0.94)	4.24 (0.91)	4.84 (1.02)
Clam Density (#/m^2)	915 (73)	913 (92)	882 (134)	914 (89)	902 (115)	821 (184)	893 (128)	852 (159)	802 (236)	774 (230)	722 (244)	696 (248)

continued on next page

	Max Extent Hypoxia											
	$\approx$ 15%			**$\approx$ 30%**			**$\approx$ 45%**			**$\approx$ 60%**		
Hypoxic Dur	**Short**	**Long**	**Fixed**	**Short**	**Long**	**Fixed**	**Short**	**Long**	**Fixed**	**Short**	**Long**	**Fixed**
Crab Biomass (g/m^2)	7.84 (0.8)	7.52 (0.77)	4.7 (0.58)	6.84 (0.87)	6.3 (0.68)	3.33 (0.52)	5.29 (0.77)	4.86 (0.57)	2.69 (0.4)	2.83 (0.42)	2.75 (0.39)	2.01 (0.31)
Mat Female Mass (g)	239.2 (5.9)	245.2 (6.5)	221.8 (8.6)	242.2 (8.3)	241.7 (8.2)	217.6 (9.4)	234.1 (6.3)	231.7 (9.1)	220.3 (9.4)	223.4 (8)	220.2 (13)	222.4 (11.1)
Mat Female CW (cm)	17.4 (0.1)	17.6 (0.1)	17.1 (0.2)	17.5 (0.1)	17.5 (0.1)	17 (0.2)	17.5 (0.1)	17.4 (0.2)	17.1 (0.2)	17.4 (0.2)	17.4 (0.4)	17.3 (0.3)
Egg (#/m^2 hr)	19.04 (13.38)	16.22 (12.75)	6.46 (7.98)	16.67 (12.55)	12 (10.74)	4.41 (6.66)	10.83 (9.94)	6.42 (7.9)	3.83 (5.88)	3.28 (5.8)	2.08 (4.48)	2.26 (4.57)
Egg per Mat Fe (#/# hr)	1794 (1250)	1750 (1362)	1261 (1501)	1893 (1418)	1653 (1472)	1252 (1839)	1828 (1655)	1397 (1718)	1280 (1962)	1283. (2289)	1007 (2214)	1195 (2418)
Recruit 7 (10^{-6}#/m^2 hr)	133.85 (456.73)	119.82 (388.57)	74.95 (275.73)	131.47 (468.41)	99.6 (343.84)	57.65 (215.23)	95.45 (325.31)	64.61 (240.68)	51.51 (188.49)	38.79 (162.63)	27.2 (121.68)	33.41 (139.27)
Recruit 12 (10^{-6}#/m^2 hr)	14.28 (25.53)	11.94 (19.91)	12.55 (25.75)	15.92 (29.51)	11.52 (20.15)	10.94 (22.62)	15.33 (28.66)	10.34 (19.22)	9.56 (19.84)	8.51 (15.94)	6 (11.53)	7.67 (15.87)

continued on next page

	Max Extent Hypoxia											
	≈ 15%			**≈ 30%**			**≈ 45%**			**≈ 60%**		
Hypoxic Dur	**Short**	**Long**	**Fixed**	**Short**	**Long**	**Fixed**	**Short**	**Long**	**Fixed**	**Short**	**Long**	**Fixed**
Recruit 18 (10^{-6}#/m^2 hr)	2.36 (3.7)	2.13 (3.33)	1.69 (2.96)	2.12 (3.51)	1.91 (3.17)	1.25 (2.31)	1.73 (3.06)	1.55 (2.78)	0.99 (1.97)	1.06 (2.08)	0.93 (1.88)	0.79 (1.6)
Gut Fullness 7-12	0.366 (0.07)	0.352 (0.063)	0.382 (0.092)	0.4 (0.069)	0.351 (0.064)	0.379 (0.091)	0.438 (0.077)	0.363 (0.068)	0.365 (0.085)	0.394 (0.078)	0.339 (0.081)	0.36 (0.094)
Gut Fullness 13-17	0.445 (0.032)	0.447 (0.031)	0.463 (0.039)	0.459 (0.033)	0.456 (0.034)	0.457 (0.045)	0.478 (0.03)	0.459 (0.039)	0.464 (0.046)	0.464 (0.039)	0.438 (0.058)	0.457 (0.051)
Gut Fullness 18+	0.43 (0.037)	0.412 (0.034)	0.434 (0.029)	0.455 (0.035)	0.427 (0.035)	0.453 (0.031)	0.492 (0.031)	0.431 (0.042)	0.443 (0.038)	0.452 (0.044)	0.419 (0.046)	0.442 (0.042)
Food Qual 7-12	0.347 (0.015)	0.346 (0.016)	0.346 (0.016)	0.347 (0.014)	0.346 (0.015)	0.345 (0.016)	0.347 (0.014)	0.347 (0.017)	0.346 (0.017)	0.35 (0.019)	0.35 (0.027)	0.343 (0.02)
Food Qual 13-17	0.415 (0.007)	0.42 (0.009)	0.405 (0.007)	0.409 (0.007)	0.418 (0.008)	0.405 (0.008)	0.402 (0.006)	0.417 (0.008)	0.407 (0.01)	0.405 (0.01)	0.412 (0.011)	0.4 (0.009)
Food Qual 18+	0.402 (0.008)	0.407 (0.008)	0.391 (0.006)	0.396 (0.008)	0.403 (0.007)	0.389 (0.007)	0.385 (0.006)	0.398 (0.01)	0.392 (0.008)	0.386 (0.009)	0.392 (0.01)	0.39 (0.009)

continued on next page

	Max Extent Hypoxia											
	≈ 15%			**≈ 30%**			**≈ 45%**			**≈ 60%**		
Hypoxic Dur	**Short**	**Long**	**Fixed**	**Short**	**Long**	**Fixed**	**Short**	**Long**	**Fixed**	**Short**	**Long**	**Fixed**
Death Aggr 7-12 (10^{-4}/hr)	6.63 (4.83)	6.1 (4.38)	6.04 (4.82)	7.31 (5.08)	5.78 (4.25)	5.76 (5.06)	7.79 (5.82)	5.57 (4.19)	5.63 (4.82)	5.74 (5.33)	4.01 (4.49)	5.08 (5.01)
Death Aggr 13-17 (10^{-4}/hr)	7.31 (3.16)	7.11 (3.38)	8.05 (3.54)	8.24 (3.78)	7.65 (3.96)	8.9 (4.85)	8.89 (4.47)	8.21 (4.94)	9.67 (5.51)	8.31 (5.11)	7.48 (5.59)	9.14 (5.77)
Death Aggr 18+ (10^{-4}/hr)	2.4 (1.82)	2.12 (1.67)	3.07 (2.24)	2.61 (2.05)	2.4 (1.97)	3.36 (2.74)	2.93 (2.61)	2.55 (2.39)	3.19 (2.99)	3.26 (3.31)	2.8 (3.22)	3.5 (3.7)

Table C.3: Effect of altering the levels of clam and background prey. Additional variables are given in Table 2. The food **Limited** case corresponds to decreasing the upper bound on clam biomass recruitment to $\rho_{cB,\text{recruit}}$=425 (g/m^2) (Default value is $\rho_{cB,\text{recruit}} = 850$ g/m^2, Table C.1) and background carrying capacity to 200 (g/m^2) (Default value is $K = 400$ g/m^2, Table C.1). The **Default** is the same as Short hypoxic duration in Table C.2. The food **Unlimited** case corresponds to turning off all clam and background mortality due to hypoxia. A Short hypoxic duration was used in all scenarios.

	Short Duration, Max Extent Hypoxia											
	≈ 15%			**≈ 30%**			**≈ 45%**			**≈ 60%**		
Food Level	**Limit**	**Def**	**Unlim**	**Limit**	**Def**	**Unlim**	**Limit**	**Def**	**Unlim**	**Limit**	**Def**	**Unlim**
Max % Hypoxic	18.6 (6.7)	17.7 (6.5)	19.4 (6.2)	33.9 (7.4)	28.1 (7.2)	30.9 (7)	49.9 (6.8)	44.9 (7.2)	46.8 (6.8)	61.8 (6.5)	61.9 (6.2)	62.9 (6)
% Hypoxic	6 (5.6)	5.7 (5.3)	6.8 (5.7)	13.5 (9.1)	10.7 (7.7)	12.6 (8.2)	24.9 (12)	20.9 (11.3)	23.3 (11.1)	36.8 (12.9)	36.9 (13)	38.3 (12.7)
DO (mg/L)	5.5 (0.7)	5.5 (0.7)	5.4 (0.7)	5.1 (0.8)	5.2 (0.8)	5.2 (0.8)	4.7 (0.9)	4.8 (0.8)	4.8 (0.9)	4.1 (0.9)	4.1 (0.9)	4 (0.9)
Hypoxic Edge (10^{-2} m/m^2)	1.14 (0.87)	1.12 (0.85)	1.26 (0.86)	2.16 (1.2)	1.82 (1.07)	2.05 (1.06)	3.34 (1.21)	3.04 (1.28)	3.29 (1.18)	4.13 (0.95)	4.13 (0.94)	4.18 (0.89)
Clam Density (#/m^2)												

continued on next page

	Short Duration, Max Extent Hypoxia											
	≈ 15%			**≈ 30%**			**≈ 45%**			**≈ 60%**		
Food Level	**Limit**	**Def**	**Unlim**	**Limit**	**Def**	**Unlim**	**Limit**	**Def**	**Unlim**	**Limit**	**Def**	**Unlim**
	448 (39)	915 (73)	915 (58)	441 (51)	914 (89)	928 (55)	436 (83)	893 (128)	947 (53)	384 (111)	774 (230)	983 (52)
Crab Biomass (g/m^2)	4.63 (0.36)	7.84 (0.8)	7.99 (0.86)	3.62 (0.47)	6.84 (0.87)	6.92 (0.83)	2.69 (0.42)	5.29 (0.77)	5.53 (0.71)	1.8 (0.3)	2.83 (0.42)	3.78 (0.55)
Mat Female Mass (g)	254.4 (10.1)	239.2 (5.9)	239.4 (6.4)	244.5 (8.6)	242.2 (8.3)	239 (6.5)	240 (12.4)	234.1 (6.3)	238.5 (6.8)	225.5 (13.6)	223.4 (8)	240.3 (8.9)
Mat Female CW (cm)	17.7 (0.1)	17.4 (0.1)	17.5 (0.1)	17.6 (0.1)	17.5 (0.1)	17.5 (0.1)	17.6 (0.2)	17.5 (0.1)	17.5 (0.1)	17.5 (0.3)	17.4 (0.2)	17.5 (0.2)
Egg ($\#/m^2$ hr)	8.88 (9.4)	19.04 (13.38)	19.3 (14.2)	6.91 (7.76)	16.67 (12.55)	16.39 (12.52)	3.62 (5.45)	10.83 (9.94)	12.45 (10.92)	1.24 (3.27)	3.28 (5.8)	7.33 (8.36)
Egg per Mat Fe (#/# hr)	1451 (1544)	1794 (1250)	1832 (1319)	1442 (1621)	1893 (1418)	1918 (1467)	1008 (1521)	1828 (1655)	1961 (1704)	744 (2170)	1283 (2289)	2004 (2285)
Recruit 7 ($10^{-6}\#/m^2$ hr)	78.91 (282.99)	133.85 (456.73)	145.21 (509.53)	67.36 (255.09)	131.47 (468.41)	126.12 (451.22)	41.92 (170.24)	95.45 (325.31)	107.33 (363.06)	18.38 (97.89)	38.79 (162.63)	79.41 (285.18)
Recruit 12 ($10^{-6}\#/m^2$ hr)	5.05	14.28	15.51	5.73	15.92	16.95	4.92	15.33	16.15	3.49	8.51	12.19

continued on next page

	Short Duration, Max Extent Hypoxia											
	≈ 15%			**≈ 30%**			**≈ 45%**			**≈ 60%**		
Food Level	**Limit**	**Def**	**Unlim**	**Limit**	**Def**	**Unlim**	**Limit**	**Def**	**Unlim**	**Limit**	**Def**	**Unlim**
	(8.43)	(25.53)	(27.74)	(9.56)	(29.51)	(31.87)	(8.62)	(28.66)	(30.72)	(6.68)	(15.94)	(22.72)
Recruit 18 (10^{-6}#/m^2 hr)	1.2 (1.91)	2.36 (3.7)	2.45 (3.89)	1.13 (1.87)	2.12 (3.51)	2.18 (3.69)	0.85 (1.61)	1.73 (3.06)	1.77 (3.14)	0.62 (1.32)	1.06 (2.08)	1.28 (2.45)
Gut Fullness 7-12	0.271 (0.055)	0.366 (0.07)	0.39 (0.069)	0.283 (0.056)	0.4 (0.069)	0.429 (0.077)	0.285 (0.049)	0.438 (0.077)	0.451 (0.091)	0.306 (0.063)	0.394 (0.078)	0.459 (0.123)
Gut Fullness 13-17	0.372 (0.041)	0.445 (0.032)	0.452 (0.031)	0.386 (0.04)	0.459 (0.033)	0.47 (0.031)	0.409 (0.043)	0.478 (0.03)	0.485 (0.028)	0.393 (0.058)	0.464 (0.039)	0.497 (0.027)
Gut Fullness 18+	0.311 (0.043)	0.43 (0.037)	0.443 (0.036)	0.336 (0.045)	0.455 (0.035)	0.478 (0.031)	0.308 (0.044)	0.492 (0.031)	0.505 (0.027)	0.319 (0.048)	0.452 (0.044)	0.518 (0.029)
Food Qual 7-12	0.344 (0.018)	0.347 (0.015)	0.347 (0.015)	0.345 (0.018)	0.347 (0.014)	0.347 (0.014)	0.345 (0.022)	0.347 (0.014)	0.345 (0.031)	0.347 (0.025)	0.35 (0.019)	0.336 (0.063)
Food Qual 13-17	0.426 (0.009)	0.415 (0.007)	0.411 (0.007)	0.42 (0.008)	0.409 (0.007)	0.404 (0.006)	0.414 (0.009)	0.402 (0.006)	0.4 (0.006)	0.419 (0.011)	0.405 (0.01)	0.4 (0.008)
Food Qual 18+	0.424 (0.01)	0.402 (0.008)	0.397 (0.008)	0.418 (0.01)	0.396 (0.008)	0.389 (0.007)	0.422 (0.012)	0.385 (0.006)	0.386 (0.005)	0.41 (0.013)	0.386 (0.009)	0.385 (0.007)

continued on next page

	Short Duration, Max Extent Hypoxia											
	≈ 15%			**≈ 30%**			**≈ 45%**			**≈ 60%**		
Food Level	**Limit**	**Def**	**Unlim**	**Limit**	**Def**	**Unlim**	**Limit**	**Def**	**Unlim**	**Limit**	**Def**	**Unlim**
Death Aggr 7-12 (10^{-4}/hr)	3.84 (2.96)	6.63 (4.83)	7.2 (5.09)	4.11 (2.83)	7.31 (5.08)	7.81 (5.58)	3.46 (2.59)	7.79 (5.82)	8.87 (14.06)	3.28 (3.43)	5.74 (5.33)	8.7 (10.36)
Death Aggr 13-17 (10^{-4}/hr)	4.82 (3.02)	7.31 (3.16)	7.39 (3.22)	5.87 (3.61)	8.24 (3.78)	8.34 (3.79)	6.67 (4.43)	8.89 (4.47)	9.12 (4.57)	6.38 (4.86)	8.31 (5.11)	9.09 (5.2)
Death Aggr 18+ (10^{-4}/hr)	1.85 (1.8)	2.4 (1.82)	2.44 (1.76)	2.43 (2.36)	2.61 (2.05)	2.6 (2.08)	2.53 (2.78)	2.93 (2.61)	2.75 (2.41)	2.99 (3.86)	3.26 (3.31)	3.01 (2.91)

Table C.4: Estuary wide summaries for altering cannibalism potential via *maximum interaction distance* (Section A.5.3). Additional variables are given in Table 3. The **Default** interaction distance corresponds to the value used in previous simulations, **Small** to decreasing this distance by a factor of 4 and **Large** represents doubling it. All simulations done using Short hypoxic duration (Table C.2).

	Short Duration, Max Extent Hypoxia											
	≈ 15%			**≈ 30%**			**≈ 45%**			**≈ 60%**		
Interact Dist	**Small**	**Default**	**Large**	**Small**	**Default**	**Large**	**Small**	**Default**	**Large**	**Small**	**Default**	**Large**
Max % Hypoxic	15.4 (6)	17.7 (6.5)	19 (6.3)	25.8 (7.2)	28.1 (7.2)	29.2 (7)	43.2 (7.3)	44.9 (7.2)	45.7 (7.2)	61.4 (6.3)	61.9 (6.2)	62.3 (6.3)
% Hypoxic	4.7 (4.7)	5.7 (5.3)	6.3 (5.6)	9.5 (7.3)	10.7 (7.7)	11.4 (8)	19.7 (11)	20.9 (11.3)	21.5 (11.4)	36.4 (12.9)	36.9 (13)	37.1 (13)
DO (mg/L)	5.5 (0.7)	5.5 (0.7)	5.4 (0.7)	5.3 (0.8)	5.2 (0.8)	5.2 (0.8)	4.9 (0.8)	4.8 (0.8)	4.8 (0.8)	4.1 (0.9)	4.1 (0.9)	4.1 (0.9)
Hypoxic Edge (10^{-2} m/m^2)	0.98 (0.82)	1.12 (0.85)	1.18 (0.86)	1.66 (1.03)	1.82 (1.07)	1.91 (1.1)	2.9 (1.27)	3.04 (1.28)	3.1 (1.28)	4.11 (0.95)	4.13 (0.94)	4.14 (0.94)
Clam Density (#/m^2)	878 (85)	915 (73)	952 (64)	888 (95)	914 (89)	951 (80)	864 (132)	893 (128)	923 (122)	758 (234)	774 (230)	789 (218)

continued on next page

	Short Duration, Max Extent Hypoxia											
	≈ 15%			≈ 30%			≈ 45%			≈ 60%		
Interact Dist	**Small**	**Default**	**Large**	**Small**	**Default**	**Large**	**Small**	**Default**	**Large**	**Small**	**Default**	**Large**
Crab Biomass (g/m^2)	12.1 (0.85)	7.84 (0.8)	4.67 (0.38)	9.93 (1.43)	6.84 (0.87)	3.62 (0.32)	8.29 (0.89)	5.29 (0.77)	2.63 (0.29)	4.43 (0.78)	2.83 (0.42)	1.65 (0.23)
Mat Female Mass (g)	252 (8.7)	239.2 (5.9)	243 (8.6)	260.4 (8.6)	242.2 (8.3)	236.6 (9.1)	246.2 (8.1)	234.1 (6.3)	229.8 (8.5)	218.8 (12)	223.4 (8)	218.6 (11.9)
Mat Female CW (cm)	17.8 (0.1)	17.4 (0.1)	17.3 (0.1)	17.7 (0.1)	17.5 (0.1)	17.1 (0.2)	17.7 (0.1)	17.5 (0.1)	17.2 (0.2)	17.6 (0.1)	17.4 (0.2)	17.1 (0.3)
Egg ($\#/m^2$ hr)	16.45 (12.75)	19.04 (13.38)	14.28 (11.18)	15.08 (12.9)	16.67 (12.55)	9.89 (9.55)	8.45 (9.46)	10.83 (9.94)	6.79 (7.68)	2.19 (4.64)	3.28 (5.8)	3.01 (5.14)
Egg per Mat Fe (#/# hr)	971 (749)	1794 (1250)	2203 (1732)	1036 (878)	1893 (1418)	2131 (2061)	704 (784)	1828 (1655)	2092 (2365)	387 (828)	1283 (2289)	1919 (3372)
Recruit 7 ($10^{-6}\#/m^2$ hr)	121.11 (472.82)	133.85 (456.73)	119.67 (414.75)	116.8 (451.65)	131.47 (468.41)	91.53 (326.21)	84.46 (329.71)	95.45 (325.31)	70.87 (257.33)	27.41 (144.76)	38.79 (162.63)	37.4 (158.16)
Recruit 12 ($10^{-6}\#/m^2$ hr)	5.29 (9.98)	14.28 (25.53)	11.27 (22.15)	4.69 (8.92)	15.92 (29.51)	10.2 (19.52)	5.15 (9.15)	15.33 (28.66)	9.04 (17.51)	2.83 (5.82)	8.51 (15.94)	6.05 (11.35)

continued on next page

	Short Duration, Max Extent Hypoxia											
	≈ 15%			**≈ 30%**			**≈ 45%**			**≈ 60%**		
Interact Dist	**Small**	**Default**	**Large**	**Small**	**Default**	**Large**	**Small**	**Default**	**Large**	**Small**	**Default**	**Large**
Recruit 18 (10^{-6}#/m^2 hr)	2.05 (2.79)	2.36 (3.7)	1.24 (2.47)	1.65 (2.28)	2.12 (3.51)	1.03 (2.11)	1.58 (2.3)	1.73 (3.06)	0.83 (1.85)	1 (1.83)	1.06 (2.08)	0.56 (1.36)
Gut Fullness 7-12	0.201 (0.038)	0.366 (0.07)	0.421 (0.186)	0.195 (0.044)	0.4 (0.069)	0.395 (0.203)	0.205 (0.042)	0.438 (0.077)	0.391 (0.199)	0.195 (0.057)	0.394 (0.078)	0.371 (0.21)
Gut Fullness 13-17	0.232 (0.047)	0.445 (0.032)	0.504 (0.028)	0.248 (0.048)	0.459 (0.033)	0.503 (0.032)	0.282 (0.047)	0.478 (0.03)	0.502 (0.039)	0.294 (0.062)	0.464 (0.039)	0.503 (0.049)
Gut Fullness 18+	0.189 (0.038)	0.43 (0.037)	0.532 (0.019)	0.187 (0.046)	0.455 (0.035)	0.534 (0.022)	0.181 (0.035)	0.492 (0.031)	0.533 (0.026)	0.19 (0.035)	0.452 (0.044)	0.529 (0.035)
Food Qual 7-12	0.343 (0.027)	0.347 (0.015)	0.299 (0.119)	0.343 (0.032)	0.347 (0.014)	0.282 (0.134)	0.344 (0.033)	0.347 (0.014)	0.283 (0.135)	0.35 (0.042)	0.35 (0.019)	0.271 (0.144)
Food Qual 13-17	0.433 (0.02)	0.415 (0.007)	0.414 (0.01)	0.425 (0.022)	0.409 (0.007)	0.415 (0.01)	0.42 (0.019)	0.402 (0.006)	0.416 (0.011)	0.437 (0.019)	0.405 (0.01)	0.413 (0.017)
Food Qual 18+	0.444 (0.013)	0.402 (0.008)	0.39 (0.005)	0.452 (0.012)	0.396 (0.008)	0.391 (0.006)	0.445 (0.014)	0.385 (0.006)	0.39 (0.007)	0.437 (0.018)	0.386 (0.009)	0.382 (0.008)
Death Aggr 7-12 (10^{-4}/hr)												

continued on next page

	Short Duration, Max Extent Hypoxia											
	≈ 15%			**≈ 30%**			**≈ 45%**			**≈ 60%**		
Interact Dist	**Small**	**Default**	**Large**	**Small**	**Default**	**Large**	**Small**	**Default**	**Large**	**Small**	**Default**	**Large**
	1.42 (1.18)	6.63 (4.83)	12.11 (19.65)	1.21 (1.17)	7.31 (5.08)	11.65 (22.6)	1.24 (1.13)	7.79 (5.82)	11.24 (22.35)	0.64 (1.38)	5.74 (5.33)	8.38 (13.92)
Death Aggr 13-17 (10^{-4}/hr)	1.74 (1.37)	7.31 (3.16)	9.3 (5.13)	2.2 (1.62)	8.24 (3.78)	9.9 (6.55)	2.95 (2.04)	8.89 (4.47)	10.29 (7.96)	2.91 (2.88)	8.31 (5.11)	10.49 (15.52)
Death Aggr 18+ (10^{-4}/hr)	0.61 (0.61)	2.4 (1.82)	2.06 (1.83)	0.85 (0.81)	2.61 (2.05)	2.29 (2.21)	1.03 (1.04)	2.93 (2.61)	2.76 (3.08)	1.26 (1.44)	3.26 (3.31)	2.93 (3.97)

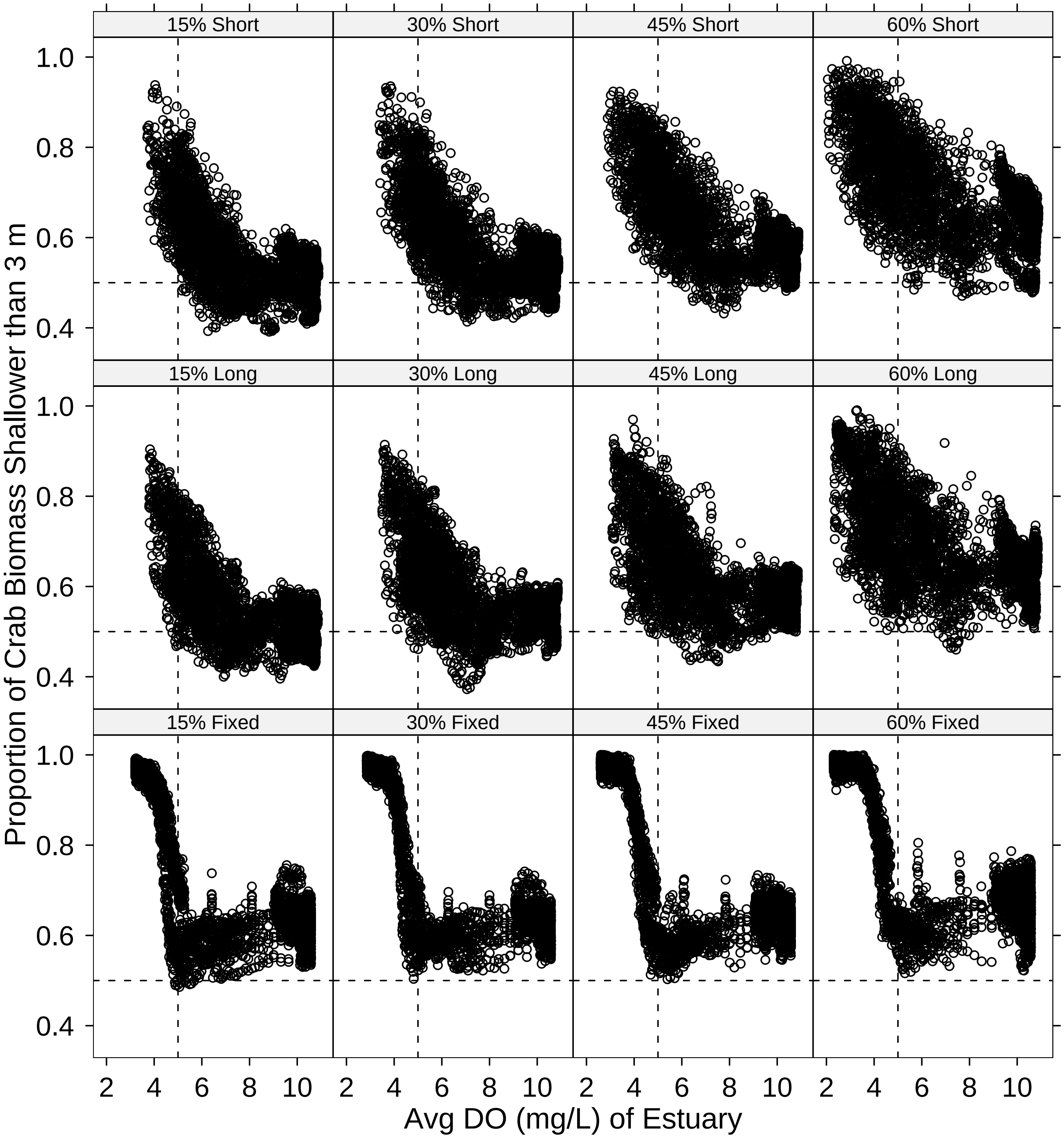

Fig. C.1: Proportion of total crab biomass shallower than 3 m vs the average DO in the estuary from the beginning of year 30 to the end of year 39 under the different hypoxic extents and durations.

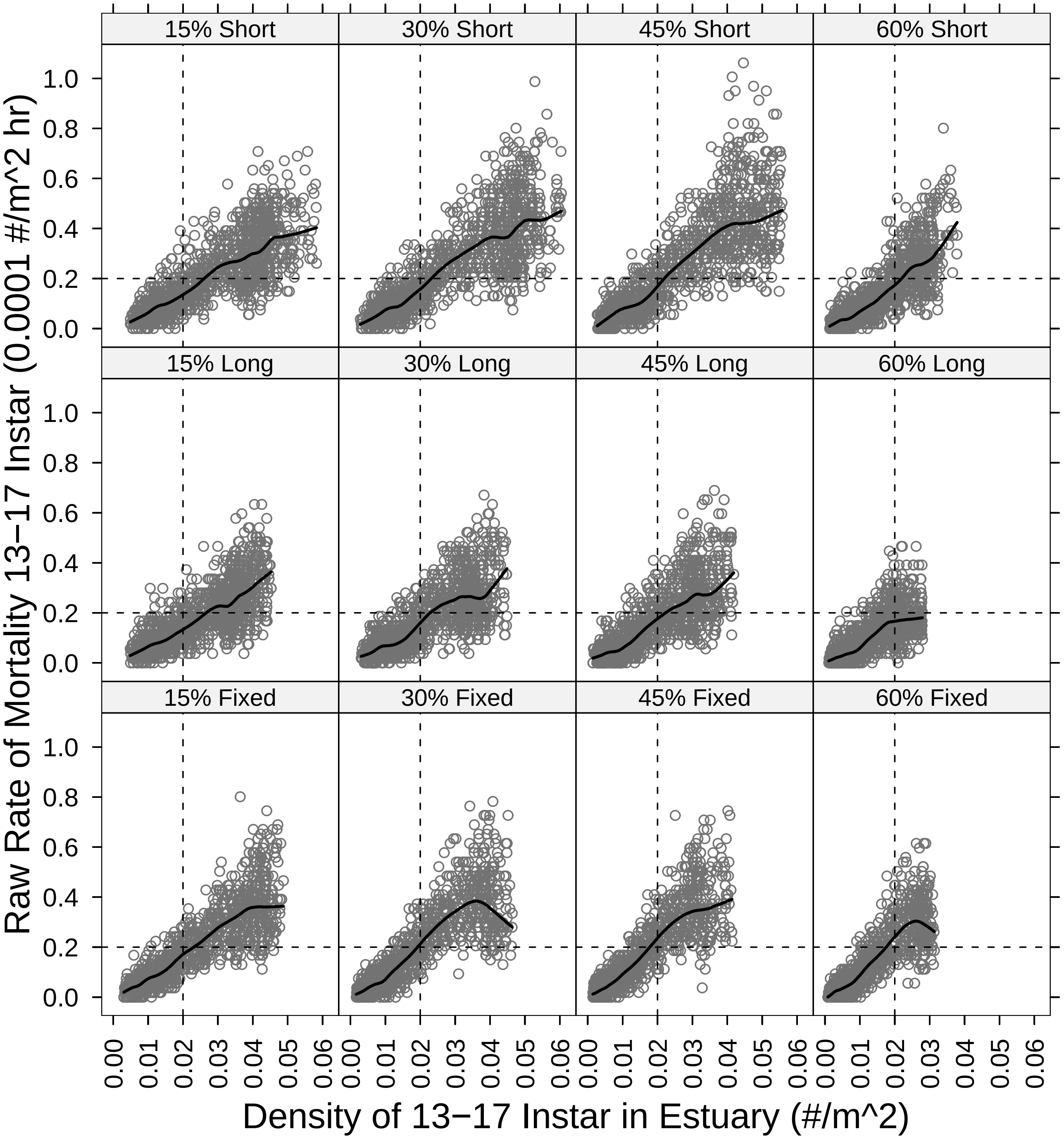

Fig. C.2: Rate of mortality ($\#.m^{-2}.hr^{-1}$) from all causes of 13 to 17 instar crabs relative to the density ($\#/m^2$) of 13 to 17 instar crabs in the estuary for the different hypoxic durations considered. Solid line generated using a Loess smoother.

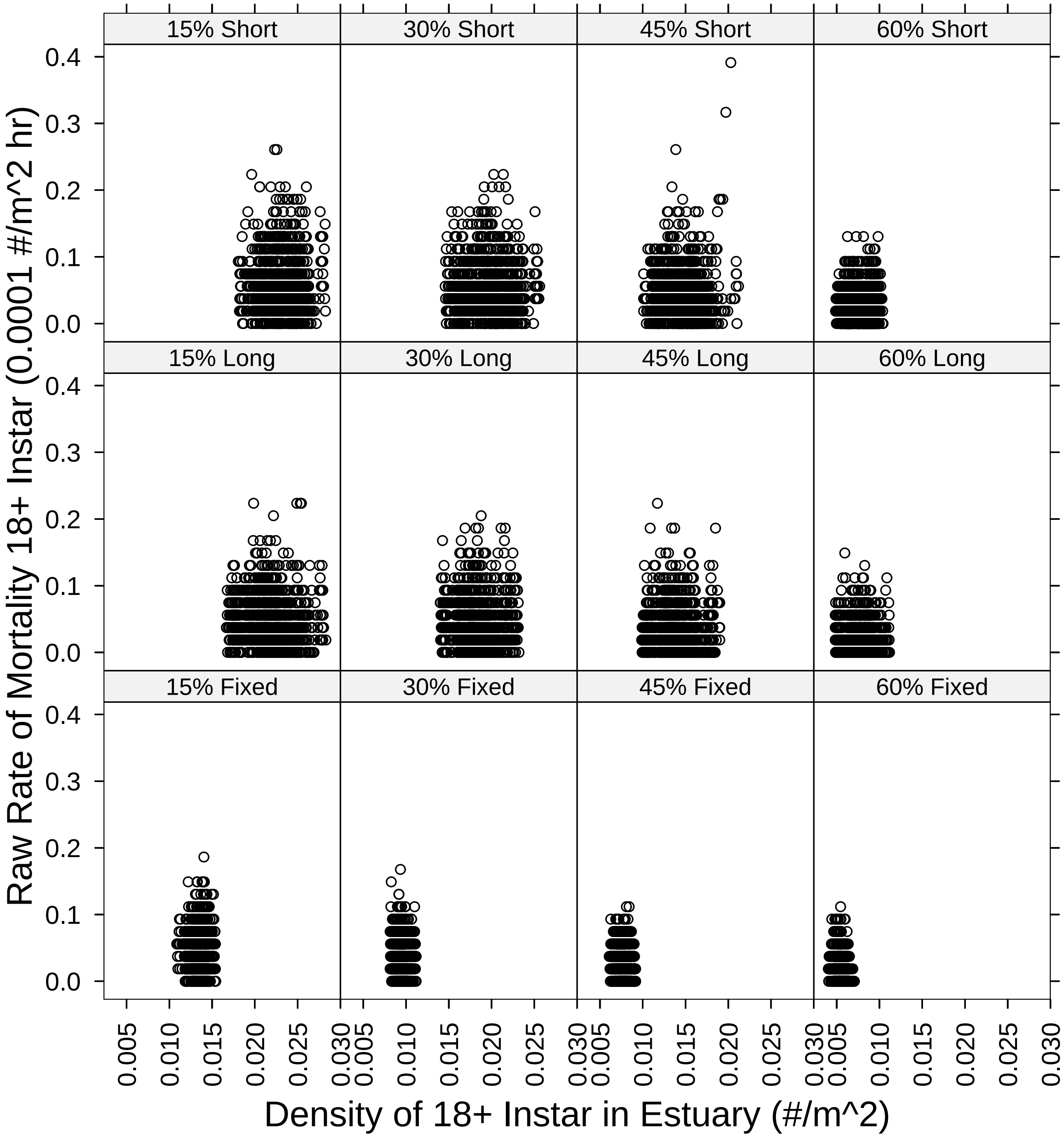

Fig. C.3: Rate of mortality ($\#.\mathrm{m}^{-2}.\mathrm{hr}^{-1}$) from all causes of 18+ instar crabs relative to the density ($\#/\mathrm{m}^2$) of 18+ instar crabs in the estuary for the different hypoxic durations considered.

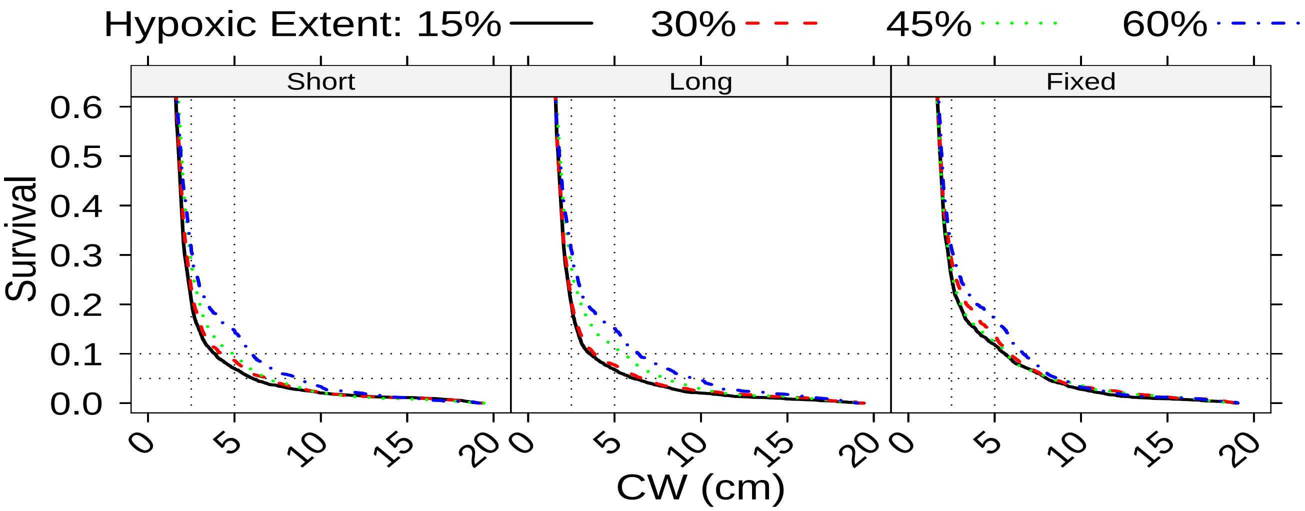

Fig. C.4: Crab survival function under three hypoxic durations and four hypoxic extents.

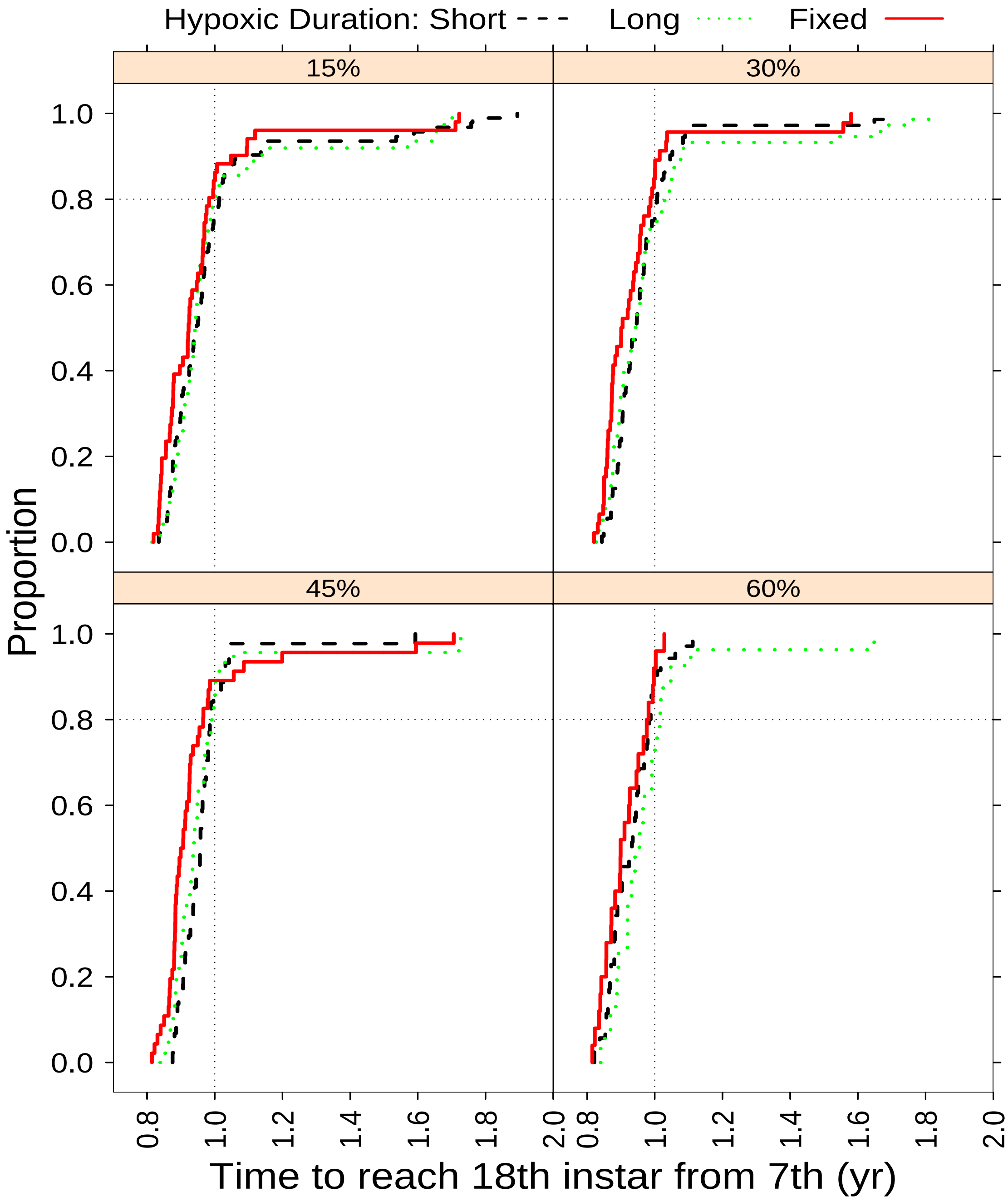

Fig. C.5: Empirical cumulative distribution function for the time it takes crabs under different hypoxic extents and durations to reach the 18th instar from the 7th.

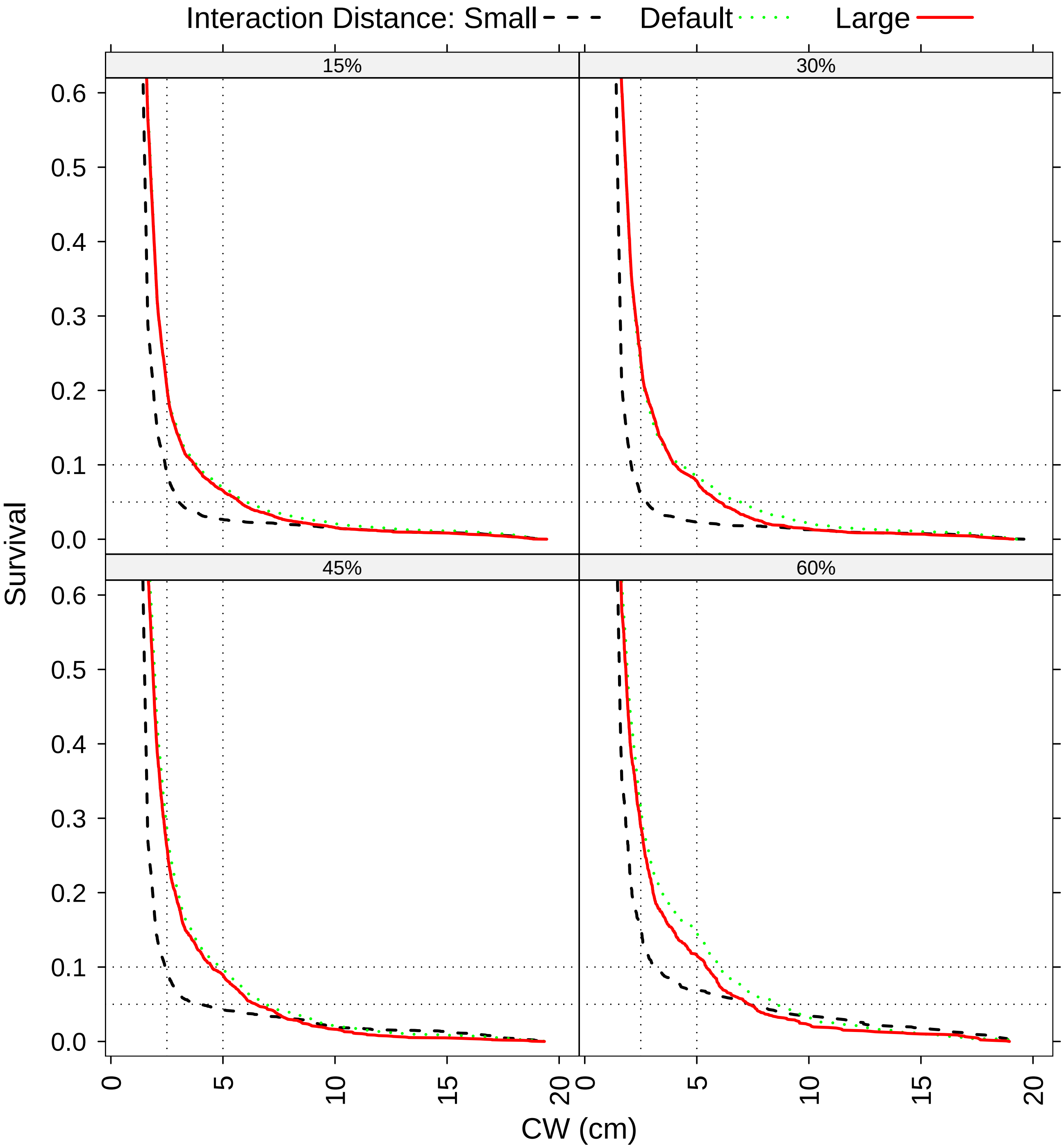

Fig. C.6: Effect of altering the *maximum interaction distance* in Scenario III on crab survival. Default corresponds to the default interaction distance used, Small to decreasing this distance by a factor of 4 and Large represents doubling it. All simulations done using Short hypoxic duration. Compare to Figs C.4 and Fig 9 in the paper.

References

Bachelet, G. (1980) Growth and recruitment of the tellinid bivalve *Macoma balthica* at the sourthern limit of its geographical distribution, the Gironde Estuary (SW France). *Marine Biology* **59**, pp. 105–117.

Balci, O. (1994) Validation, verification, and testing techniques throughout the life cycle of a simulation study. *Annals of Operations Research* **53**, pp. 121–173.

Balci, O. (1997) Principles of simulation model validation, verification, and testing. *Transactions of the Society for computer simulation international* **14**, pp. 3–12.

Bänsch, E. (1991) Local mesh refinement in 2 and 3 dimensions. *Impact of Computing in Science and Engineering* **3**, pp. 181–191.

Bensch, A., Bacher, C., Baud, J. & Martin, J. L. (1992) Modélisation de la croissance de *Ruditapes philippinarum* dans un système expérimental. *IFREMER Actes de Colloques* **13**, pp. 71–82.

Beukema, J. J. & de Vlas, J. (1989) Tidal-current transport of thread-drifting postlarval juveniles of the bivalve *Macoma balthica* from the Wadden Sea to the North Sea. *Marine Ecology Progress Series* **52**, pp. 193–200.

Booth, C. E. & McMahon, B. R. (1992) Aerobic capacity of the blue crab, *Callinectes sapidus. Physiological Zoology* **65**, pp. 1074–1091.

Borsuk, M., Higdon, D., Stow, C. & Reckhow, K. (2001a) A Bayesian hierarchical model to predict benthic oxygen demand from organic matter loading in estuaries and coastal zones. *Ecological Modelling* **143**, pp. 165–181.

Borsuk, M., Powers, S. & Peterson, C. (2002) A survival model of the effects of bottom-water hypoxia on the population density of an estuarine clam (*Macoma balthica*). *Canadian Journal of Fisheries and Aquatic Sciences* **59**, pp. 1266–1274.

Borsuk, M. E., Stow, C. A., Luettich Jr., R. A., Paerl, H. W. & Pinckney, J. L. (2001b) Modelling oxygen dynamics in an intermittently stratified estuary: estimation of process rates using field data. *Estuarine, Coastal and Shelf Science* **52**, pp. 33–49.

Bouma, H., Duiker, J., de Vries, P. P., Herman, P. & Wolff, W. J. (2001) Spatial pattern of early recruitment of *Macoma balthica* (L.) and *Cerastoderma edule* (L.) in relation to sediment dynamics on a highly dynamic intertidal sandflat. *Journal of Sea Research* **45**, pp. 79–93.

Bourget, E. (1983) Seasonal variations of cold tolerance in intertidal mollusks and relation to environmental conditions in the St Lawrence Estuary. *Canadian Journal of Zoology* **61**, pp. 1193–1201.

Braess, D. (1997) *Finite Elements*. Cambridge University Press.

Buzzelli, C. P., Luettich Jr, R. A., Powers, S. P., Peterson, C. H., McNinch, J. E., Pinckey, J. L. & Paerl, H. W. (2002) Estimating the spatial extent of bottom-water hypoxia and habitat degradation in a shallow estuary. *Marine Ecology Progress Series* **230**, pp. 103–112.

Cadman, L. R. & Weinstein, M. P. (1985) Size-weight relationships of postecdysial juvenile blue crabs (*Callinectes sapidus* Rathbun) from the lower Chesapeake Bay. *Journal of Crustacean Biology* **5**, pp. 306–310.

Chapra, S. C. (1997) *Surface Water-Quality Modeling*. New York: McGraw-Hill.

Churchill Jr., E. P. (1917-1918) Life history of the blue crab. *Bulletin of the U.S. Bureau of Fisheries* **36**.

Clark, M. E., Wolcott, T. G., Wolcott, D. L. & Hines, A. H. (1999) Foraging and agonistic activity co-occur in free-ranging blue crabs (*Callinectes sapidus*): observation of animals by ultrasonic telemetry. *Journal of Experimental Marine Biology and Ecology* **233**, pp. 143–160.

Commito, J. A. (1982) Effects of *Lunatia heros* predation on the population dynamics of *Mya arenaria* and *Macoma balthica* in Maine, USA. *Marine Biology* **69**, pp. 187–193.

Crisp, D. J. (1984) Energy flow measurement. In: *Methods for the study of marine benthos* (Holme, H. A. & McIntyre, A. D., eds.), chap. 9. Blackwell Scientific Publications, 2 edn.

Cummins, K. W. & Wuycheck, J. C. (1971) Caloric equivalents for investigations in ecological energetics. *International Association of Theoretical and Applied Limnology. Mitteilungen. Communications* **18**, pp. 1–120.

Das, T. & Stickle, W. B. (1993) Sensitivity of crabs *Callinectes sapidus* and *C. similis* and the gastropod *Stramonita haemastoma* to hypoxia and anoxia. *Marine Ecology Progress Series* **98**, pp. 263–274.

Das, T. & Stickle, W. B. (1994) Detection and avoidance of hypoxic water by juvenile *Callinectes sapidus* and *C. similis*. *Marine Biology* **120**, pp. 593–600.

Dietrich, C. R. & Newsam, G. N. (1993) A fast and exact method for multidimensional gaussian stochastic simulations. *Water Resources Research* **29**, pp. 2861–2869.

Dittel, A. I., Hines, A. H., Ruiz, G. M. & Ruffin, K. K. (1995) Effects of shallow water refuge on behavior and density-dependent mortality of juvenile blue crabs in Chesapeake Bay. *Bulletin of Marine Science* **57**, pp. 902–916.

Eggleston, D. B. (1990) Foraging behavior of the blue crab, *Callinectes sapidus* on juvenile oysters, *Crassostrea virginica*: effects of prey density and size. *Bulletin of Marine Science* **46**, pp. 62–82.

Eggleston, D. B. (1998) Population dynamics of the blue crab in North Carolina: statistical analyses of fisheries survey data. Tech. rep., North Carolina State University, Department of Marine, Earth and Atmospheric Sciences, Raleigh NC, 27695-8208. Final report for contract M-6053 to the North Carolina Department of Environmental Health and Natural Resources, Division of Marine Fisheries.

Epifanio, C. E. (1995) Transport of blue crab (*Callinectes sapidus*) larvae in the waters off mid-Atlantic states. *Bulletin of Marine Science* **57**, pp. 713–725.

Etherington, L. L. & Eggleston, D. B. (2000) Large-scale blue crab recruitment: linking postlarval transport, post-settlement planktonic dispersal, and multiple nursery habitats. *Marine Ecology Progress Series* **204**, pp. 179–198.

Fisher, M. R. (1999) Effect of temperature and salinity on size at maturity of female blue crabs. *Transactions of the American Fisheries Society* **128**, pp. 499–506.

Freeman, J. A., Kilgus, G., Laurendeau, D. & Perry, H. M. (1987) Postmolt and intermolt molt cycle stages of *Callinectes sapidus*. *Aquaculture* **61**, pp. 201–209.

Garvine, R. W., Epifanio, C. E., Epifanio, C. C. & Wong, K.-C. (1997) Transport and recruitment of blue crab larvae: a model with advection and mortality. *Estuarine, Coastal and Shelf Science* **45**, pp. 99–111.

Gilbert, M. A. (1973) Growth rate, longevity and maximum size of *Macoma balthica* (L.). *Biological Bulletin* **145**, pp. 119–126.

Gilbert, M. A. (1978) Aspects of the reproductive cycle in *Macoma balthica* (bivalvia). *The Nautilus* **92**, pp. 21–24.

Guerin, J. L. & Stickle, W. B. (1992) Effects of salinity gradients on the tolerance and bioenergetics of juvenile blue crabs (*Callinectes sapidus*) from water of different environmental salinities. *Marine Biology* **114**, pp. 391–396.

Harvey, M. & Vincent, B. (1989) Spatial and temporal variations of the reproductive cycle and energy allocation of the bivalve *Macoma balthica* (L.) on a tidal flat. *Journal of Experiemental Marine Biology and Ecology* **129**, pp. 199–217.

Heck Jr, K. L. & Coen, L. D. (1995) Predation and the abundance of juvenile blue crabs: a comparison of selected east and gulf coast (USA) studies. *Bulletin of Marine Science* **57**, pp. 877–883.

Hines, A. H. (In Press) Ecology of juvenile and adult blue crabs. In: *Biology of the Blue Crab* (Kennedy, V. S. & Cronin, L. E., eds.). College Park: Maryland Sea Grant College Program, pp. xx–xx.

Hines, A. H. & Comtois, K. (1985) Vertical distribution of infauna in sediments of a subestuary of central Chesapeake Bay. *Estuaries* **8**, pp. 296–304.

Hines, A. H. & Ruiz, G. M. (1995) Temporal variation in juvenile blue crab mortality: Nearshore shallows and cannibalism in Chesapeake Bay. *Bulletin of Marine Science* **57**, pp. 884–901.

Holland, A. F., Mountford, N. K., Hiegel, M. H., Kaumeyer, K. R. & Mihursky, J. A. (1980) Influence of predation on infaunal abundance in Upper Chesapeake Bay. *Marine Biology* **57**, pp. 221–235.

Holland, A. F., Mountford, N. K. & Mihursky, J. A. (1977) Temporal variation in upper bay mesohaline benthic communities: I. The 9-m mud habitat. *Chesapeake Science* **18**, pp. 370–378.

Holland, A. F., Shaughnessy, A. T. & Hiegel, M. H. (1987) Long-term variation in mesohaline Chesapeake Bay macrobenthos: spatial and temporal patterns. *Estuaries* **10**, pp. 227–245.

Honkoop, P. J. C. & Beukema, J. J. (1997) Loss of body mass in winter in three intertidal bivalve species: and experiemental and observation study of the interacting effects between water temperature, feeding time and feeding behaviour. *Journal of Experimental Marine Biology and Ecology* **212**, pp. 277–297.

Honkoop, P. J. C., van der Meer, J., Beukema, J. J. & Kwast, K. (1998) Does temperature-influenced egg production predict the recruitment in the bivalve *Macoma balthica*? *Marine Ecology Progress Series* **164**, pp. 229–235.

Houlihan, D. F., Govind, C. K. & Haj, A. E. (1985) Energetics of swiming in *Callinectes sapidus* and walking in *Homarus americanus*. *Comparative biochemistry and physiology. A* **82**, pp. 267–279.

Hummel, H. (1985a) An energy budget for a *Macoma balthica* (Mollusca) population living on a tidal flat in the Dutch Wadden sea. *Netherlands Journal of Sea Research* **19**, pp. 84–92.

Hummel, H. (1985b) Food intake of *Macoma balthica* (mollusca) in relation to seasonal changes in its potential food on a tidal flat in the Dutch Wadden Sea. *Netherlands Journal of Sea Research* **19**, pp. 52–76.

Hyer, P. V., Fang, C. S., Ruzecki, E. P. & Hargis Jr., W. J. (1971) Hydrography and hydrodynamics of virginia estuaries. II. Studies of the distribution of salinity and dissolved oxygen in the upper York system. Tech. Rep. 13, Virginia Institute of Marine Science, Gloucester Point, Virginia. Special Report in Applied and Marine Science and Ocean Engineering.

Ihaka, R. & Gentleman, R. (1996) R: A language for data analysis and graphics. *Journal of Computational and Graphical Statistics* **5**, pp. 299–314.

Jachowski, R. L. (1974) Agonistic behavior of the blue crab, *Callinectes sapidus* Rathbun. *Behaviour* **50**, pp. 232–253.

Kannupandi, T., Krishnan, T., Soundarapandian, P. & Shanmugam, A. (1999) Yolk utilization in an estuarine edible crab *Thalamita crenata* (Latreille). *Indian Journal of Fisheries* **46**, pp. 289–294.

Kennedy, V. S. & Mihursky, J. A. (1971) Upper temperature tolerances of some estuarine bivalves. *Chesapeake Science* **12**, pp. 193–204.

Kim, S. Y. (1990) *Physical processes and fine-grained sediment dynamics in the Neuse River Estuary, North Carolina*. Ph.D. thesis, University of North Carolina, Chapel Hill, NC.

Kitchell, J. & Stewart, D. (1977) Applications of a bioenergetics model to yellow perch (*Perca flavescens*) and walleye (*Stizostedion vitreum vitreum*). *Journal of the Fisheries Research Board Canada* **35**, pp. 1922–1935.

Kleijnen, J. P. (1995) Verification and validation of simulation models. *European Journal of Operational Research* **82**, pp. 145–162.

Laird, C. E. & Haefner Jr, P. A. (1976) Effects of intrinsic and environmental factors on oxygen consumption in the blue crab *Callinectes sapidus* Rathbun. *Journal of Experimental Marine Biology and Ecology* **22**, pp. 171–178.

Laughlin, R. A. (1982) Feeding habits of the blue crab *Callinectes sapidus* Rathbun in the Apalachicola estuary, Florida. *Bulletin of Marine Science* **32**, pp. 807–822.

Leffler, C. W. (1972) Some effects of temperature on the growth and metabolic rate of juvenile blue crabs *Callinectes sapidus*, in the laboratory. *Marine Biology* **14**, pp. 104–110.

Lipcius, R. N., Seitz, R. D., Seebo, M. S. & Colón-Carrión, D. (2005) Density, abundance and survival of the blue crab in seagrass and unstructured salt marsh nurseries of Chesapeake Bay. *Journal of Experimental Marine Biology and Ecology* **319**, pp. 69–80.

deFur, P. L. (1990) Respiration during ecdysis at low salinity in blue crabs, *Callinectes sapidus* Rathbun. *Bulletin of Marine Science* **46**, pp. 48–54.

Lowery, T. A. & Tate, L. G. (1986) Effect of hypoxia on hemolymph lactate and behavior of the blue crab *Callinectes sapidus* Rathbun in the laboratory and field. *Comparative Biochemistry and Physiology* **85A**, pp. 689–692.

Luettich Jr., R. A., Martens, C. S., McNinch, J. E., Paerl, H. W., Pinckney, J. L., Peterson, C. H., Alperin, M. & Wells, J. T. (1999) Neuse river estuary MODeling and MONitoring project: Monitoring phase. Tech. Rep. Draft 4, Water Resources Research Institute of the University of North Carolina.

Mantelatto, F. L. M. & Christofoletti, R. A. (2001) Natural feeding activity of the crab *Callinectes ornatus* (Portunidae) in Ubatuba Bay (Sao Paulo, Brazil): influence of season, sex, size and molt stage. *Marine Biology* **138**, pp. 585–594.

Mauersberger, P. (1983) General principles in deterministic water quality modeling. In: *Mathematical Modeling of Water Quality* (Orlob, G., ed.), chap. 3. New York: John Wiley and Sons, pp. 42–115.

McErlean, A. J. (1964) Characteristics of *Macoma balthica* populations in the middle Patuxent Estuary. *Chesapeake Science* **5**, pp. 200–208.

McGaw, I. J. & Reiber, C. L. (2000) Integrated physiological responses to feeding in the blue crab *Callinectes sapidus*. *The Journal of Experimental Biology* **203**, pp. 359–368.

McMahon, B. R. (2001) Respiratory and circulatory compensation to hypoxia in crustaceans. *Respiration Physiology* **128**, pp. 349–364.

McMahon, R. F. & Wilson, J. G. (1981) Seasonal respiratory responses to temperature and hypoxia in relation to burrowing depth in three intertidal bivalves. *Journal of Thermal Biology* **6**, pp. 267–277.

Moksnes, P.-O., Lipcius, R. N., Pihl, L. & van Montfrans, J. (1997) Cannibal-prey dynamics in young juveniles and postlarvae of the blue crab. *Journal of Experimental Marine Biology and Ecology* **215**, pp. 157–187.

Newcombe, C. L., Cambell, F. & Eckstine, A. M. (1949) A study of the form and growth of the blue crab *Callinectes sapidus* Rathbun. *Growth* **13**, pp. 71–96.

Nichols, F. H. & Thompson, J. K. (1982) Seasonal growth in the bivalve *Macoma balthica* near the southern limit of its range. *Estuaries* **5**, pp. 110–120.

North Carolina Department of Environment, Health and Natural Resources (1993) Neuse River basinwide water quality management plan. Raleigh, NC.

O'Leary Amsler, M. & George, R. Y. (1984) The effect of temperture on the oxygen consumption and development rate of the embryos of *Callinectes sapidus* Rathbun. *Journal of Experimental Marine Biology and Ecology* **82**, pp. 221–229.

Olmi III, E. J. & Bishop, J. H. (1983) Variations in total width-weight relationships of blue crabs *Callinectes sapidus*, in relation to sex, maturity, molt stage and carapace form. *Journal of Crustacean Biology* **3**, pp. 575–581.

Orth, R. J. & van Montfrans, J. (1987) Utilization of a seagrass meadow and tidal marsh creek by blue crabs *Callinectes sapidus*. I. Seasonal and annual variations in abundance with emphasis on post-settlement juveniles. *Marine Ecology Progress Series* **41**, pp. 283–294.

Pihl, L., Baden, S. P. & Diaz, R. J. (1991) Effects of periodic hypoxia on distribution of demersal fish and crustaceans. *Marine Biology* **108**, pp. 349–360.

Posey, M. H., Alphin, T. D., Harwell, H. & Allen, B. (2005) Importance of low salinity areas for juvenile blue crabs, *Callinectes sapidus* Rathbun, in river-dominated estuaries of southeastern Uunited States. *Journal of Experimental Marine Biology and Ecology* **319**, pp. 81–100.

Prager, M. H., McConaugha, J. R., Jones, C. M. & Geer, P. J. (1990) Fecundity of blue crab *Callinectes sapidus* in Chesapeake Bay: Biological, statistical and management considerations. *Bulletin of Marine Science* **46**, pp. 170–179.

Pullen, E. J. & Trent, W. L. (1970) Carapace width-total weight relations of blue crabs from Galveston Bay, Texas. *Transactions of the American Fisheries Society* **99**, pp. 795–798.

Ripley, B. D. (1987) *Stochastic Simulation*. John Wiley & Sons.

Rosenberg, R., Loo, L.-O. & Moller, P. (1992) Hypoxia, salinity and temperature as structuring factors for marine benthic communities in a eutrophic area. *Netherlands Journal of Sea Research* **30**, pp. 121–129.

Rugolo, L. J., Knotts, K. S., Lange, A. M. & Crecco, V. A. (1998) Stock assessment of Chesapeake Bay blue crab (*Callinectes sapidus* Rathbun). *Journal of Shellfish Research* **17**, pp. 906–930.

Ryer, C. H., van Montfrans, J. & Orth, R. J. (1990) Utilization of a seagrass meadow and tidal marsh creek by blue crabs *Callinectes sapidus.* II. Spatial and temporal patterns of molting. *Bulletin of Marine Science* **46**, pp. 95–104.

Rykiel Jr., E. J. (1996) Testing ecological models: the meaning of validation. *Ecological Modelling* **90**, pp. 229–244.

Schnoor, J. (1996) *Environmental modeling: fate and transport of polutants in water, air, and soil*. New York: Wiley.

Schönfisch, B. & de Roos, A. (1999) Synchronous and asynchronous updating in cellular automata. *Biosystems* **51**, pp. 123–143.

Sedgewick, R. (1992) *Algorithms in C++*. Reading, Massachusetts: Addison-Wesley Publishing Company.

Seitz, R. D., Lipcius, R. N., Stockhausen, W. T., Delano, K. A., Seebo, M. S. & Gerdes, P. D. (2003a) Potential bottom-up control of blue crab distribution at various spatial scales. *Bulletin of Marine Science* **72**, pp. 471–490.

Seitz, R. D., Marshall, L., Hines, A. H. & Clark, K. (2003b) Effects of hypoxia on predator-prey dynamics of the blue crab *Callinectes sapidus* and Baltic clam *Macoma balthica* in Chesapeake bay. *Marine Ecology-Progress Series* **257**, pp. 179–188.

Selberg, C. D., Eby, L. A. & Crowder, L. B. (2001) Hypoxia in the Neuse River Estuary: Responses of blue crabs and crabbers. *North American Journal of Fisheries Management* **21**, pp. 358–366.

Smith, L. D. (1990) Patterns of limb loss in the blue crab, *Callinectes sapidus* Rathbun, and the effects of autotomy on growth. *Bulletin of Marine Science* **46**, pp. 23–36.

Smith, L. D. (1995) Effects of limb autotomy and tethering on juvenile blue crab survival from cannibalism. *Marine Ecology Progress Series* **116**, pp. 65–74.

Smith, L. D. & Hines, A. H. (1991) The effect of cheliped loss on blue crab *Callinectes sapidus* Rathbun foraging rate on soft-shell clams *Mya arenaria* L. *Journal of Experimental Marine Biology and Ecology* **151**, pp. 245–256.

Smith, S. G. (1997) *Models of Crustacean growth dynamics*. Ph.D. thesis, University of Maryland, College Park, MD.

Solidoro, C., Pastres, R., Canu, D. M., Pellizzato, M. & Rossi, R. (2000) Modelling the growth of *Tapes philippinarum* in northern Adriatic lagoons. *Marine Ecology Progress Series* **199**, pp. 137–148.

Spitzer, P. M., Heck Jr., K. L. & Valentine, J. F. (2003) Then and now: a comparison of paterns in blue crab post-larval abundance and post-settlement mortality during the early and late 1990s in the Mobile Bay system. *Bulletin of Marine Science* **72**, pp. 435–452.

Sullivan, E. T. & Gaskill, D. (1998) Effects of anoxia on the value of bottom habitat for fisheries production in the Neuse River Estuary. Tech. rep., DMF Final Report for FRG Project, Morehead City. Http://www.marine.unc.edu/neuse/modmon/.

Szaniawska, A., Wolowicz, M. & Wenne, R. (1986) Energetic values of the body of *Macoma balthica* L. from the Gulf of Gdansk. *Oceanologia* **24**, pp. 55–62.

Tagatz, M. E. (1968) Growth of juvenile blue crabs, *Callinectes sapidus* Rathbun, in the St. Johns River, Florida. *Fishery Bulletin* **67**, pp. 281–288.

Tagatz, M. E. (1969) Some relations of temperature acclimation and salinity to thermal tolerance of the blue crab *Callinectes sapidus*. *Transactions of the American Fisheries Society* **4**, pp. 713–716.

Tallqvist, M. (2001) Burrowing behaviour of the baltic clam *Macoma balthica*: effects of sediment type, hypoxia and predator presence. *Marine Ecology Progress Series* **212**, pp. 183–191.

Tang, Q. (1985) Modifications of the Ricker stock recruitment model to account for environmentally induced variation in recruitment with particular reference to the blue crab fishery in Chesapeake Bay. *Fisheries Research* **3**, pp. 13–21.

Taylor, D. L. & Eggleston, D. B. (2000) Effects of hypoxia on an estuarine predator-prey interaction: foraging behavior and mutual interference in the blue crab *Callinectes sapidus* and the infaunal clam prey *Mya arenaria*. *Marine Ecology Progress Series* **196**, pp. 221–237.

Tischendorf, L. (1997) Modelling individual movements in heterogeneous landscapes: potentials of a new approach. *Ecological Modelling* , pp. 33–42.

van den Avyle, M. J. (1984) Species profiles: life histories and environmental requirements of coastal fishes and invertebrates (South Atlantic) – blue crab. U.S. Fish and Wildlife Service. FWS/OBS-82/11. U.S. Army Corps of Engineers, TR EL-82-4.

van der Meer, J., Beukema, J. J. & Dekker, R. (2001) Long-term variability in secondary production of an intertidal bivale population is primarily a matter of recruitment variability. *Journal of Animal Ecology* **70**, pp. 159–169.

van Engle, W. A. (1958) The blue crab and its fishery in Chesapeake Bay. *Commerical Fisheries Review* **20**, pp. 6–17.

van Montfrans, J., Epifanio, C. E., Knott, D. M., Lipcius, R. N., Mense, D. J., Metcalf, K. S., Olmi III, E. J., Orth, R. J., Posey, M. H., Wenner, E. L. & West, T. L. (1995) Settlement of blue crab postlavae in western North Atlantic estuaries. *Bulletin of Marine Science* **57**, pp. 834–854.

Wallace, J. C. (1973) Feeding, starvation and metabolic rate in the shore crab *Carcinus maenas*. *Marine Biology* **20**, pp. 277–281.

Waller, L. M. (1996) *The Population Dynamics of the clam Macoma mitchelli and its potential as a bioindicator in the Neuse River Estuary, North Carolina*. Master's thesis, North Carolina State University.

Wang, W. X. & Widdows, J. (1993) Calorimetric studies on the energy metabolism of an infaunal bivalve, *Abra tenuis* under normoxia, hypoxia and anoxia. *Marine Biology* **116**, pp. 73–79.

Wilson, J. G. (1981) Temperature tolerance of circatidal bivalves in relation to their distribution. *Journal of Thermal Biology* **6**, pp. 279–286.

Wolcott, T. G. & Hines, A. H. (1990) Ultrasonic telemetry of small-scale movements and microhabitate selection by molting blue crabs (*Callinectes sapidus*). *Bulletin of Marine Science* **46**, pp. 83–94.

Yilmaz, L. & Balci, O. (1997) Object-oriented simulation model verification and validation. In: *The Proceedings of the 1997 Summer Computer Simulation Conference* (Obaidat, M. S. & Illgen, J., eds.). Arlington, Virginia: The Society for Computer Simulation International.

Zeigler, B. P., Praehoffer, H. & Kim, T. G. (2000) *Theory of Modeling and simulation*. New York: Academic Press, 2 edn.